

# **DOE Low Temperature Plasma Centers and User Facilities Annual Meeting**

**Center for Low Temperature Plasma Interactions with Complex  
Surfaces (PICI)**

**Sandia Plasma Research Facility (PRF)**

**Princeton Collaborative Low Temperature Research Facility  
(PCRf)**

**Center for Studies of Plasma-Assisted Combustion and  
Plasma Catalysis (PACC)**

**December 7-8, 2023  
Hilton Garden Inn Reagan National Airport  
Arlington, VA**

We gratefully acknowledge the funding from  
**The U.S. Department of Energy Office of Science  
Fusion Energy Sciences Program**  
Grants DE-SC0020232, DE-NA0003525, DE-AC02-09CH11466, DE-SC0020233



U.S. DEPARTMENT OF  
**ENERGY**

Office of  
Science

## Schedule

Thursday, December 7, 2023			
	Time (Eastern)	Speaker	Title
<b>8:15 – 8:30 am</b> <a href="#"><u>Welcome</u></a> (Salon 1 & 2)			
	8:15 – 8:30	Mark J. Kushner	Introduction to Annual Meeting
<b>8:30 – 10:10 am</b> <a href="#"><u>Oral Session I: PICI</u></a> (Salon 1 & 2).			
1	8:30 – 8:50	Steven Shannon	SIW Propagation over Complex Dielectric Topologies
2	8:50 – 9:10	Brian Bentz	Tomographic Optical Emission Spectroscopy of Surface Ionization Waves
3	9:10 – 9:30	Aditya Bhan	Pathways and Timescales for Oxidative and Reductive N <sub>2</sub> Conversion by Low Temperature, Atmospheric Pressure Plasma Catalysis
4	9:30 – 9:50	Selma Mededovic Thagard	Exploring the Degradation Pathways of PFOA in a Radio Frequency Driven Atmospheric Pressure Plasma Jet
5	9:50 – 10:10	Peter Bruggeman	The Impact of Plasma-Liquid Interactions on Near-Interfacial Plasma Properties
<b>10:10 – 10:30 am</b> <i>Break</i>			
<b>10:30 am – 12:10 pm</b> <a href="#"><u>Oral Session II: PCRF</u></a> (Salon 1 & 2).			
1	10:30 – 10:50	Yevgeny Raitses	Princeton Collaborative Low Temperature Plasma Research Facility (PCRF): Status Update and New Solicitation of User Proposals
2	10:50 – 11:10	Sophia Gershman	Plasma in Contact with Liquid and Solid Materials for Environmental and Bio Applications (PCRF User Projects)
3	11:10 – 11:30	Mikhail Shneider	Dielectric Permittivity of Cell Membranes in a Physiological Solution Interacting with Low-Temperature Plasma
4	11:30 – 11:50	Igor Kaganovich	Modeling of Modern Plasma Processing Reactors: Plasma Physics and Surface Chemistry
5	11:50 – 12:10	Willca Villafana	Modeling Low-Temperature Plasmas with EDIPIC-2D: An Open-Source and Versatile Particle-In-Cell Code
6	12:10 – 12:30	Shurik Yatom	Measurement and Reduction of Ar Metastable Densities by Nitrogen Admixing in Electron Beam-generated Plasmas
<b>12:30 – 1:50 pm</b> <i>Lunch</i>			

<b>Thursday, December 7, 2023 (continued)</b>			
	<b>Time (Eastern)</b>	<b>Speaker</b>	<b>Title</b>
<b>1:50 – 2:50 pm</b> <b><u><a href="#">Oral Session III: PACC</a></u> (Salon 1 &amp; 2).</b>			
1	1:50 – 2:10	Igor Adamovich	Ns Pulse and Hybrid Ns Pulse / RF Discharges for Plasma Catalysis and Plasma Fuel Reforming
2	2:10 – 2:30	Yiguang Ju	Plasma Assisted Combustion and Control of Plasma Dynamics for Manufacturing
3	2:30 – 2:50	Bruce Koel	Plasma-Assisted Catalytic Synthesis of NH <sub>3</sub>
<b>2:50 – 3:00 pm</b> <b>Group Photo</b>			
<b>3:00 – 3:10 pm</b> <b>Break</b>			
<b>3:10 – 4:30 pm</b> <b>Poster Session I (Salon 3 &amp; 4)</b>			
<b>4:30 – 4:40 pm</b> <b>Break</b>			
<b>4:40 – 6:00 pm</b> <b>Poster Session II (Salon 3 &amp; 4)</b>			
<b>6:00 pm</b> <b>End of Day 1</b>			
<b>Friday, December 8, 2023</b>			
<b>8:30 – 9:50 am</b> <b><u><a href="#">Oral Session IV: PRF</a></u> (Salon 1 &amp; 2).</b>			
1	8:30 – 8:50	Shane Sickafoose	Sandia National Laboratories Plasma Research Facility (PRF)
2	8:50 – 9:10	Lucas Beving	Understanding Sheath Expansion in Flowing Plasmas
3	9:10 – 9:30	Christopher Kliewer	Nonlinear Optical Diagnostics Laboratory for Low-Temperature Plasma-Assisted Chemistry
4	9:30 – 9:50	Nils Hansen	Opportunities for Mass Spectrometry to Study Plasma-Assisted Chemical Transformations
5	9:50 – 10:10	Jonathan Frank	Imaging of Methyl Radical and Hydrogen Peroxide in Plasmas by Photofragmentation Laser-Induced Fluorescence
<b>10:10 – 10:30 pm</b> <b>Break</b>			
<b>10:30 – 11:30 am</b> <b><u><a href="#">Oral Session V: PICI</a></u> (Salon 1 &amp; 2).</b>			
1	10:30 – 10:50	Gottlieb Ohrlein	Plasma/Catalyst Contributions for N <sub>2</sub> Oxidation and Dry Reforming of Methane
2	10:50 – 11:10	Igor Adamovich	Characterization of Plasma Jets Impinging on Dielectric and Metal Surfaces
3	11:10 – 11:30	Mark J. Kushner	Shaping Liquid Surfaces for Selective Plasma Interactions
<b>11:30 – 11:40 am</b> <b>Break</b>			
<b>11:40 am – 12:40 pm</b> <b><u><a href="#">Group Discussion</a></u> (Salon 1 &amp; 2).</b>			
<b>12:40 pm</b> <b>End of Day 2</b>			

*Poster Session I. Thursday, December 7, 3:10 – 4:30 pm*

	<b>Presenter</b>	<b>Title</b>
1	Sonia Arumuganainar	Design of Ordered Mesoporous Oxides for Dielectric Barrier Discharge-assisted Catalysis of Ammonia Synthesis
2	Yevgeny Raitses	Electron Beam Generated Plasmas and Their Applications
3	Sai Raskar	Measurements of Excited Metastable Species and Ionization in a Nonequilibrium Heated Plasma Reactor
4	Brian Bentz	Mapping Electron Density with Laser-Collision Induced Fluorescence in the Budapest Capacitively Coupled Plasma Reference Cell
5	Ning Liu	Ferroelectrics-induced Surface Charge in Plasma
6	Shurik Yatom	Temperature Prediction in OES using Neural Networks
7	Brian Bayer	Availability and Reactivity of N <sub>2</sub> (v) for NH <sub>3</sub> Synthesis by Plasma Catalysis
8	Jordyn Polito	Computational Investigation of Mechanisms Leading to Reduction in Cell Viability by Changing Atmospheric Pressure Plasma Jet Configuration
9	Zhiyu Shi	Numerical Modeling of Plasma Assisted Deflagration to Detonation Transition in a Microscale Channel
10	Yerbolat Ussenov	Synthesis of Dust Nanoparticles in RF Discharge Plasma
11	Kseniia Konina	Atmospheric Pressure Plasma Jet Treatment of Polypropylene Materials with Non-Smooth Interfaces
12	Matthew Berry	Ammonia Generation in a “Hybrid” High Repetition Rate Ns Pulse / RF Discharge Sustained over a Catalytic Surface
13	Victor Miller	Data-Driven Dimensionless Number Discovery in a Nanosecond Pulsed Low Temperature Plasma
14	Matthew Hopkins	Electron-Field Instability: Excitation of Electron Plasma Waves by an Electric Field
15	Ketong Shao	Interpretable Attention-Based Transfer Learning for Plasma Catalysis
16	Hamzeh Telfah	Spatially- and Time-Resolved Measurements of HO <sub>2</sub> Radicals in a Ns Pulse Atmospheric Pressure Plasma Jet

**Poster Session II. Thursday, December 7, 4:40 – 6:00 pm**

	<b>Presenter</b>	<b>Title</b>
1	Zihan Lin	Kinetic Modeling Analysis of Ar Addition to Atmospheric Pressure N <sub>2</sub> -H <sub>2</sub> Plasma for Plasma-Assisted Catalytic Synthesis of NH <sub>3</sub>
2	Sophia Gershman	The Role of Dielectric Properties of Biological Targets in non-thermal Plasma Treatment
3	Michael Hinshelwood	Study of Surface Interactions During Plasma Catalytic Dry Reforming of Methane
4	Grant Gorman	Particle-In-Cell Simulations of the Anode Sheath in DC Discharges
5	Xingqian Mao	Ignition Enhancement and NO <sub>x</sub> Formation of NH <sub>3</sub> /Air Mixtures by Non-equilibrium Plasma Discharge
6	Louis Hoffenberg	Molecular Dynamics Simulation of Vapor-Phase Nucleation of Metal Nanoparticles in a Reactive Plasma Atmosphere
7	Mahreen Khan	Improved Matching and Power Measurements in PICI reference RF Jet
8	Foluke (Jennifer) Ganzallo	Understanding Ionic Interactions and Distributions at Plasma-Liquid Interfaces and Their Influence on Liquid Phase Chemistry
9	Mackenzie Meyer	CH <sub>3</sub> Radical Generation in Microplasmas for Up-Conversion of Methane
10	Yiteng Zheng	Nickel Nitride on Plasma-Assisted Ammonia Synthesis over Nickel Catalysts
11	Oluwatosin Ohiro	Microkinetic Model for Low-Temperature Plasma Assisted Catalysis by Fe and Ni Catalysts for Ammonia Synthesis
12	Sai Raskar	Spatio-Temporal Electric Field Distributions in an Atmospheric Plasma Jet Impinging on a Microchannel Array Surface
13	Keegan Orr	Measurements and Kinetic Modeling of O <sub>2</sub> Vibrational Kinetics in O <sub>2</sub> -Ar Mixtures Partially Dissociated by a Ns Pulse Discharge
14	Stanislav Musikhin	Studies of Catalyst Nanoparticles Synthesis Using Metal Arc Discharge: Experiment and Modeling
15	Tanubhav Srivastava	Femtosecond TALIF to Measure Atomic Sodium Densities in a Glow Discharge with NaCl Solution Electrode
16	James Trettin	Mechanistic Insights into Plasma-Assisted Catalysis by <i>Operando</i> DRIFTS

## Abstracts – Oral Presentations

### [I-1] SIW Propagation over Complex Dielectric Topologies

Steven Shannon, Joshua Morsell

North Carolina State University, Raleigh NC USA (scshannon@ncsu.edu)

The interaction between surface ionization wave fronts and single step-up and step-down topologies on dielectric surfaces have been studied using gated CCD imaging of wave propagation through a dielectric plate with a transparent indium tin oxide (ITO) grounded backplane. Integrated intensity and wavelength selected intensities for the helium triplet states  $3^3S$  (706.5 nm) and  $3^3D$  (587.6 nm) were used to study SIW propagation velocity, reduced fields and estimated electron temperature in the SIW front. Variations in gas composition above the dielectric surface are also taken into account using a mixed helium / air model to account for changes in relative emission intensity with respect to electron energy and gas composition. A radial increase in electron temperature is observed, and attributed to radial variation in the gas composition due to mixing of the helium APPJ feedgas with surrounding air. SIW “bunching” at step surfaces is observed; propagation over the step topologies is characterized as a function of SIW energy and step height revealing conditions where the SIW can “hop” a step or where a step can sufficiently arrest the motion of an SIW. Finally, increased propagation velocity is observed along the corners of step features compared to flat surfaces. This topology study is expanded to include propagation and escape of SIW’s from channel grooves of varying height and width; the fraction of the SIW that is retained in the channel groove depends on the energy of the pulse and the surface area of the groove.[1]

Figure 1 illustrates these observations. In Figure 1 (I) the propagation of the SIW along the channel at B moved a greater distance than the SIW on the flat surface to the right of the step at 348ns, revealing a higher velocity of propagation along step discontinuities than flat surfaces. The emission profiles perpendicular to the channel at A, also plotted at various times in Figure 1 (II) show compression of the SIW as it moves toward the step along with an initial reduction in emission, followed by a re-intensification of emission after the SIW passes over the step discontinuity.

#### References

[1] Morsell, J. K., Trosan, D., Stapelmann, K., & Shannon, S. (2023). *Plasma Sources Science and Technology*. DOI 10.1088/1361-6595/acf9c9

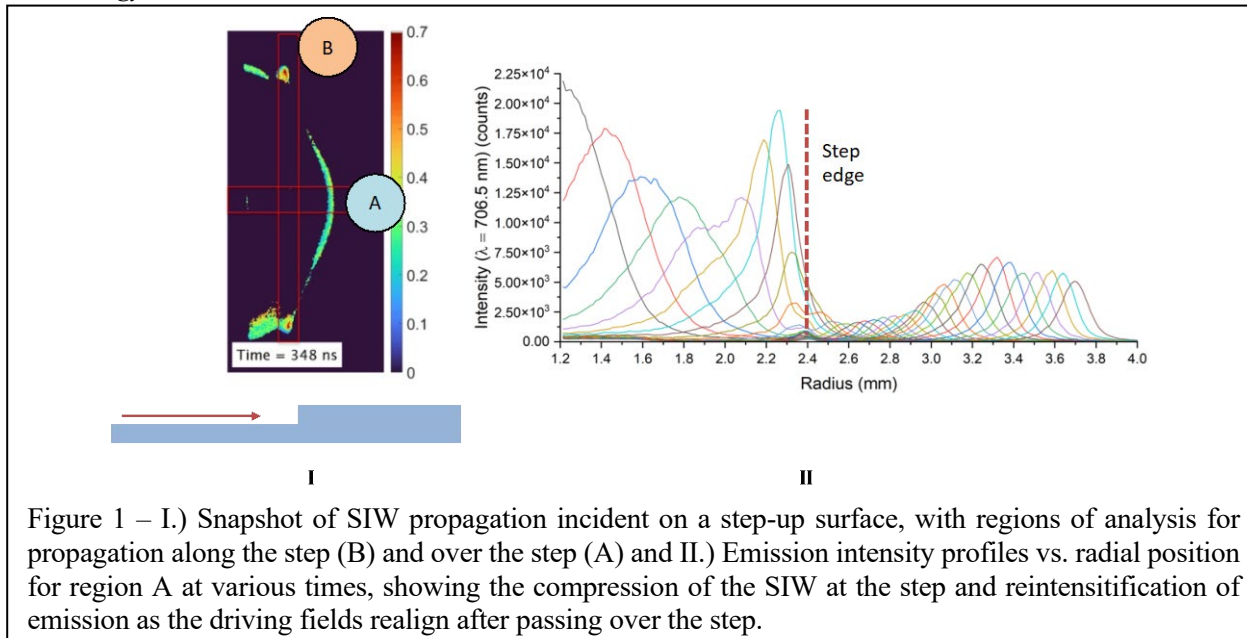


Figure 1 – I.) Snapshot of SIW propagation incident on a step-up surface, with regions of analysis for propagation along the step (B) and over the step (A) and II.) Emission intensity profiles vs. radial position for region A at various times, showing the compression of the SIW at the step and reintensification of emission as the driving fields realign after passing over the step.

# [I-2] Tomographic Optical Emission Spectroscopy of Surface Ionization Waves

Brian Z. Bentz

Sandia National Laboratories, Albuquerque, New Mexico, USA  
(bzbentz@sandia.gov)

Applications of non-thermal plasmas at atmospheric pressures often involve formation of surface ionization waves (SIWs) that experience variable geometrical and electrical material properties as they propagate, leading to 3D configurations that are non-symmetric and spatially complex. Furthermore, interactions with ambient air create reactive oxygen and nitrogen species (RONS) with distributions that cannot be fully characterized with 1D or 2D diagnostics. To better assess the species distributions, a tomographic optical emission spectroscopy (Tomo-OES) diagnostic was developed and its ability to study evolution of SIWs in 3D was evaluated. Light emissions from He (706.5 nm),  $N_2^+$  (391.4 nm), and  $N_2$  (337.1 nm) were imaged by an intensified camera at ten angular projections and the respective time-resolved 3D emission was reconstructed. Emission from He revealed the core of the SIW and emission from  $N_2^+$  and  $N_2$  indicated effects of entrainment of ambient air. Penning ionization of  $N_2$  created a ring or outer layer of  $N_2^+$  that spatially converged to form the ‘plasma bullet’ or spatially diverged across the surface as part of a SIW. The SIW entered trenches of size 150  $\mu\text{m}$ , leading to decreases in plasma light emission in regions above the trenches (see Figure 1). The plasma light emission was higher in regions with trenches compared to a planar surface, possibly due to effects of field enhancement.

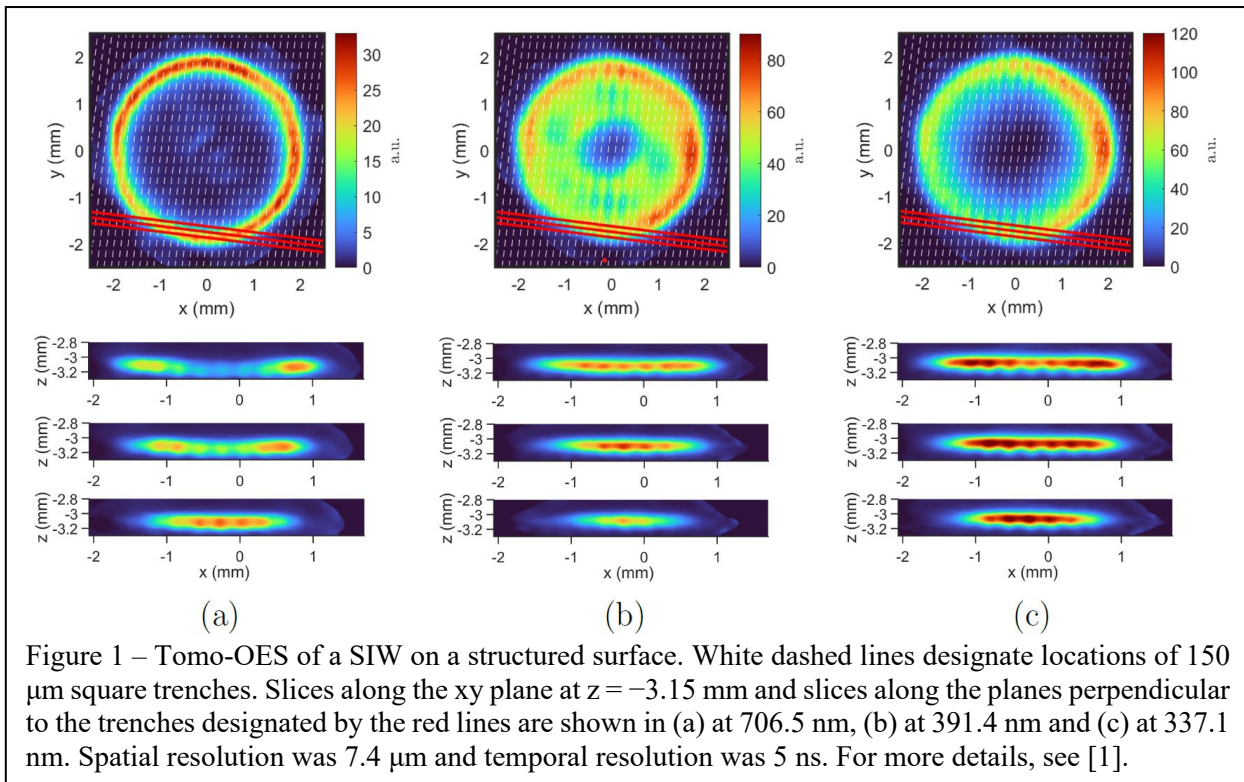


Figure 1 – Tomo-OES of a SIW on a structured surface. White dashed lines designate locations of 150  $\mu\text{m}$  square trenches. Slices along the xy plane at  $z = -3.15$  mm and slices along the planes perpendicular to the trenches designated by the red lines are shown in (a) at 706.5 nm, (b) at 391.4 nm and (c) at 337.1 nm. Spatial resolution was 7.4  $\mu\text{m}$  and temporal resolution was 5 ns. For more details, see [1].

This work was supported by the U.S. Department of Energy Office of Fusion Energy Sciences (DE-SC0020232) and the Sandia Laboratory Directed Research and Development (LDRD) program. Sandia is managed and operated by NTESS under DOE NNSA contract DE-NA0003525.

## References

[1] B. Z. Bentz, Plasma Sources Sci. Tech. **32**, 105003, (2023).

# [I-3] Pathways and Timescales for Oxidative and Reductive N<sub>2</sub> Conversion by Low Temperature, Atmospheric Pressure Plasma Catalysis

Brian Bayer<sup>a</sup>, Peter Bruggeman<sup>b</sup> and Aditya Bhan<sup>a</sup>

(a) University of Minnesota, Department of Chemical Engineering and Materials Science  
(bayer116@umn.edu, abhan@umn.edu)

(b) University of Minnesota, Department of Mechanical Engineering (pbruggem@umn.edu)

Activation of N<sub>2</sub> in nonthermal plasma to form radicals and excited species opens new pathways for N<sub>2</sub> fixation by heterogeneous catalysis at near ambient temperatures and pressures. Here, we enumerate densities of N radicals and N<sub>2</sub>(v) (vibrationally excited N<sub>2</sub>) produced in an atmospheric pressure plasma jet by molecular beam mass spectrometry (MBMS) and assess their reactivity for reductive N<sub>2</sub> fixation to NH<sub>3</sub> and oxidative N<sub>2</sub> fixation to NO<sub>x</sub> by measuring consumption of plasma-derived species and formation of products with and without catalyst present.

For reduction of N<sub>2</sub> in Ar/N<sub>2</sub>/H<sub>2</sub> plasma, the plasma jet produces measurable densities of N, H, NH<sub>3</sub>, and N<sub>2</sub>(v). The presence of catalyst increases the rate of N and N<sub>2</sub>(v) conversion and extent of NH<sub>3</sub> formation. Rates and quantities of N consumption in Fe, Ni, or Ag catalyst beds correlate 1:1 with rates and quantities of NH<sub>3</sub> formation for sufficient concentrations of H and H<sub>2</sub> (Figure 1) [1]. Through MBMS-validated state-to-state vibrational kinetic modeling, we show that N<sub>2</sub>(v), though produced in quantities exceeding N by 100×, is not reactive for NH<sub>3</sub> formation at the investigated experimental operating conditions. The dominant loss of N<sub>2</sub>(v) in the catalyst bed occurs due to vibrational relaxation on the catalyst surface, which prevents N<sub>2</sub>(v) from reacting in NH<sub>3</sub>-forming reactions on the surface [2].

For oxidation of N<sub>2</sub> in Ar/N<sub>2</sub>/O<sub>2</sub> plasma, N can react with O<sub>2</sub> to form NO in the gas phase, although the reaction of N with NO to form N<sub>2</sub> limits the ability of N to produce NO with a high yield. Plasma and gas-phase N<sub>2</sub> oxidation processes are not 100% selective to NO formation. In the presence of an Ag catalyst, the rate of N consumption increases and NO is formed with ~100% selectivity when the O<sub>2</sub> concentration exceed 3 mol% (Figure 2). For the investigated process conditions, the rate of mass transfer rather than the kinetics of surface reactions dictates how fast N can react on the surface to form NO. Above a threshold NO density, N can be consumed in reactions with NO in the gas phase more quickly than it can diffuse to the surface and react to form NO, which limits the ability of the surface to catalyze NO formation from N [3].

## References

- [1] Bayer et al. ACS Catal. 13 (2023) 4, 2619-2630
- [2] Bayer et al. Plasma Sources Sci. Technol. In review
- [3] Bayer et al. Chem. Eng. J. Submitted

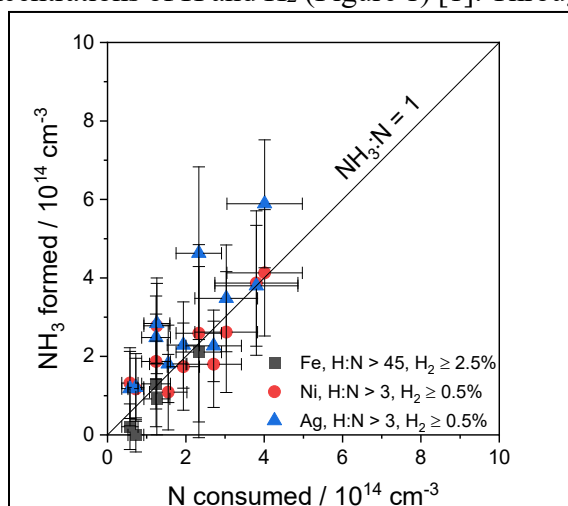


Figure 1 – Correlation between N consumption and NH<sub>3</sub> formation in packed beds of Fe, Ni, and Ag

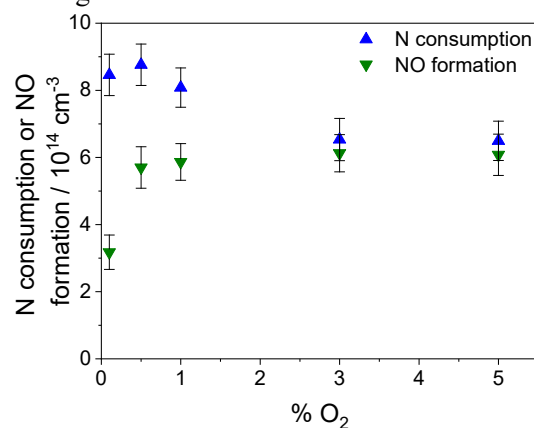


Figure 2 – N consumption and NO formation in a packed bed of Ag catalyst for different O<sub>2</sub> concentrations



## [I-4] Exploring the Degradation Pathways of PFOA in a Radio Frequency Driven Atmospheric Pressure Plasma Jet

Md. Akibur Rahman and Selma Mededovic Thagard

Department of Chemical and Biomolecular Engineering, Clarkson University, Potsdam, NY, 13699  
(md.rahm@clarkson.edu, smededov@clarkson.edu)

Poly- and perfluoroalkyl substances (PFAS), a large and complex group of synthetic chemicals known for their outstanding physical and chemical properties, have found widespread use in consumer products globally. Unfortunately, they have become ubiquitous in our environment, causing various health issues, and are resistant to conventional treatment (oxidation) methods. Plasmas generated in systems where gas contacts the surface of a liquid have shown promise in degrading both long-chain and, to some extent, short-chain PFAS. Published plasma studies have demonstrated exceptionally high removal rates for these compounds. However, critical details remain elusive, including the specific species responsible for their degradation, the byproducts formed, and the complex relationships among operational parameters, compound transport and adsorption at the plasma-liquid interface and their subsequent removal.

This study aims to elucidate the degradation pathways of perfluorooctanoic acid (PFOA), a long-chain PFAS. We employ an RF-driven atmospheric-pressure plasma jet directed over the aqueous surface of a flow-through cuvette, which serves as the reactor. To bridge the knowledge gaps pertaining to the removal of these compounds using electrical discharge plasmas, we investigated the effects of liquid flow rate, starting compound concentration and gas type on PFOA degradation. Furthermore, we identified degradation byproducts and attempted to close the fluorine mass balance. Our experiments also involved the use of chemical probes to scavenge reactive oxidative and reductive species, facilitating

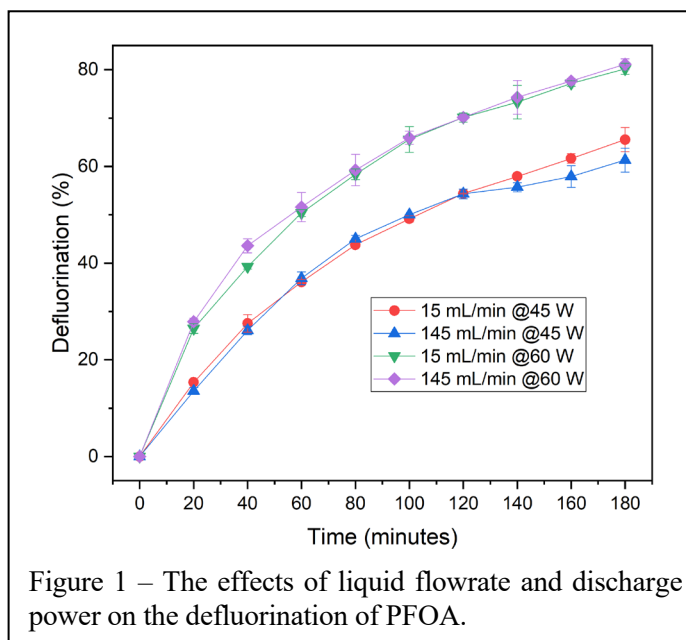


Figure 1 – The effects of liquid flowrate and discharge power on the defluorination of PFOA.

a deeper understanding of degradation pathways. The results of our investigation reveal that under carefully selected conditions, PFOA defluorination reaches approximately 80%, a level not previously observed in any other plasma system (Figure 1). Additionally, we discuss differences between RF and traditionally employed pulsed DC plasmas in degrading PFAS.

## [I-5] The Impact of Plasma-Liquid Interactions on Near-Interfacial Plasma Properties

Gaurav Nayak, Tanubhav Srivastava, Jianan Wang, Yuanfu Yue and Peter Bruggeman

Department of Mechanical Engineering, University of Minnesota, 111 Church St SE, Minneapolis, Minnesota, 55455, USA (pbruggem@umn.edu)

The interaction of liquids with low temperature atmospheric pressure plasmas has been investigated intensively due to its large potential in many applications. The strong coupling between the plasma and the liquid phase can lead to huge changes in the local plasma properties in the vicinity of the liquid phase and significantly enhances the complexity of the underpinning processes. This coupling does not only significantly impact the transport of reactive species into the liquid phase, the driving force behind many applications, but can also impact the plasma dynamics, stability and kinetics. We have shown that a significant amount of water vapor can be introduced in the gas phase plasma by plasma-enhanced evaporation [1]. Interestingly, in the case of a liquid anode, this can lead to a suppression of a glow discharge instability [2]. In collaboration with Prof. Dogariu, we have recently extended this work to the transfer of solutes from the liquid to the plasma gas phase which shows interesting and highly distinctive phenomena in the case of liquid anode and cathode, in strong contrast with the very similar plasma-enhanced water evaporation for both polarities. We will discuss in detail the underlying processes and the impact on plasma kinetics.

In the case of droplets, the plasma-liquid interface is no longer a driven electrode as in the cases discussed above but is at floating potential. Nonetheless similar effects were found. Droplet evaporation also significantly impacts the plasma surrounding the droplet, leading to a strong inhomogeneity in the plasma (see Figure 1). Using continuum radiation measurements, spatially resolved electron properties were determined in the presence of droplets in the plasma, allowing for the estimation of  $e^-$ /ion fluxes to the droplet. The gas-phase OH radical densities and water vapor concentrations were determined spatially along the plasma length and in the vicinity of the droplet using OH-LIF measurements [3]. These measurements were recently extended to time resolved measurements surrounding the droplet allowing us to investigate transient evaporation effects coupled with droplet transport. We studied the impact of this strong coupling on plasma-induced liquid phase chemistry in collaboration with Prof. Mededovic and showed that such interactions can even lead to highly unexpected trends in liquid phase conversions.

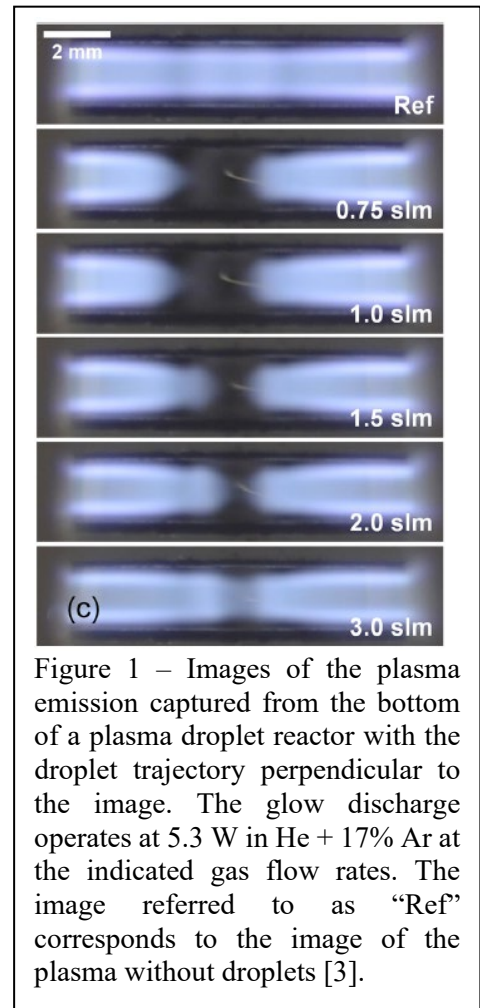


Figure 1 – Images of the plasma emission captured from the bottom of a plasma droplet reactor with the droplet trajectory perpendicular to the image. The glow discharge operates at 5.3 W in He + 17% Ar at the indicated gas flow rates. The image referred to as “Ref” corresponds to the image of the plasma without droplets [3].

### References

- [1] Y. Yue, V. S. S. K. Kondeti, N. Sadeghi, P. J. Bruggeman 2022 Plasma Sources Sci. Technol. 31 025008
- [2] Y. Yue, P. Bruggeman 2022 Plasma Sources Sci. Technol. 31 124004
- [3] G. Nayak, J. Wang, R. Li, D. Aranzales, S. Mededovic Thagard, P. Bruggeman 2023 Plasma Process Polym. 20:e2200222

## [II-1] Princeton Collaborative Low Temperature Plasma Research Facility (PCRF): Status Update and New Solicitation of User Proposals

Yevgeny Raitses<sup>a</sup>, Igor Kaganovich<sup>a</sup>, Mikhail Shneider<sup>b</sup>, Sophia Gershman<sup>a</sup>, Arthur Dogariu<sup>b</sup>,  
Shurik Yatom<sup>a</sup>, Anatoli Morozov<sup>b</sup>, Nirbhav S. Chopra<sup>a</sup>, and Willca Villafana<sup>a</sup>

(a) PCRF, Discovery Plasma Science Department, Princeton Plasma Physics Laboratory  
(yraitses@pppl.gov)

(b) PCRF, Mechanical and Aerospace Engineering Department, Princeton University

The Princeton Collaborative Low Temperature Plasma Research Facility (PCRF) provides the scientific communities and industry access to state-of-the-art research capabilities, including advanced diagnostics, plasma sources and computational codes, theory support, and expertise for comprehensive characterization of low temperature plasmas (LTPs) with focuses on 1) plasma-liquid and plasma-solid interactions, 2) collective phenomena in LTP, and 3) use of LTP in modern applications (e.g. nanomaterials synthesis and processing, microelectronics and quantum systems, energy, sustainability, aerospace, bio/med/agro). Since the beginning of the facility operation in 2019, 86 collaborative users from the plasma and other scientific communities, including from universities, national labs, and industry, were awarded with runtime at the PCRF. In this presentation, we will overview PCRF research, capabilities and opportunities for collaboration.

This work is supported by the US Department of Energy through contract DE-AC02-09CH11466.

### References

[1] <http://pcrf.pppl.gov>

### **New Solicitation of Collaborative Research Proposals**

**Call for proposals opens: October 9th, 2023**

**Call for proposals closes: December 15th, 2023**

**External Review: ~ 1.5 month**

**Notification of Principal Investigators: by February 5, 2024**

## [II-2] Plasma in Contact with Liquid and Solid Materials for Environmental and Bio Applications (PCRF User Projects)

S. Gershman <sup>a</sup>, N. Sponsel <sup>b</sup>, R. Walker <sup>c</sup>, J. Sutter <sup>d</sup>, M. Carreon <sup>e</sup>, J. Foster <sup>c</sup>, V. Miller <sup>d</sup>,  
K. Stapelmann <sup>b</sup>

(a) Princeton Plasma Physics Laboratory, Princeton, NJ (sgershma@pppl.gov)

(b) North Carolina State University, Raleigh, NC (nlsponse@ncsu.edu, kstapel@ncsu.edu)

(c) University of Michigan, MI (rzpinsky@umich.edu, JEFOSTER@umich.edu)

(d) Drexel University, Philadelphia, PA (js4932@drexel.edu, van54@drexel.edu)

(e) University of Arkansas, Fayetteville, AR (mc138@uark.edu)

Plasma in contact with liquid and solid materials is subject to feedback that affects plasma properties and propagation. Recent PCRF projects ranging from discharges in gas bubbles to gas and polymer conversion to biological applications, highlight the ubiquitous nature of these interactions.

For example, solution conductivity effects discharge evolution in water solutions with argon bubbles on different time scales. For a sharp electrode tip ( $25 \pm 10 \mu\text{m}$ ) and a short voltage rise time ( $dV/dt < 4 \text{ kV/ns}$ ), electrostriction effects dominate in deionized water and discharge initiates in the water at the tip of the anode. The discharge in the water rapidly extends ( $\sim 10^4 \text{ m/s}$ ) to the apex of the bubble and light emitted from inside the bubble begins to form (Figure 1) [1, 2]. For the same voltage pulse at higher conductivity ( $1.6 \text{ mS/cm}$ ) electric breakdown is observed only when the gas bubble comes into direct contact with the electrode and multiple emission nodes were observed at different timescales (Figure 2) [2]. At high conductivities and longer time scales, the liquid assumes the role of a poorly conducting electrode affecting the discharge formation and propagation in the water/gas system.

The properties of liquid substrates affect the circuit properties of non-thermal plasma treatment systems and hence the power delivered to biological substrates as shown by observations of cell suspensions [3 and S. Gershman poster, PICI, 2023]. Interactions with porous silica catalyst in plasma assisted ammonia synthesis and plasma de-polymerization of common plastic are also discussed [4, 5]

### References

- [1] N. L Sponsel et al J. Vac. Sci. Technol. A 40, 063002 (2022)
- [2] N. L Sponsel et al J. Phys. D: Appl. Phys. 56 505202 (2023)
- [3] J. Sutter et al Plasma 6(3), 577-591 (2023)
- [4] S. Gershman, et al. Plasma Chem Plasma Process 42, 731–757 (2022).
- [5] R. Walker et al Plasma Process and Polym 2023 – in review

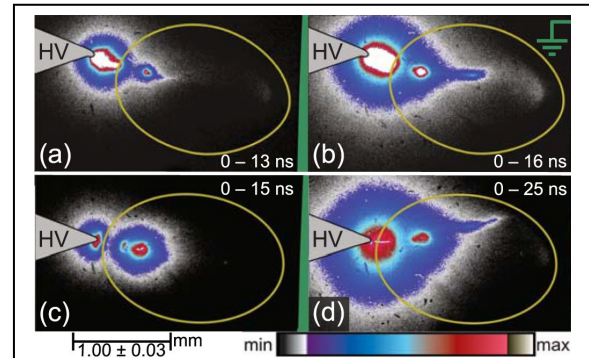


Figure 1 - Ionization wave propagation for an Ar gas bubble in deionized water for pin-to-rod electrodes.  $V_{\text{peak}} = 22 \text{ kV}$ ,  $t_{\text{rise}} = 7 \text{ ns}$ ,  $d = 2 \text{ mm}$  gap,  $r_{\text{tip}} = 25 \mu\text{m}$ ,  $d_{\text{bub}} = 1.7 \text{ mm}$ , water gap (a, b) –  $270 \mu\text{m}$ , (c, d) –  $70 \mu\text{m}$ .

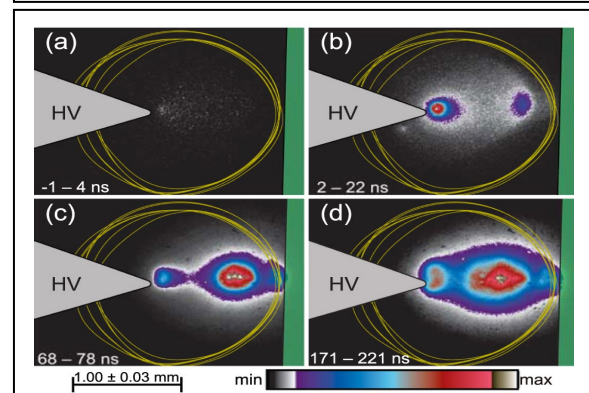


Figure 2 - (a) Diffuse discharge across the bubble before  $V_{\text{peak}}$  is reached, (b) corona-like discharge at the electrode during voltage fall; (c, d) discharge bridging and expanding during subsequent voltage oscillations.  $\sigma = 1.6 \text{ mS/cm}$ ,  $d = 1.04 \text{ mm}$  gap,  $d_{\text{bub}} = 1.75 \text{ mm}$ .

## [II-3] Dielectric Permittivity of Cell Membranes in a Physiological Solution

### Interacting with Low-Temperature Plasma

Mikhail N. Shneider<sup>a</sup> and Mikhail Pekker<sup>b</sup>

(a) Princeton University, Princeton NJ 08544 (m.n.shneider@gmail.com)

(b) Retired (pekkerm@gmail.com)

As was shown in [1], the interaction of non-equilibrium plasma with a physiological solution changes the ionic composition of the solution and, consequently, the drop of osmotic pressure across the cell membranes. In [2], it was supposed that the displacement of water from membranes and, consequently, the change in their dielectric constant, are different in healthy and cancer cells due to a noticeable difference in the mechanical properties of these cells.

Considering the water contained in the lipid membrane as an impurity with a relative volume, to estimate the effective permittivity of the membrane  $\varepsilon_m$ , it is convenient to use the simplest approximate Rayleigh formula for the permittivity of two substances, one of which is continuous, and the second is uniformly distributed small droplets of the impurity substance [3]:

$$\varepsilon_m = \varepsilon_e \left( 1 + f \frac{3(\varepsilon_i - \varepsilon_e)}{\varepsilon_i + 2\varepsilon_e - f(\varepsilon_i - \varepsilon_e)} \right). \quad (1)$$

Here,  $\varepsilon_m$ ,  $\varepsilon_e$ , and  $\varepsilon_i$  are the respective permittivities of the mixture, the main medium, and the impurity droplets. Substituting in (1) the values of the permittivity  $\varepsilon_e = 2$  for a dehydrated phospholipid membrane and  $\varepsilon_i = \varepsilon_w = 81$  for water, we obtain the dependence of the membrane permittivity  $\varepsilon_m$  according to the volume fraction of water  $f$  (see Fig.1).

We assume that the surface charge on the membrane and its thickness changes little when the solution interacts with the plasma, then  $U_m \sim 1/\varepsilon_m$ . The water content dependence of the ratio  $U_m(f)/U_m(f=0)$  is shown in Fig.1.

In our opinion, the saturation of the membrane with water explains the marked decrease in resting potential in the nervous tissue observed in [4] and, accordingly, the decrease in the threshold of sodium channel opening (threshold of action potential excitation).

M.N.S. acknowledges partial support by the Princeton Collaborative Research Facility (PCRF) supported by the U.S. DOE under contract No. DE-AC02-09CH11466.

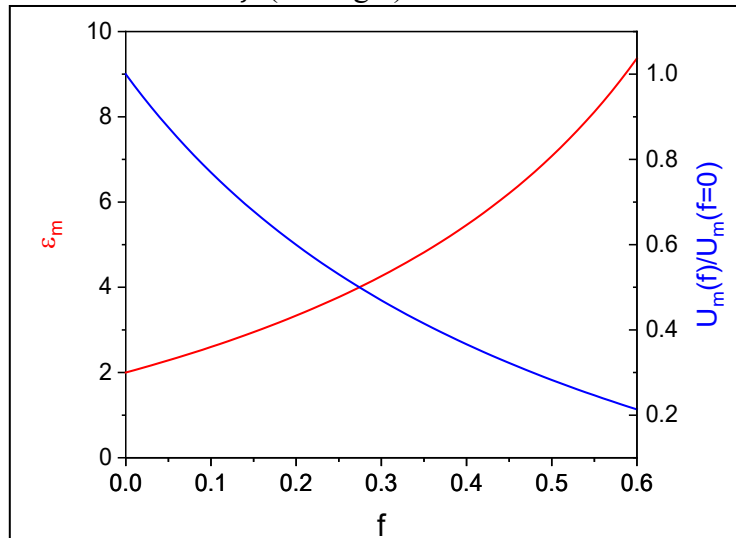


Figure 1 – Dependences of the effective dielectric constant  $\varepsilon_m$ , and the relative potential difference across the membrane on the water content  $f$ . for  $\varepsilon_e=2$  and  $\varepsilon_i=\varepsilon_w=81$  at a fixed value of the surface charge and thickness.

### References

- [1] M.N. Shneider, M. Pekker, J. Appl. Phys. **123**, 204701 (2018).
- [2] M.N. Shneider, M. Pekker, Plasma Research Express, **1**, 045001 (2019).
- [3] A. Sihvola, Subsurface Sensing Technologies and Applications, **1** (4), 393 (2000).
- [4] B. Hille, A.M. Woodhull, B.I. Shapiro, Phil. Trans. R. Soc. London. B. **270**, 301 (1975).

## [II-4] Modeling of Modern Plasma Processing Reactors: Plasma Physics and Surface Chemistry

Igor D. Kaganovich, Dmytro Sydorenko, Yuri Barsukov, Stephane Ethier, Alexander V. Khrabrov, Andrew Tasman Powis, Willca Villafana, Sierra Jubin, Salman Sarwar

Princeton Plasma Physics Laboratory (ikaganov@pppl.gov)

Fabrication of nanoelectronics devices requires processing of features with sub-10 nm dimensions, with some structures in logic and memory devices being less than 40 atoms wide. To achieve these goals, a multidisciplinary approach is needed that integrates and advances our understanding and predictability of complex processes involving plasma chemistry, plasma-surface interactions, and surface science. Correspondingly, we have developed modeling capabilities in all these areas. This includes particle-in-cell codes to model low pressure discharges and quantum chemistry modeling of volume and surface chemistries and using ML/AI techniques to develop reaction pathways.

For plasma processing, there is a need to simulate large plasma devices via kinetic means, because the Electron Velocity Distribution Function in these devices is non-Maxwellian and therefore a fluid treatment is insufficient to accurately capture the physics. The method of choice for many fully kinetic simulations has been the particle-in-cell (PIC) technique due to relatively ease of implementation of the method and that it can be parallelized effectively over many processors and accelerated on GPUs. However, PIC codes that use standard explicit schemes are constrained by the requirement to resolve the short length and time scales associated with the plasma Debye radius and plasma frequency respectively. This makes it extremely challenging to perform long time 2D PIC simulations for large plasma devices. For this reason, many 2D kinetic simulations of plasmas have been limited to small or artificially scaled systems. Energy conserving or implicit methods must be used to remove these limitations. Effects of numerical noise in simulations using PIC code need to be analyzed and taken into account.

At PPPL we have developed two codes EDIPIC-2D and LTP-PIC-3D. EDIPIC-2D is an open-source code that includes features for simulations of practical devices (e.g., we incorporated complex geometry and complex boundary conditions) and has been used for modeling of several plasma devices. LTP-PIC-3D is a high-performance scalable PIC code which incorporates best programming practices and multi-level parallelism. This code was upgraded to operate efficiently on the latest CPU/GPU architectures for additional performance improvements. Simulation results are benchmarked against other codes, and where available, analytical theory. These codes have been applied to study plasma processing applications, such as capacitively coupled plasmas, electron beam produced plasmas, inductively coupled, hollow cathodes [1].

To model surface processes we used a combination of quantum chemistry methods and molecular dynamics. For analysis of chemical reaction pathways, we employed direct sensitivity analysis and an uncertainty-aware strategy for plasma mechanism reduction with directed weighted graphs.

Work being performed within the Princeton Collaborative Research Facility (PCRF) is supported by the US Department of Energy through contract DE-AC02-09CH11466. The code development was funded by the PPPL LDRD program and CRADA collaborations with Applied Materials. Resources of the National Energy Research Scientific Computing Center (NERSC) were used for high performance computation.

### References

[2] see latest Refs. <https://orcid.org/my-orcid?orcid=0000-0003-0653-5682>.

## [II-5] Modeling Low-Temperature Plasmas with EDIPIC-2D: An Open-Source and Versatile Particle-In-Cell Code

Willca Villafana<sup>a</sup>, Dmytro Sydorenko<sup>b</sup>, Alexander V. Khrabrov<sup>a</sup>, Igor D. Kaganovich<sup>a</sup>, Sierra Jubin<sup>a</sup>, Andrew Tasman Powis<sup>a</sup>, Salman Sarwar<sup>a</sup>, Stéphane Ethier<sup>a</sup>, Shahid Rauf<sup>c</sup>

(a) Princeton Plasma Physics Laboratory (wvillafa@pppl.gov)

(b) University of Alberta

(c) Applied Materials Inc

Low-temperature plasmas find extensive use across diverse industrial applications, frequently exhibiting kinetic phenomena. Investigating these non-equilibrium behaviors necessitates the utilization of a Particle-In-Cell (PIC) technique. In this context, we showcase recent applications of this approach along with new developments using the open-source 2D PIC code, EDIPIC [1,2,3,4,5].

Within the Princeton Collaborative Low-Temperature Plasma Research Facility, EDIPIC-2D is being used to investigate a wide variety of systems having applications in space propulsion, plasma processing, and the semiconductor industry.

In this context, we provide illustrations of modeling an Electron Cyclotron Resonance (ECR) plasma cathode, a hollow cathode, and Langmuir probes, comparing the results with experimental observations. We also detail the code implementations necessary to facilitate these simulations, including the utilization of cylindrical coordinates and external circuits.

Furthermore, recent efforts on modeling capabilities on Capacitively and Inductively Coupled Plasma Discharges, relevant to the semiconductor industry are reported. In particular, the use of Darwin [6] in a PIC code is for the first time described.

Finally, theoretical considerations regarding the numerical noise in PIC simulations are detailed [7].

Work being performed within the Princeton Collaborative Research Facility (PCRF) is supported by the US Department of Energy through contract DE-AC02-09CH11466. The code development was funded by the PPPL LDRD program and collaborations with Applied Materials by CRADA.

### References

[1] <https://github.com/PrincetonUniversity/EDIPIC-2D>

[2] S. Rauf, D. Sydorenko, S. Jubin, W. Villafana, S. Ethier, A. Khrabrov, and I. Kaganovich, “Particle-in-cell modeling of electron beam generated plasma,” *Plasma Sources Sci. Technol.* 32(5), 055009 (2023).

[3] S. Simha, S. Sharma, A. Khrabrov, I. Kaganovich, J. Poggie, and S. Macheret, “Kinetic simulation of a 50 mTorr capacitively coupled argon discharge over a range of frequencies and comparison to experiments,” *Physics of Plasmas* 30(8), 083509 (2023).

[4] H. M. Sun, J. Chen, I. D. Kaganovich, A. Khrabrov, and D. Sydorenko, *Phys. Rev. Lett.* **129**, 125001 (2022).

[5] H. M. Sun, J. Chen, I. D. Kaganovich, A. Khrabrov, and D. Sydorenko, *Phys. Rev. E* **106**, 035203 (2022).

[6] Gibbons M. R. and D. W. Hewett, “The Darwin Direct Implicit Particle-in-Cell (DADIPIC) Method for Simulation of Low Frequency Plasma Phenomena”, *J. Comput. Phys.* 120, 231 (1995).

[7] S. Jubin et al. “Numerical thermalization in 2D PIC simulations: Practical estimates for low temperature plasma simulations”, submitted at *Physics of Plasmas* (2023).

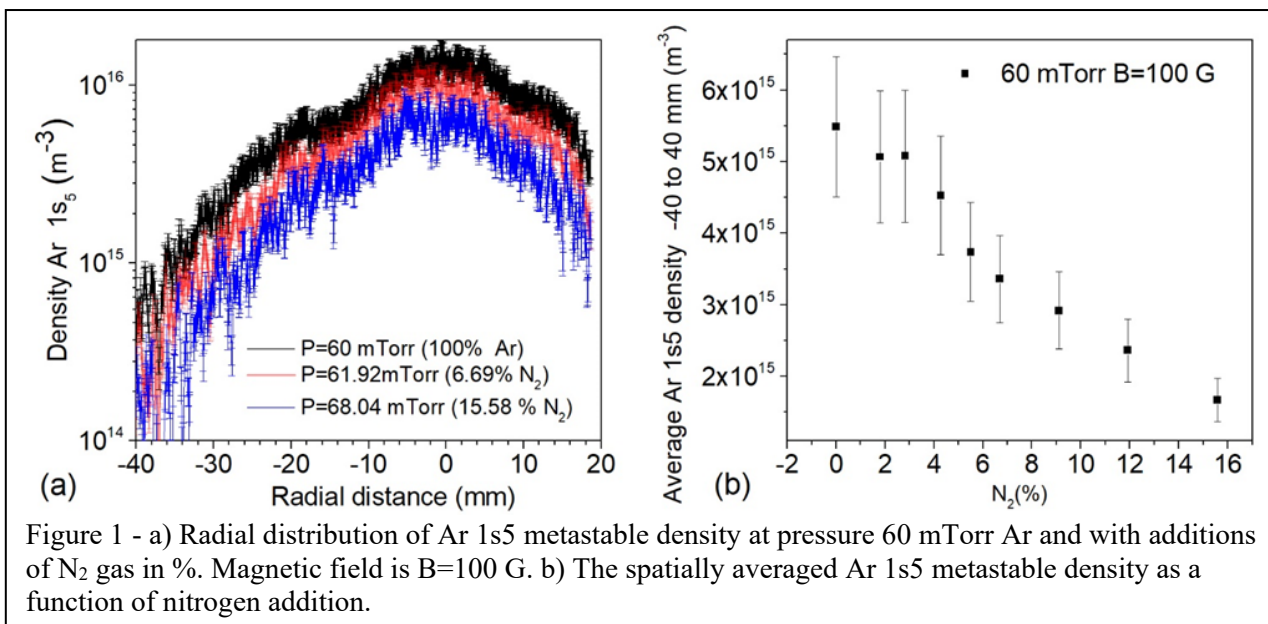
## [II-6] Measurement and Reduction of Ar Metastable Densities by Nitrogen Admixing in Electron Beam-generated Plasmas

Shurik Yatom<sup>a</sup>, Nirbhav Chopra<sup>a</sup>, Santosh Kondeti<sup>a</sup>, Tzvetelina B. Petrova<sup>b</sup>, Yevgeny Raitses<sup>a</sup>, David R. Boris<sup>b</sup>, Michael J. Johnson<sup>b</sup> and Scott G. Walton<sup>b</sup>

(a) Princeton Plasma Physics Laboratory, Princeton, NJ 08450 (syatom@pppl.gov)

(b) Naval Research Laboratory, Plasma Physics Division, Washington DC, 20375

Electron beam (e-beam) generated plasmas are useful for material processing applications such as deposition and etching because the plasmas deliver a large fluence of very low energy of ions to surfaces. Metastable species produced in the beam-region can also transport significant energy to the plasma periphery and surfaces. In this work, we have investigated the spatially resolved density of metastable Ar 1s<sub>5</sub> species produced in an Ar and Ar/N<sub>2</sub> e-beam generated plasma at pressures of 60–67 mTorr using laser-induced fluorescence (LIF). The experiments provide the first direct measure of absolute density and reduction of Ar 1s<sub>5</sub> in an e-beam generated plasma when argon is diluted with nitrogen. These results are consistent with previous predictions of numerical modeling and measurements using optical emission spectroscopy. The present spatially resolved LIF measurements directly quantify the reduction of Ar 1s<sub>5</sub> in the e-beam generated plasma by nitrogen admixing. This reduction was observed in the region of the electron beam and in the plasma periphery, where substrates are usually placed. For example, up to a threefold reduction of the density of Ar 1s<sub>5</sub> was measured when the argon background was diluted with 15.5% nitrogen at pressure of 60 mTorr. Ar 1s<sub>5</sub> reduction is attributed to excitation exchange with nitrogen molecules as well as the cooling of plasma electrons via inelastic collisions with nitrogen molecules.



This work is supported by the Princeton Collaborative Research Facility (PCRF), which is supported by the U.S. Department of Energy (DOE) under Contract No. DE-AC02-09CH11466 and the Naval Research Laboratory Base Program.



# [III-1] Ns Pulse and Hybrid Ns Pulse / RF Discharges for Plasma Catalysis and Plasma Fuel Reforming

Igor V. Adamovich

Department of Mechanical and Aerospace Engineering  
The Ohio State University, Columbus, OH 43210, USA  
(adamovich.1@osu.edu)

Ammonia generation during the plasma-catalytic synthesis in a “hybrid” ns pulse / RF discharge sustained at a high pulse repetition rate in a heated plasma flow reactor [1] is studied by Fourier Transform Infrared Spectroscopy (FTIR). The ns pulse discharge is operated in burst mode, up to 300 pulses per burst at a pulse repetition rate of 10 kHz, and burst repetition rate of 10 Hz. During each pulse burst, additional energy is coupled to the plasma by the sub-breakdown 13.56 MHz RF bursts, generated between the ns pulses. The RF peak voltage is kept sufficiently low, to prevent additional ionization, dissociation, and electronic excitation of the N<sub>2</sub>-H<sub>2</sub> mixture in the reactor. The burst mode operation is used to increase the peak N<sub>2</sub> vibrational temperature, enhanced by the vibration-vibration (V-V) exchange, as was done in our previous work [2]. The measurements are made in a 10% H<sub>2</sub>-N<sub>2</sub> mixture, at the pressure of P=190 Torr and temperature of T=573 K, with Ni-, Co-, and Ru-Al<sub>2</sub>O<sub>3</sub> catalyst pellets placed in the reactor. The results quantify the effect of N<sub>2</sub> vibrational excitation on the ammonia yield, compared to the mechanism driven by the reactions of the plasma-generated N and H atoms on the catalyst surface.

Kinetics of the plasma-catalytic CH<sub>4</sub>-CO<sub>2</sub> reforming and CH<sub>4</sub>-O<sub>2</sub> oxidative coupling to higher hydrocarbons are studied in a fused silica six-arm cross plasma flow reactor with optical access, similar to that used in our previous work [3]. The reacting mixture in Ar buffer is excited by a plane-to-plane ns pulse discharge, with the cathode heated by a button heater up to T=1000 K, and a receptacle with a catalyst disk (Ni-, Co-, Fe, or Cu-Al<sub>2</sub>O<sub>3</sub>) placed on the top of the heater. The reaction products are analyzed by an FTIR spectrometer. A complementary apparatus, a heated plasma flow reactor coupled with a supersonic flow expansion has been developed for studies of the plasma chemical conversion of hydrocarbon fuels, at fuel-lean conditions. The fuel-oxidizer flow (0.1-0.2% CH<sub>4</sub> and 1-2% O<sub>2</sub> in Ar buffer) is heated in a thermal energy storage system, a stainless steel pipe filled with alumina ceramic beads and placed in a tube furnace heated to T<sub>0</sub>=600-900 K. Downstream, the heated flow is excited by a 100 kHz ns pulse discharge in the plasma section, at P<sub>0</sub>=0.5-1.0 atm, to generate the radical species. The flow is subsequently expanded through a converging-diverging nozzle into a Mach 4 supersonic test section. The rapid supersonic expansion freezes the chemical reactions, such that the products can be analyzed spectroscopically, at the low temperature and pressure in the supersonic section. The concentrations of the reaction products are predicted by kinetic modeling and measured by mid-IR Quantum Cascade Laser Absorption Spectroscopy and Cavity Ring Down Spectroscopy (in progress). For this, the diagnostic section is equipped with arms with optical access windows or high-reflectivity mirrors. The results isolate the dominant reaction pathways controlling the methane conversion branching, between C<sub>2+</sub> species formation and oxidation to CO.

## References

1. X. Yang et al, Plasma Sources Sci. Technol. **32**, 064003 (2023).
2. I. Gulko et al, Plasma Sources Sci. Technol. **29**, 104002 (2020).
3. D. van den Bekerom et al, Plasma Sources Sci. Technol. **31**, 095018 (2022).

## [III-2] Plasma Assisted Combustion and Control of Plasma Dynamics for Manufacturing

Yiguang Ju

Department of Mechanical and Aerospace Engineering, Princeton University, Princeton, NJ 08544, USA  
(yju@princeton.edu)

Pressure gain combustion and ammonia combustion are important for carbon reduction and the increase of energy conversion efficiency. Moreover, plasma assisted manufacturing using renewable electricity provides a great opportunity to further increase energy efficiency and mitigate carbon emissions from fossil energy. However, understanding the mechanism of plasma assisted combustion and emissions remains to be challenging. In addition, novel methods to control plasma properties and reactivity for electrified manufacturing need to be developed.

In this study, we examined low temperature chemistry (LTC) enhancement by nanosecond (ns) dielectric barrier discharge (ns-DBD) plasma on a dimethyl ether (DME)/oxygen (O<sub>2</sub>)/Argon (Ar) premixture for deflagration to detonation (DDT) in a micro channel [1]. It was found that non-equilibrium plasma generated active species and enhanced LTC and DDT. In situ laser diagnostics and computational modeling are conducted to examine formaldehyde (CH<sub>2</sub>O) laser induced fluorescence (LIF) via plasma enhanced LTC. The results show that with an appropriate number of discharge pulses, plasma enhanced the LTC of DME and increased CH<sub>2</sub>O formation and low temperature ignition, leading to accelerated DDT. Therefore, the present study clearly demonstrated that plasma enhanced LTC plays an important role in accelerating DDT.

In-situ diagnostics and plasma modeling were also conducted to understand the mechanism of plasma assisted ammonia oxidation and non-equilibrium NO<sub>x</sub>/N<sub>2</sub>O reaction pathways and to develop an experimentally validated predictive model [2]. It is found that the nonequilibrium plasma controls the NO<sub>x</sub> formation by supplying O/H/N atoms via electron-impact dissociation and collisional quenching of excited species. The N<sub>2</sub>O formation follows a two-step mechanism, where electron-impact reactions first provide amine radicals which then further react with NO<sub>x</sub> to generate N<sub>2</sub>O.

To control plasma properties and reactivity, we studied the effect of ferroelectric PZT (Pb(Zr<sub>x</sub>Ti<sub>(1-x)</sub>)O<sub>3</sub>) barrier electrodes on electric field, surface charge, and afterglow discharge. The results showed that the ferroelectric PZT manifests spontaneous electric polarization to enable an increase of surface charge by two orders of magnitude compared to dielectric barrier discharge an alumina electrode. In situ measurements of electric field revealed that the fast electric polarization of ferroelectric materials increases the electric field and almost doubled the breakdown electric field compared to the static breakdown electric field. Moreover, it is shown that ferroelectric materials dramatically extended the afterglow time and increased plasma instability.

By using carbon enhanced electrode materials, we developed a plasma setup consisting of a pair of carbon-fiber-tip enhanced electrodes that enable the generation of a uniform, ultrahigh-temperature and stable plasma (up to 8000 K) at atmospheric pressure via a combination of vertically-oriented long and short carbon fibers [3]. The long carbon fibers help initiate the plasma through micro spark discharge at a low breakdown voltage while the short carbon fibers expand the discharge into a volumetric and stable ultrahigh temperature plasma. As a proof-of-concept, we utilized this plasma process to synthesize various extreme materials in seconds, including ultrahigh temperature ceramics (e.g., Hf(C,N)) and refractory metal alloys.

### References

- [1] M. Vorenkamp, S. Steinmetz, X. Mao, Z. Shi, A. Starikovskiy, Y. Ju and C. Klierer, *AIAA Journal*, 2023, p.1-7.
- [2] H. Zhong, X. Mao, N. Liu, Z. Wang, T. Ombrello, Y. Ju, *Combustion & Flame*, 256, p.112948.
- [3] H Xie et al., *A Stable Atmospheric-Pressure Plasma for Extreme-Temperature Synthesis*, *Nature*, 2023, in press.

### [III-3] Plasma-Assisted Catalytic Synthesis of NH<sub>3</sub>

Bruce E. Koel

Department of Chemical and Biological Engineering, Princeton University, Princeton, NJ, USA  
(bkoel@princeton.edu)

Our recent research continues to address fundamental issues related to plasma-assisted catalytic synthesis of NH<sub>3</sub>. These include understanding the dominant reaction pathways that produce the ammonia product, addressing the low energy yield and how one can try to improve it, determining the effects of the catalyst support particles, and probing how the catalyst surface is modified by the plasma. This talk will report on and will discuss several aspects of our work and results for the synthesis of ammonia from N<sub>2</sub> and H<sub>2</sub> in dielectric barrier discharge (DBD) reactors using AC and nanosecond pulsed discharges and packed with catalyst support particles or supported metal catalysts in the discharge zone. In addition, development of reactors for in situ and operando characterization of catalysts and surface species in the presence of plasma discharges will be discussed.

Previously, using a zero-dimensional plasma kinetic model we showed that under the conditions of our experiments, ammonia synthesis proceeds principally by the formation of reactive radicals in the gas phase, which then adsorb and participate in Eley–Rideal (E–R) reactions on both the metal and support material surfaces.[1] Measurements using an electron-ionization molecular beam mass spectrometer (MBMS) connected directly to a plasma reactor detected NNH radicals in the gas phase, indicating that this reactive species should be considered further in the reaction kinetics.[2]

Experiments on the effect of catalyst support particle porosity on the conversion of NH<sub>3</sub> synthesis used two different particles of the same diameter (~1.5 mm) porous silica (SiO<sub>2</sub>) (pore size: 8 nm) and smooth, nonporous soda lime glass beads.[3] Penetration of the plasma into the pores of the particles was unlikely, however reactive species generated in the plasma outside the particles could diffuse into the pores. The N<sub>2</sub> conversion and energy yield of NH<sub>3</sub> increased with applied voltage for both particle types. These values were consistently higher when using the SiO<sub>2</sub> beads, but the effect of these two different supports on the physical properties of the discharge was negligible. High resolution optical emission spectra revealed that the concentrations of N<sub>2</sub><sup>+</sup>, atomic N, and atomic H (H<sub>α</sub>, H<sub>β</sub>) in the plasma discharge were lower with the porous SiO<sub>2</sub> beads, indicating that these active species participate in heterogeneous reactions at support particle surfaces and that the larger surface area presented by the porous particles led to higher rates of depletion of these intermediates and a higher rate of ammonia synthesis. This research has now been extended to synthetically-controlled pore sizes and surface areas of ordered mesoporous materials (OMMs).

Kinetic modeling analysis of Ar addition to atmospheric pressure N<sub>2</sub>-H<sub>2</sub> plasma revealed new insights into the role of Ar in N radical production, H interactions, and NH<sub>3</sub> dissociation.[4] We also investigated the formation of nickel nitride on a Ni catalyst for ammonia synthesis using ex-situ surface characterization. Updates will be provided on our development of reactors for in situ and operando characterization of catalysts and surface species in the presence of plasma discharges using DRIFTS, ATR-FTIR, ESEM, and XAS. Results from investigations of the dynamics of supported Pt catalysts during CO oxidation under a DBD plasma jet using operando DRIFTS will be discussed.

#### References

- [1] Z. Chen, B.E. Koel, S. Sundaresan, J. Physics D: Appl. Phys. **55**, 055202 (2022).
- [2] H. Zhao, G. Song, Z. Chen, X. Yang, C. Yan, S. Abe, Y. Ju, S. Sundaresan, B.E. Koel, ACS Energy Lett. **7**, 53 (2022).
- [3] Z. Chen, S. Jaiswal, A. Diallo, S. Sundaresan, B.E. Koel, J. Phys. Chem. A **126**, 8741 (2022).
- [4] Z. Lin, S. Abe, Z. Chen, S. Jaiswal, B.E. Koel, J. Phys. Chem. A, submitted (2023). (arXiv:2310.03307 [physics.plasm-ph])

## [IV-1] Sandia National Laboratories Plasma Research Facility (PRF)

Shane M. Sickafoose, Brian Z. Bentz, Jonathan Frank, Grant Gorman, Nils Hansen, Matthew M. Hopkins, Christopher Kliewer, Sebastian Pfaff, Lucas Beving

Sandia National Laboratories (smsicka@sandia.gov)

This presentation will provide an update on the activities and structure of Sandia's Low-Temperature Plasma Research Facility (PRF), funded by DOE Office of Science, Office of Fusion Energy Sciences, General Plasma Science. The PRF is a resource available to anyone in the International Low-Temperature Plasma (LTP) community to access the advanced resources available at Sandia (not restricted to the US collaborators). Capabilities are accessed through an annual proposal process which opens immediately following the GEC conference. Available resources include both experimental and modeling capabilities that represent many person-years and millions of dollars of development through DOE and other investments (some for decades). Examples of real-time diagnostics include Laser-Induced Fluorescence (LIF), Laser-Collision-Induced Fluorescence (LCIF), Photofragmentation LIF (PF-LIF), and Molecular Beam Mass Spectrometry (MBMS). Advanced modeling capabilities are also available, including state-of-the-art PIC-DSMC modeling tools along with access to Sandia's high-performance computing (HPC) capabilities (many 10K's of cores).

The presentation will include an overview of expertise and capabilities available, an explanation of the proposal process, and a summary of select recent projects.

This work used the capabilities of the SNL Plasma Research Facility, supported by DOE SC FES. SNL is managed and operated by NTESS under DOE NNSA contract DE-NA0003525.

## [IV-2] Understanding Sheath Expansion in Flowing Plasmas

Lucas Beving<sup>a</sup>, Matthew Hopkins<sup>a</sup> Greg Severn<sup>b</sup>

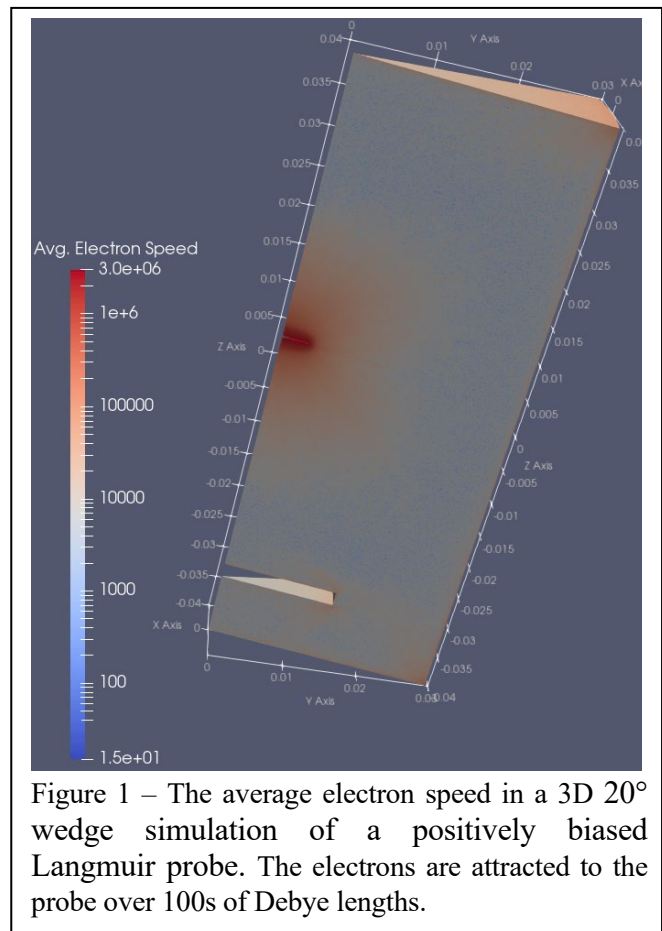
(a) Sandia National Laboratories (lpbevin@sandia.gov)

(b) University of San Diego (severn@sandiego.edu)

Sheaths are the non-neutral regions that form on probes, walls, and even dust immersed in a quasineutral bulk plasma. Understanding the specific properties of sheaths is critical to plasma applications, like etching, or even basic diagnostics like Langmuir probes. It is currently understood that properties of the sheath, like the width, are determined by gas pressure, electron temperature and density, and the potential applied to the non-plasma side of the sheath. Here, we describe the development of 2D and 3D particle-in-cell simulations that will characterize how a flowing plasma, directed at the sheath, affects sheath expansion.

In the context of Langmuir probes, a model for the expansion of the sheath is necessary to properly analyze the signal from the probe, since the sheath width determines the effective collection area of the probe. However, the current model of sheath expansion does not account for the effects of a flowing plasma, like those found in the presheath. Furthermore, recent experiments have indicated that the current model of sheath expansion fails in the presheath, where there is significant plasma flow [1]. Specifically, the current model predicts an electron density that is significantly larger than the ion density! Based on these results, we will leverage simulations of a Langmuir probe at different potentials near a biased electrode to correct the current model. Specifically, the simulations will allow us to determine the effective collection area of the probe immersed in a plasma flow.

However, simulations of a Langmuir probe sweep pose several difficulties. For instance, the area of the simulated probe must be much smaller the wall if it is to be biased above the plasma potential and so simulate the electron saturation regime [2]. This is easily satisfied in 3D simulations, though they are very expensive: a simulation of a 3D 20° cylindrical wedge is shown in Fig. 1 and required nearly a week on 2560 cores and produce several TB of data. Alternatively, simulating the same probe in 2D requires a much larger area than in 3D to maintain a probe that is small enough compared to the wall. Ultimately, 2D simulations are more computationally efficient even with the larger domain.



This work used the capabilities of the SNL Plasma Research Facility, supported by DOE SC FES. SNL is managed and operated by NTESS under DOE NNSA contract DE-NA0003525.

### References

[1] P. Li et al, Plasma Sources Sci. Technol. **29** 025015 (2020).

[2] S. Baalrud et al, Plasma Sources Sci. Technol. **29** 053001 (2020).

## [IV-3] Nonlinear Optical Diagnostics Laboratory for Low-Temperature Plasma-Assisted Chemistry

Christopher J. Kliewer<sup>a</sup>, Yiguang Ju<sup>b</sup>, Madeline Vorenkamp<sup>b</sup>, Timothy Y. Chen<sup>c</sup>

(a) Sandia National Laboratories, Livermore, California, USA (cjkliew@sandia.gov)

(b) Princeton University, Princeton, New Jersey, USA (yju@princeton.edu)

(c) Applied Materials, Santa Clara, California, USA (Timothy\_chen@amat.com)

Low temperature plasmas (LTP) provide opportunities for enhancing high-value energy conversion processes in both energy efficiency and chemical selectivity. LTP technology is additionally a critical component of the semiconductor manufacturing process. Nonequilibrium distributions of electronic and molecular rovibronic excitations as well as active speciation in non-thermal equilibrium plasmas offer unique control over the outcome of chemical reactions and process optimization. While the understanding of low temperature plasma assisted chemistry is still emerging, clear benefits have already been demonstrated in such fields as plasma assisted catalysis and plasma assisted combustion. However, improved understanding of the underlying chemical kinetic mechanisms requires new capabilities in in-situ probing of plasma-chemistry interactions.

Ultrafast nonlinear spectroscopy methods provide incisive tools for probing the chemistry and dynamics of low-temperature plasma assisted chemistry. Figure 1 demonstrates a culmination of research in the past two years in which temperature, electric field, and formaldehyde concentrations were measured by fs/ps CARS, two-beam EFISH, and laser-induced fluorescence during the plasma-induced oxidation of dimethyl ether. The combined data allowed for a detailed comparison to numerical modeling.

In the previous year, our group has further developed a coherent one-dimensional fs/ps coherent Raman spectroscopy imaging approach for the detection of atomic species such as F, Cl, and O. Coherent transitions between spin-orbit split electronic levels are used to generate the coherent Raman signals. Detection limits and near-surface imaging capabilities were studied. The spatial distribution of these radicals is of critical importance to semi-conductor etch processes.

This work was supported by Sandia National Laboratories' Plasma Research Facility, funded by the U.S. Department of Energy Office of Fusion Energy Sciences. Sandia is managed and operated by NTESS under DOE NNSA contract DE-NA0003525.

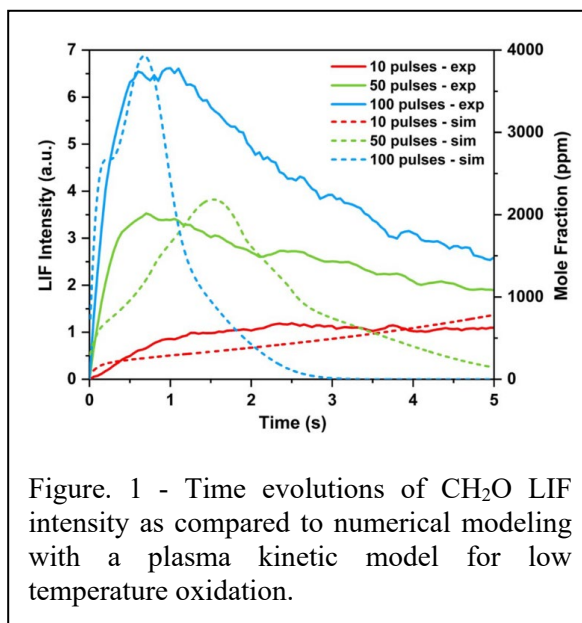


Figure. 1 - Time evolutions of CH<sub>2</sub>O LIF intensity as compared to numerical modeling with a plasma kinetic model for low temperature oxidation.

## [IV-4] Opportunities for Mass Spectrometry to Study Plasma-Assisted Chemical Transformations

Nils Hansen

Collaborative Plasma Research Facility, Sandia National Laboratories, Livermore, CA 94550 USA  
(nhansen@sandia.gov)

Mass spectrometry is a perfect analytical tool to study complex reaction networks as found in many environments and applications. Using this technique, unprecedentedly detailed chemical insights are generated as it allows for simultaneous and sensitive detection of all intermediates and products of the reaction network without prior knowledge of their identity. This presentation highlights the basic concepts of our mass spectrometry approaches to study the reaction networks of plasma-assisted chemical transformations that enable a transition to clean energy. The first part of the talk highlights chemical insights from molecular-beam mass spectrometry with single-photon and electron ionization into the accelerating effects of non-thermal plasma on ethylene combustion and ammonia decomposition and oxidation. The second part highlights time-dependent species measurements to gain chemical insights into plasma-assisted chemical looping combustion of simple hydrocarbons by CuO/NiO and plasma-assisted polymer upcycling using a low-temperature CO<sub>2</sub> plasma.

## [IV-5] Imaging of Methyl Radical and Hydrogen Peroxide in Plasmas by Photofragmentation Laser-Induced Fluorescence

Jonathan H. Frank<sup>a</sup>, Francesco di Sabatino<sup>a</sup>, Sebastian Pfaff<sup>a</sup>, Dirk van den Bekerom<sup>a</sup>, Ammar M. Alkhalifa<sup>b</sup>, Deanna A. Lacoste<sup>b</sup>, Maria J. Herrera Quesada<sup>c</sup>, Katharina Stapelmann<sup>c</sup>

- (a) Plasma Research Facility, Sandia National Laboratories (jhfrank@sandia.gov)  
(b) Clean Combustion Research Center, King Abdullah University of Science and Technology  
(deanna.lacoste@kaust.edu.sa)  
(c) Dept. of Nuclear Engineering, North Carolina State University (kstapel@ncsu.edu)

The methyl radical ( $\text{CH}_3$ ) and hydrogen peroxide ( $\text{H}_2\text{O}_2$ ) are key reactive species in plasma assisted processes such as combustion, catalysis, surface decontamination, and biomedical treatments. Imaging of  $\text{CH}_3$  and  $\text{H}_2\text{O}_2$  is challenging because they cannot be detected directly by laser-induced fluorescence. We present our recent developments in 2D imaging of these species in plasmas using photofragmentation laser-induced fluorescence (PF-LIF). The target molecule,  $\text{CH}_3$  or  $\text{H}_2\text{O}_2$ , is photodissociated by a UV pump laser to produce  $\text{CH}$  or  $\text{OH}$  fragments, respectively. These photofragments are then detected with LIF imaging using an overlapping probe laser beam for LIF excitation. For  $\text{CH}_3$  PF-LIF measurements, transitions in the B-X band of  $\text{CH}$  are excited, and fluorescence from the overlapping A-X(0,0), A-X(1,1), and B-X(0,1) bands is detected with the A-state populated by collisional B-A electronic energy transfer. For  $\text{H}_2\text{O}_2$  PF-LIF measurements, the probe laser excites transitions in the A-X(1,0) band of  $\text{OH}$ , and fluorescence is detected from A-X(1,1) and (0,0) bands. These non-resonant detection schemes enable interrogation near surfaces.

We demonstrate PF-LIF imaging measurements of  $\text{CH}_3$  in a repetitively pulsed glow discharge across a lean premixed methane-air flame to provide insights into the chemical effects of the plasma on enhanced flame stabilization (Fig. 1a). We also used PF-LIF to measure the distribution of  $\text{H}_2\text{O}_2$  mole fraction in the effluent of the RF driven COST microplasma reference jet issuing into nitrogen and air atmospheres (Fig. 1b). We are investigating interactions of the jet with surfaces and exploring opportunities for detection of  $\text{HO}_2$ , another key reactive species in water-laden plasmas. Detailed studies of these key reactive species in canonical low-temperature plasma systems are needed to provide fundamental insights into plasma chemistry and data sets that challenge plasma modeling.

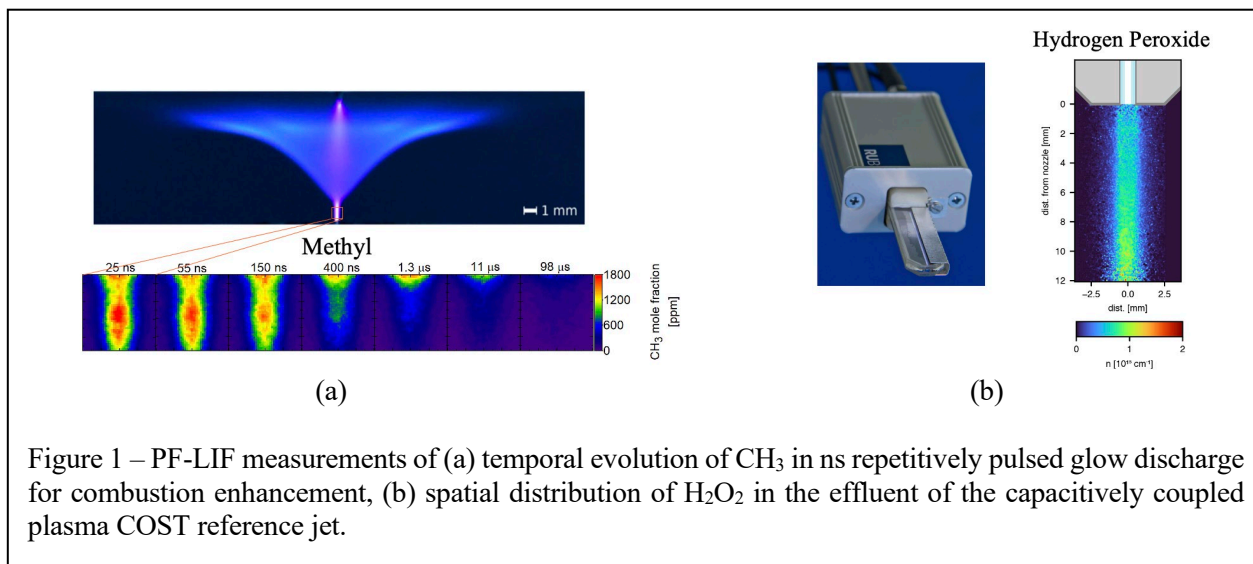


Figure 1 – PF-LIF measurements of (a) temporal evolution of  $\text{CH}_3$  in ns repetitively pulsed glow discharge for combustion enhancement, (b) spatial distribution of  $\text{H}_2\text{O}_2$  in the effluent of the capacitively coupled plasma COST reference jet.



# [V-1] Plasma/catalyst Contributions for N<sub>2</sub> Oxidation and Dry Reforming of Methane

Michael Hinshelwood and Gottlieb S. Oehrlein

Department of Materials Science and Engineering and the Institute for Research in Electronics and Applied Physics, University of Maryland, College Park, MD 20742, USA (oehrlein@umd.edu)

The coupling of catalysts and atmospheric-pressure plasma has the potential to improve the efficiency of nitrogen fixation reactions such as nitrogen oxidation. Understanding the changes that the catalyst undergoes during plasma exposure is key to improving performance. In this study, exposure of a Pt-Al<sub>2</sub>O<sub>3</sub> powder catalyst to an Ar/N<sub>2</sub>/O<sub>2</sub> non-equilibrium atmospheric-pressure plasma-jet was investigated. Products downstream of the interaction were analyzed with Fourier transform infrared spectroscopy while surface species were analyzed with diffuse reflectance infrared Fourier transform spectroscopy (DRIFTS). To separate the effects of plasma and catalyst, the catalyst temperature was ramped cyclically between 100 °C and 350 °C during plasma exposure.

Results reveal both long-lasting and transient changes taking place on the catalyst surface during plasma exposure. Long-lasting changes arise from the filling of nitrate sites on the Al<sub>2</sub>O<sub>3</sub> support. Subsequent thermal cycles demonstrate a repeatable hysteresis pattern of NO and NO<sub>2</sub> production. The plasma acts primarily as a source of NO and O<sub>3</sub> reactants while the catalyst enables adsorption of these reactants at low temperatures and their subsequent reaction at high temperatures to form NO<sub>2</sub>. The catalyst also promotes oxidation of incoming NO at high temperatures where oxidants in the plasma would otherwise be destroyed. Thus, two NO oxidation pathways occur during thermal cycling: one via surface reactants adsorbed at low temperature, and the other by reactants arriving at the surface at high temperature.

Fig. 1 shows the relationship between NO<sub>2</sub> and NO downstream products during thermal cycling. With high-power O<sub>2</sub>-rich plasma, NO<sub>2</sub> production rate increase is almost vertical with respect to NO production rate during initial heating due to stored NO. Pt-O formed at low temperatures appears to be critical for NO oxidation in this case, as at high temperatures NO increases at the expense of NO<sub>2</sub> suggesting surface oxygen depletion.

Additional work has focused on plasma dry-reforming of methane over a Ni-SiO<sub>2</sub>/Al<sub>2</sub>O<sub>3</sub> catalyst to investigate plasma-catalyst enhancement and coking reduction. DRIFTS measurements reveal that exposure to Ar/CH<sub>4</sub> plasma results in the buildup of hydrogenated carbon, carbonate, and CO species on the catalyst surface. Similar species may form during catalyst coking[1]. Variation of such peaks with catalyst temperature and plasma composition can shed light on surface interactions important for plasma dry reforming.

## References

[1] Zhang, S., Y. Li, A. Knoll, and G. S. Oehrlein, *J. Phys. D: Appl. Phys.* **53**, 215201 (2020).

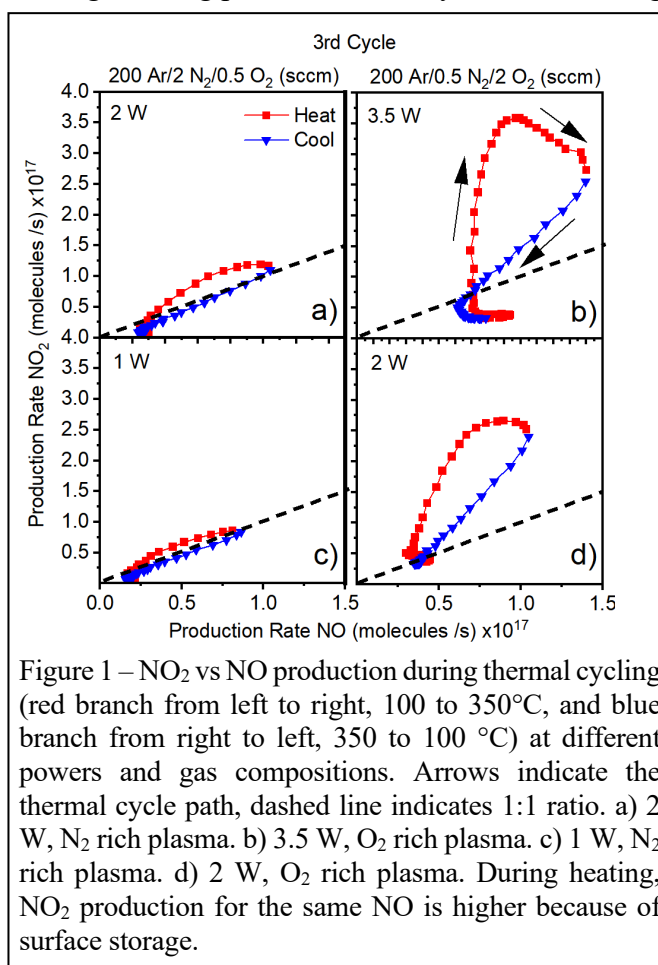


Figure 1 – NO<sub>2</sub> vs NO production during thermal cycling (red branch from left to right, 100 to 350°C, and blue branch from right to left, 350 to 100 °C) at different powers and gas compositions. Arrows indicate the thermal cycle path, dashed line indicates 1:1 ratio. a) 2 W, N<sub>2</sub> rich plasma. b) 3.5 W, O<sub>2</sub> rich plasma. c) 1 W, N<sub>2</sub> rich plasma. d) 2 W, O<sub>2</sub> rich plasma. During heating, NO<sub>2</sub> production for the same NO is higher because of surface storage.

## [V-2] Characterization of Plasma Jets Impinging on Dielectric and Metal Surfaces

Igor V. Adamovich

Department of Mechanical and Aerospace Engineering,  
The Ohio State University, Columbus, OH 43210, USA  
(adamovich.1@osu.edu)

The electric field distribution in the ionization waves propagating over a microchannel array dielectric surface, with the channels either empty or filled with distilled water, is measured by ps Electric Field Induced Second Harmonic (EFISH) generation. The surface ionization wave is initiated by the atmospheric pressure N<sub>2</sub>-Ar plasma jet impinging on the surface and powered by ns pulse discharge bursts. The results show that the electric field inside the microchannels, specifically its horizontal component, is enhanced by up to a factor of 2. The field enhancement region is localized within the channels. The vertical electric field inside the channels lags in time compared to the field measured at the ridges, indicating the transient reversal of the ionization wave propagation direction across the channels. This is consistent with the phase-locked plasma emission images and confirmed by the modeling predictions, which show that the ionization wave “jumps” over the empty channels and propagates into the channels only after the jump between the adjacent ridges. When the channels are filled with water, the wave speed increases by up to 50%, due to the higher effective dielectric constant of the surface. No evidence of a significant electric field enhancement near the dielectric surface, predicted by the modeling calculations, has been detected, due to the limited spatial resolution, ~100 μm. It is likely that the electric field at the water surface may be even higher than that predicted in the plasma. Probing it would require reflecting the pump laser beam off the water surface, as has been done in surface-enhanced fs EFISH experiments [1]. The results of Ref. [1] suggest that continuum models of the interfacial shielding, even without plasma, may not reflect the structural complexity on the molecular level, demonstrating the need for the direct plasma-water interface diagnostic and modeling effort.

The absolute, spatially-resolved, and time-resolved number density of HO<sub>2</sub> radical is measured in a quasi-2-D, atmospheric pressure “curtain” plasma jet powered by a train of ns discharge pulses. The plasma is sustained in an H<sub>2</sub>O vapor – O<sub>2</sub> – He flow with a co-flow of dry air, impinging on a copper foil target. The water vapor is added to the baseline O<sub>2</sub>-He flow in a bubbler filled with distilled, deionized water. The measurements are made using the previously developed pulsed Cavity Ring Down Spectroscopy (CRDS) diagnostic near 1.5 μm. The ring-down cavity is formed between two high-reflectivity mirrors placed at the ends of the stainless steel “arms” purged with dry air, with the plasma jet placed in the gap between the arms. Both the water vapor in the jet and HO<sub>2</sub> generated in the plasma have been measured. The results exhibit a rapid accumulation of HO<sub>2</sub> during the ns pulse discharge burst, followed by the decay in the afterglow on a ms time scale. The modeling predictions significantly overpredict the HO<sub>2</sub> decay rate, indicating the deficiencies in the previously developed H<sub>2</sub>O-O<sub>2</sub>-He plasma chemical reaction mechanism. In the O<sub>2</sub>-He plasma jet impinging on a liquid water surface, HO<sub>2</sub> has not been detected. The most likely reason is the rapid decay of the metastable He atoms and O atoms generated in the plasma in the evaporation/mixing layers, which precludes the efficient generation of H atoms, the dominant precursors for HO<sub>2</sub> generation.

### References

1. K.K. Ray et al, J. Phys. Chem. C **127** 30, 14949 (2023).

### [V-3] Surface Ionization Waves and the Shape of Water

Scott Doyle <sup>a</sup>, Kseniia Konina <sup>a</sup>, Mackenzie Meyer <sup>a</sup>, Sai Raskar <sup>b</sup>, Igor V. Adamovich <sup>b</sup>  
Joshua Morsell <sup>c</sup>, Steven Shannon <sup>c</sup>, Selma Mededovic Thagard <sup>d</sup> and Mark J. Kushner <sup>a</sup>

(a) University of Michigan, Ann Arbor, MI

(b) The Ohio State University, Columbus, OH

(c) North Carolina State University, Raleigh, NC

(d) Clarkson University, Potsdam, NY

(mjkush@umich.edu)

The interactions of atmospheric pressure plasmas with surfaces are sensitive to the shape of the surface due to electric field enhancement, charging and their associated feedback to the plasma. Previous studies have shown the propensity for surface ionization waves (SIWs) over solid surfaces to transition from surface-hugging to hopping, depending on the shape, periodicity and dielectric constant of the surface. The mode of SIW propagation then determines the fluxes (and fluences) of charged particles, photons and reactive species onto the surface. The ability to shape liquid surfaces to take advantage of these SIW propagation trends is far more limited. Liquid surfaces can be shaped to some degree by their containers (e.g., liquids in channels, hydrophobic vs hydrophilic surfaces) and by inducing waves on the surface. In fact, surfaces treated by plasmas are rarely perfectly planar due to the occurrence of capillary waves and turbulence. The context of investigating plasma interactions with shaped liquid surfaces is at least two-fold. These are PDSE (plasma-driven solution electrolysis) and plasma remediation of surfactant-like contaminants where control of fluxes of reactants to the surface would be beneficial.

In this talk, results will be discussed from computational investigations of atmospheric pressure plasmas with shaped water surfaces. These investigations were conducted with the 2-dimensional *nonPDPSIM* modeling platform. As a baseline, SIWs interacting with dry and water filled channels and steps on dielectric surfaces will be discussed, emphasizing the ability to focus or disperse plasma generated fluences to the surfaces. These trends will be extended to investigations of plasma interactions with liquids of varying conductivity that have been acoustically shaped into wavy surfaces. The implications of plasma interactions with shaped-liquids for materials synthesis and contaminant remediation will be discussed.

## Abstracts – Poster Presentations

### [PI-1] Design of Ordered Mesoporous Oxides for Dielectric Barrier Discharge-assisted Catalysis of Ammonia Synthesis

Sonia E. Arumuganainar, Stavroula Sartzetakis, Michele L. Sarazen and Bruce E. Koel

Department of Chemical and Biological Engineering, Princeton University, 41 Olden Street, Princeton, NJ 08544 (seka@princeton.edu)

Plasma-assisted catalytic studies, using dielectric barrier discharges (DBDs), have often shown that metal nanoparticles supported on porous oxides (traditional thermal catalysts) have surprisingly similar  $N_2$  conversions to the metal-free porous oxides alone, indicating there are significant support contributions that need to be understood to improve the low energy yields of DBD-assisted catalysis.[1] Synthetically-controlled pore sizes and surface areas of ordered mesoporous materials (OMMs) maintain material composition while systematically probing porosity effects on  $N_2$  conversion and DBD properties. Interestingly, SBA-15 (a silica-based OMM) has demonstrated higher  $N_2$  conversion than non-ordered analogs.[2] In order to take advantage of this, along with desirable aspects of  $\gamma$ -alumina (i.e., higher  $N_2$  conversions reported for bulk  $\gamma$ -alumina relative to silica and potential  $NH_3$  adsorption on  $\gamma$ -alumina acid sites that shields  $NH_3$  from decomposition in the plasma), we synthesized  $\gamma$ -alumina-coated SBA-15 (5-15 wt. % Al) via a reported wetness impregnation procedure.[3] The samples are represented by x-SBA-15, where x is the target nominal Al weight loading. As shown in Figure 1, the alumina coat completely covers the silica surface and preserves the ordered porosity of SBA-15 based on FTIR and  $N_2$  physisorption data, respectively.

10-SBA-15, alongside uncoated SBA-15, was pelletized prior to testing in our DBD reactor for larger voids between support particles in the packed bed, which promotes a more homogenous discharge. Higher initial  $N_2$  conversions were measured on OMM pellets relative to pelletized powders of non-ordered oxides, extending insights for ordered silica to  $\gamma$ -alumina. As shown in Figure 2, OMM pellets yielded higher steady-state  $NH_3$  yields than commercial beads commonly used as supports in DBD reactors, even though lower electron densities were measured on the pellets (likely due to its smaller interparticle voids inhibiting plasma generation). Ex situ temperature programmed desorption measurements on the catalyst supports showed the highest  $NH_3$  uptake for 10-SBA-15 pellets, highlighting its ability to shield  $NH_3$  from undesired decomposition in the plasma. Together, these results inform the rational design of OMM porosity and functionality to optimize DBD properties, catalytic activity,  $NH_3$  uptake and energy yield of DBD-assisted catalysis of  $NH_3$  synthesis.

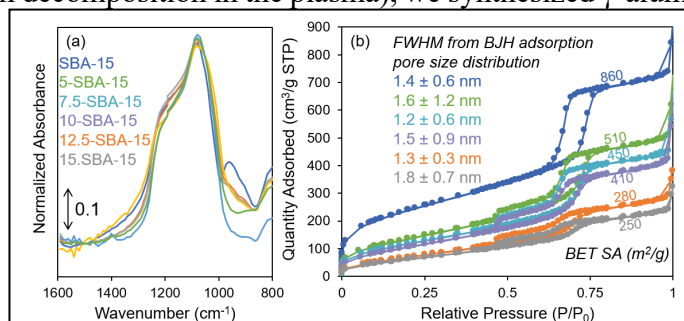


Figure 1 – (a) FTIR and (b)  $N_2$  adsorption-desorption isotherms (FWHM from BJH pore size distribution and BET surface area insetted) of synthesized SBA-15 and its alumina-coated composites of different weight loadings.

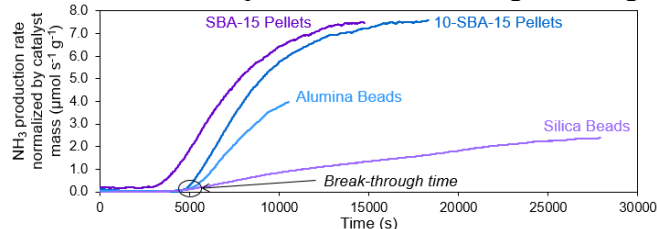


Figure 2 – Time profile of  $NH_3$  effluent rate from the DBD reactor containing different porous oxide supports.

## References

- [1] Z. Chen, B. E. Koel and S. Sundaresan, J. Phys. D Appl. Phys. **55** (5), 055202 (2022).
- [2] F. Gorky, S. R. Guthrie, C. S. Smoljan, J. M. Crawford, M. A. Carreon and M. L. Carreon, J. Phys. D Appl. Phys. **54** (26), 264003 (2021).
- [3] Z. Babaei, A. Najafi Chermahini and M. Dinari, Chem. Eng. J. **352**, 45 (2018).

## [PI-2] Electron Beam Generated Plasmas and Their Applications

Yevgeny Raitses, Nirbhav S. Chopra, Shurik Yatom, and Emma Devin

Discovery Plasma Science Department, Princeton Plasma Physics Laboratory (yraitses@pppl.gov)

Low temperature plasmas generated by electron beams (e-beams) are promising for applications requiring efficient generation of ions and radicals in low pressure environments ranging from hundreds of microTorr to hundreds of mTorr [1,2]. For example, it was recently shown that an e-beam generated plasma with applied crossed electric and magnetic fields (ExB) operating with argon-hydrogen gas mixture in the several mTorr pressure range can generate fluxes of hydrogen atoms and ions, enabling low damage hydrogenation on an atomically thin 2D material such as graphene [3] and hydrogen passivation of diamond and silicon substrates for quantum sensor applications [4, 5]. In this talk, we will report results of a number of PCRF User and Host Team research projects on e-beam generating plasmas and their applications [3-8]. Specifically, we will compare plasma properties and stability of

e-beam generated plasmas produced by different electron sources, including an ion-induced secondary electron emission (iSEE) cathode, a thermionic cathode and an RF plasma cathode. The focus will be on electron and ion kinetic properties, chemical composition and characteristic instabilities generating dynamic and stationary plasma structures. In the described experiments, electrostatic probes, optical emission spectroscopy, ns and CW Laser-Induced Fluorescence (LIF) and fs-Two-Photon Absorption LIF (TALIF) diagnostics were used to characterize the plasma. Measurements revealed i) the effect of the nitrogen addition on the density of argon metastables (Fig. 1) [6], ii) the formation of the warm electrons and of ions [7], and iii) ExB rotating spoke driven by gradient-drift instabilities. Experimental results are compared with predictions of recent Particle-in-Cell simulations predicting various regimes of e-beam-plasma instabilities [8].

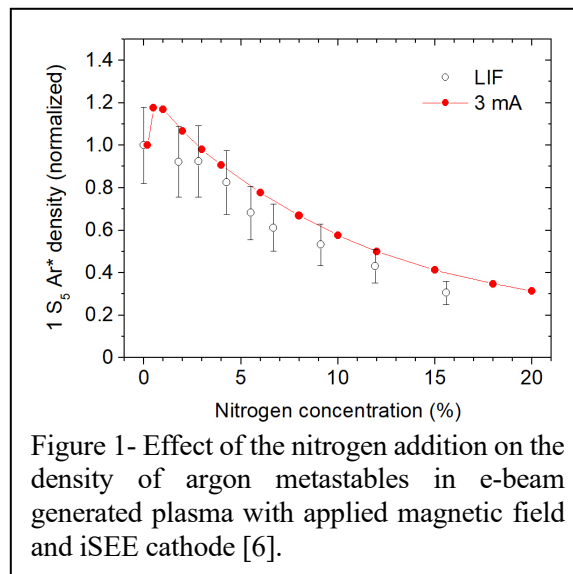


Figure 1- Effect of the nitrogen addition on the density of argon metastables in e-beam generated plasma with applied magnetic field and iSEE cathode [6].

This work was performed at the Princeton Collaborative Research Facility (PCRF) supported by the US Department of Energy through contract DE-AC02-09CH11466.

### References

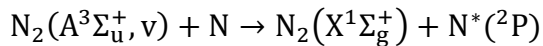
- [1] S. G. Walton, D. R. Boris, et al., ECS J. Solid State Sci. Technol. **4**, N5033 (2015)
- [2] D. B. Zolotukhin, V. A. Burdovitsin, E. M. Oks, Phys. Plasmas **24**, 093502 (2017)
- [3] F. Zhao, Y. Raitses, X. Yang, A. Tan, and C. G. Tully, Carbon **177**, 244 (2021).
- [4] C. Pederson, et al., Optical tuning of the diamond Fermi level measured by correlated scanning probe microscopy and quantum defect spectroscopy, submitted for journal publication.
- [5] T. Schenkel, "Plasma based hydrogen doping of semiconductors for color center qubit optimization", PCRF Collaborative Research Project, 2023
- [6] S. Yatom et al., "Measurement and reduction of Ar metastable densities by nitrogen admixing in electron beam generated plasmas", submitted for journal publication.
- [7] N. S. Chopra, Y. Raitses, and I Romadanov, "EEDF and warm ions in an electron beam generated ExB plasma" to presented at this meeting
- [8] H. Sun, J. Chen, I. D. Kaganovich et al., Phys. Rev. Lett. **129**, 125001 (2022).

# [PI-3] Measurements of Excited Metastable Species and Ionization in a Nonequilibrium Heated Plasma Reactor

Sai Raskar, Hamzeh Telfah and Igor V. Adamovich

Department of Mechanical and Aerospace Engineering, Ohio State University, Columbus, OH 43210  
(raskar.1@osu.edu, telfah.1@osu.edu, adamovich.1@osu.edu)

One of the key ionization processes in nonequilibrium plasmas is associative ionization in collisions of excited metastable molecules and atoms. The objective of the present work is to generate N and O atoms, both in their ground electronic states,  $N(^4S)$  and  $O(^3P)$ , and excited metastable states,  $N(^2D, ^2P)$  and  $O(^1D, ^1S)$ , in a laboratory experiment, and to study their associative ionization generating  $N_2^+$  and  $NO^+$  ions. The focus of the experiment discussed below is on the generation and detection of the excited metastable states of nitrogen, as well as molecular nitrogen ions. To generate excited metastable species of nitrogen, we use a heated plasma flow reactor. The heating of the flow in the reactor is critical for  $N_2^+$  measurements, since it shifts the equilibrium in the rapid ion conversion reaction,  $N_2^+ + N_2 + N_2 \leftrightarrow N_4^+ + N_2$  toward  $N_2^+$ , such that it can be detected and measured with confidence. A slow flow of nitrogen, at a pressure of  $P = 100$  Torr is heated in a tube furnace to the temperature of up to  $T=1000$  K, and excited by a burst of high peak voltage (25 kV), ns duration pulses (10 ns), at high pulse repetition rate (100 kHz). The main objective of the discharge burst excitation is the efficient generation of N atoms and a long-lived metastable nitrogen molecules,  $N_2(A^3\Sigma_u^+)$ , by electron impact. These species serve as precursors for the excited metastable atoms in the afterglow, when  $N_2(A^3\Sigma_u^+, v)$  is quenched by the ground state N atoms,



which subsequently decay by associative ionization,  $N^*(^2P) + N^*(^2P) \rightarrow N_2^+ + e^-$ . Figure 1 plots the  $v=0$  population measured during a 20-pulse burst at different furnace temperatures. Figure 2 plots the Cavity Ring Down Spectrum (CRDS) of  $N_2^+$  ions generated in the plasma flow reactor during a 60-pulse discharge burst at  $T=800$  K, compared to the LIFBASE synthetic spectrum. The inference of the  $N_2^+$  number density from CRDS spectra and the associative ionization rate coefficient are underway.

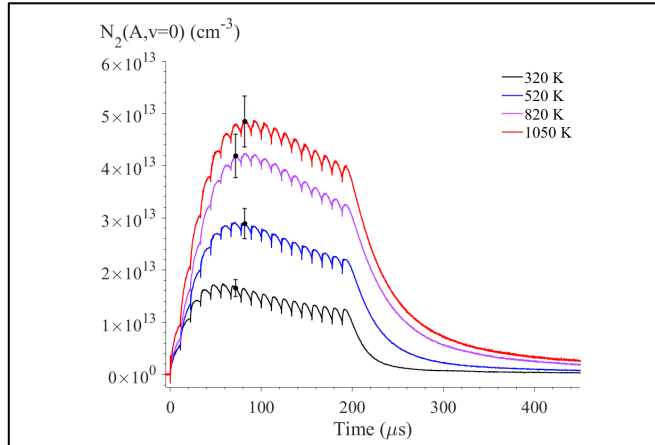


Figure 1 – Time-resolved  $N_2(A^3\Sigma_u^+, v = 0)$  population measured in heated plasma flow reactor at different temperatures.

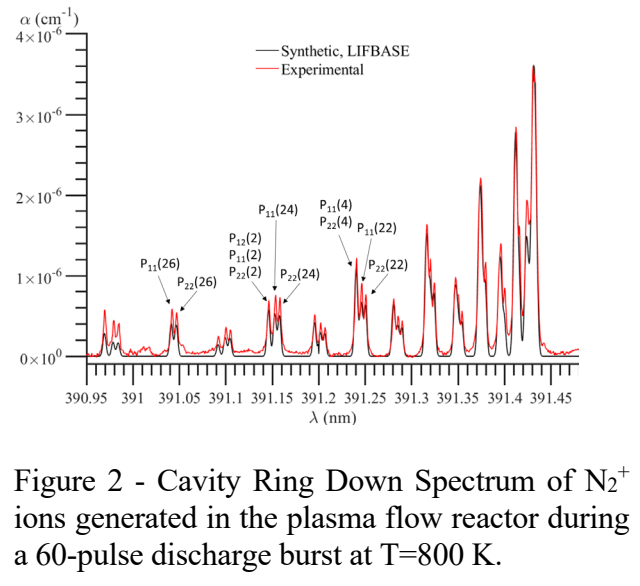


Figure 2 - Cavity Ring Down Spectrum of  $N_2^+$  ions generated in the plasma flow reactor during a 60-pulse discharge burst at  $T=800$  K.

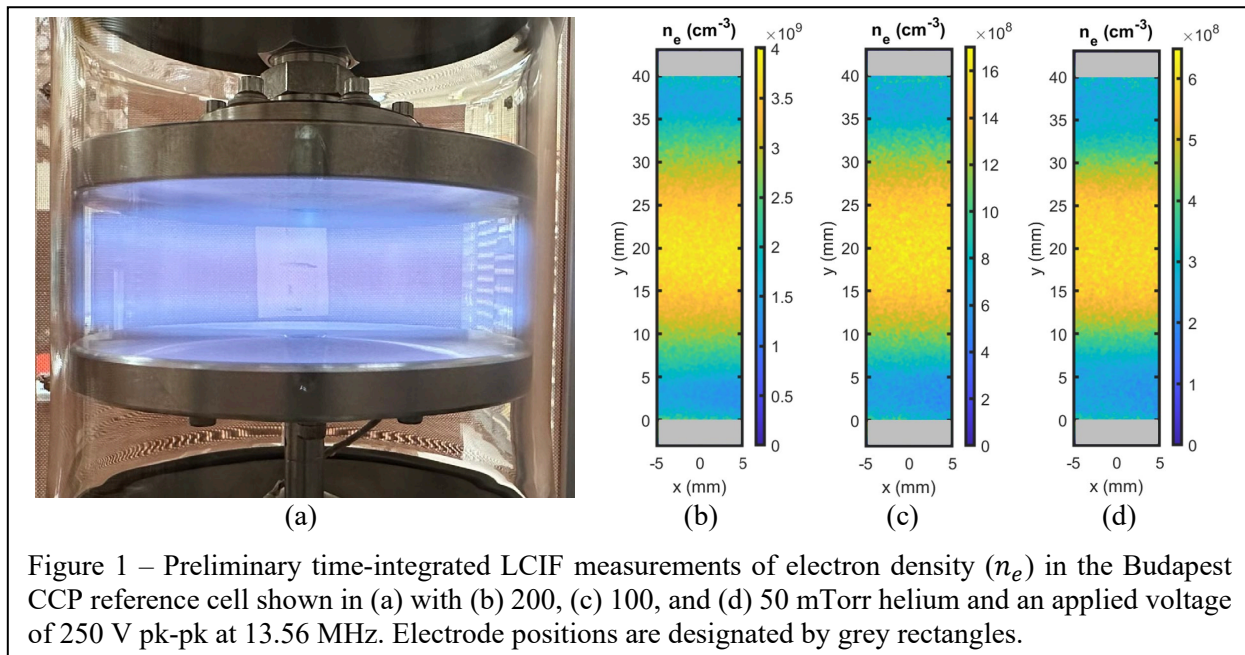
## [PI-4] Mapping Electron Density with Laser-Collision Induced Fluorescence in the Budapest Capacitively Coupled Plasma Reference Cell

Brian Z. Bentz<sup>a</sup>, Kevin Youngman<sup>a</sup>, Peter Hartmann<sup>b</sup>, Aranka Derzsi<sup>b</sup>, and Zoltan Donko<sup>b</sup>

(a) Sandia National Laboratories, Albuquerque, New Mexico, USA (bzbentz@sandia.gov)

(b) Wigner Research Centre for Physics, Budapest, Hungary (donko.zoltan@wigner.hu)

Electron density is a key plasma parameter influencing production of radicals and active species playing major roles in applications such as plasma etch and deposition, key processes for fabrication of microelectronics. However, accurate measurement of electron densities in low pressure RF-driven plasma reactors can be surprisingly difficult. Electrical probes perturb the plasma and can have large error factors or cannot be used due to limitations of probe theories or probe design [1]. Laser-collision induced fluorescence (LCIF) diagnostics present an established alternative where the electron density can be mapped in 2D without perturbing the plasma and in regimes (density, temperature, pressures, size, duration, magnetic fields, etc.) not easily accessed with electrical probes [2]. The technique relies on the transfer of laser-excited electrons to nearby and more energetic levels with collisional excitation rates that depend minimally on the electron temperature. The measurement uncertainty can be conservatively estimated as 50%, depending primarily on the uncertainty in the rate constants or experimental calibration. Shown in Fig. 1, preliminary LCIF measurements were performed in a Budapest reference cell built at Sandia for collaborative validation of plasma parameters and simulation codes [3].



This work was supported by Sandia National Laboratories' Plasma Research Facility, funded by the U.S. Department of Energy Office of Fusion Energy Sciences. Sandia is managed and operated by NTESS under DOE NNSA contract DE-NA0003525.

### References

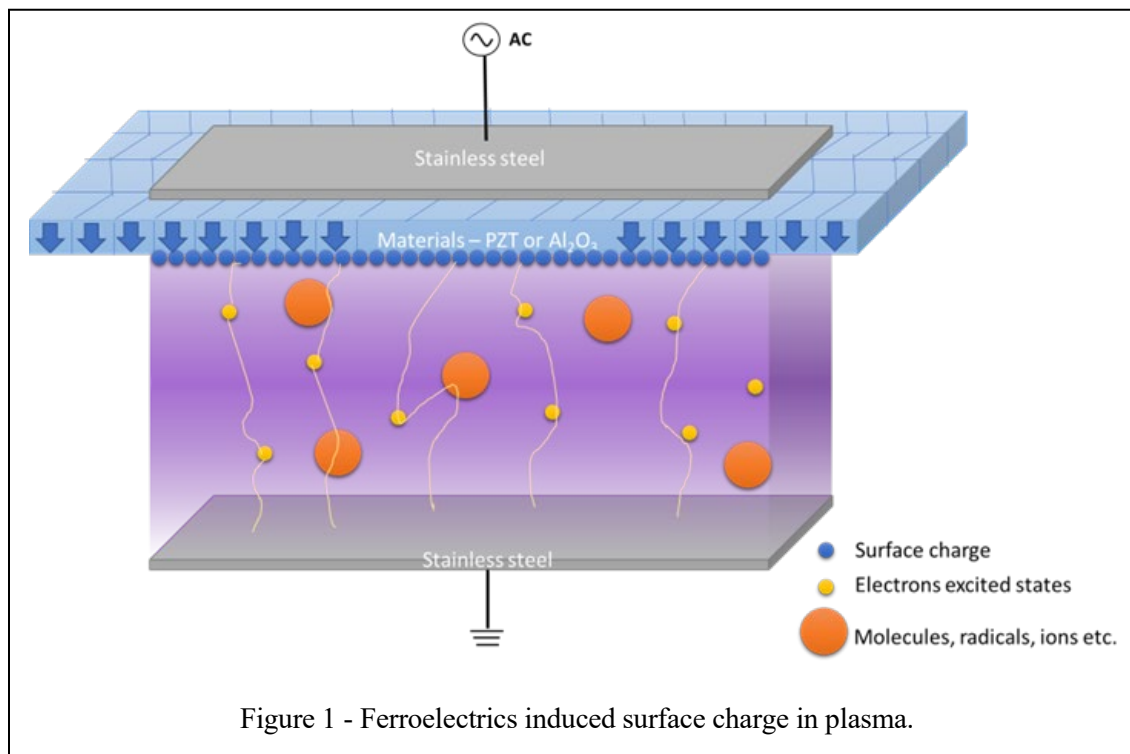
- [1] V. Godyak, J. Appl. Phys. **129**, 041101, (2021).
- [2] E. V. Barnat and K. Frederickson, Plasma Sources Sci. Tech. **19**, 055015 (2010).
- [3] J. Ďurian, P. Hartmann, Š. Matejčík, A. R. Gibson, and Z. Donkó, Plasma Sources Sci. Technol. **31**, 095001, (2022).

## [PI-5] Ferroelectrics-induced Surface Charge in Plasma

Yijie Xu, Ning Liu, Ying Lin, Xingqian Mao, Mikhail N Shneide and, Yiguang Ju

Department of Mechanical and Aerospace Engineering, Princeton University, Princeton, NJ 08544, USA  
(nl7@princeton.edu)

Non-equilibrium low-temperature plasma has been widely investigated because its energetic electrons, ions, and excited species can initiate and facilitate chemical reactions with reduced kinetic barriers and new non-equilibrium pathways. However, plasma applications on catalysis and synthesis have been limited by low energy efficiency and extra heating for assistance. Here, we report a plasma discharge with significantly enhanced electric field and density through a ferroelectric PZT ( $\text{Pb}(\text{Zr}_x\text{Ti}_{1-x})\text{O}_3$ ) barrier electrode design [1]. Due to an asymmetric crystal structure, the ferroelectric PZT manifests spontaneous electric polarization to enable a large surface charge of  $10^{-1} \mu\text{C}/\text{cm}^2$  in the discharge region, two orders of magnitude higher than that from the classic dielectric alumina barrier. This significant charge accumulating on the surface then considerably enhances the electric field and the concentration and energy of reactive species (e.g., electrons) in the plasma, making the plasma more temporally sustainable when alternating the power polarity. Furthermore, the surface charge induces a high current through the electrodes, enabling self-Joule-heating. The ferroelectric barrier discharge (FBD) is expected to offer a promising pathway toward energy-efficient and sustainable plasma catalysis and synthesis.



### References

[1] Liu, Ning, Yijie Xu, Xingqian Mao, Yiguang Ju, and Ying Lin. "Ferroelectrics-induced Surface Charge in Plasma." *Bulletin of the American Physical Society* (2023).



# [PI-6] Temperature Prediction in OES using Neural Networks

Shurik Yatom<sup>a</sup> and Amy Zheng<sup>b</sup>

(a) Princeton Plasma Physics Laboratory

(b) University of Pennsylvania

An optical emission spectrum pertains information on vibrational and rotational temperatures of the emitting species and may contain information on the density of each species. Current measurement techniques involve high-end equipment, expertise, and a significant investment in time and data analysis. With the machine learning approach, data analysis can be performed in real-time without involving other resource-consuming methods. This project targets plasmas abundant in technological, biomedical, and environmental applications, such as C<sub>2</sub>, N<sub>2</sub>.

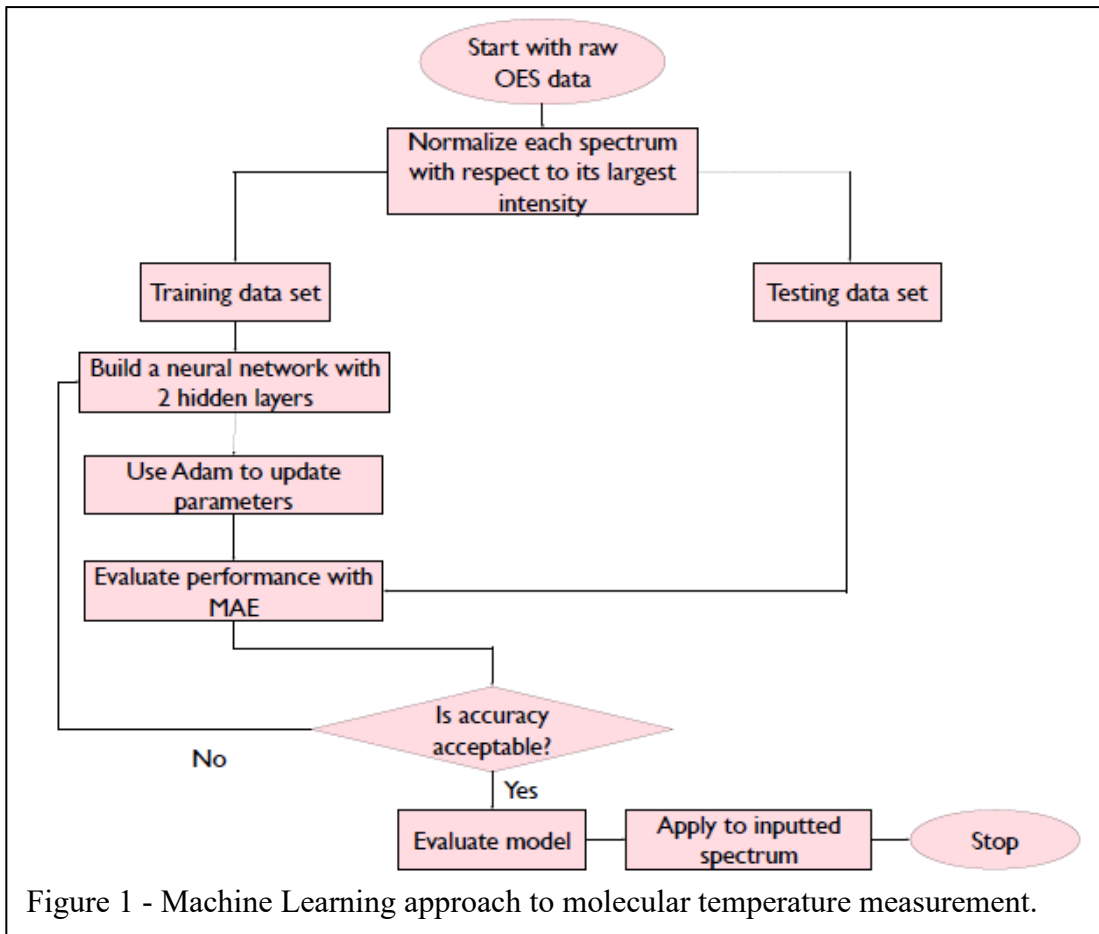


Figure 1 - Machine Learning approach to molecular temperature measurement.

This work is supported by the Princeton Collaborative Research Facility (PCRF), which is supported by the U.S. Department of Energy (DOE) under Contract No. DE-AC02-09CH11466.

# [PI-7] Availability and Reactivity of $N_2(v)$ for $NH_3$ Synthesis by Plasma Catalysis

Brian Bayer<sup>a</sup>, Sai Raskar<sup>b</sup>, Igor V. Adamovich<sup>b</sup>, Peter Bruggeman<sup>c</sup> and Aditya Bhan<sup>a</sup>

(a) University of Minnesota, Department of Chemical Engineering and Materials Science  
(bayer116@umn.edu, abhan@umn.edu)

(b) The Ohio State University, Department of Mechanical and Aerospace Engineering (raskar.1@osu.edu,  
adamovich.1@osu.edu)

(c) University of Minnesota, Department of Mechanical Engineering (pbruggem@umn.edu)

Vibrational excitation of  $N_2$  ( $N_2(v)$ ) has been proposed to enhance  $NH_3$  formation by plasma catalysis, though quantification of  $N_2(v)$  in nonthermal plasmas interfacing catalytic surfaces and an assessment of its ability to undergo  $NH_3$ -forming surface reactions have not been performed to verify these claims. Here, we analyze production of  $N_2(v)$  in an Ar/ $N_2$ / $H_2$  radiofrequency atmospheric pressure plasma jet and loss of  $N_2(v)$  by gas-phase reactions and reactions on catalytic surfaces with vibrational state-to-state kinetic models and molecular beam mass spectrometry (MBMS) measurements to probe whether  $N_2(v)$  contributes to catalytic  $NH_3$  formation.

MBMS-validated state-to-state kinetic models show that ~40-50% of  $N_2$  is vibrationally excited in the effluent of the plasma jet, and total  $N_2(v>0)$  densities exceed the N density by 100 $\times$  (Figure 1) [1]. Depletion of the populations of  $N_2(v>8)$  occurs due to fast vibrational-translational relaxation of  $N_2(v)$  with H and  $H_2$ .

MBMS measurements with and without catalyst present show that loss of  $N_2(v)$  in the catalyst bed arises from surface reactions rather than gas-phase reactions. The state-to-state kinetic model shows that the MBMS-measured loss of  $N_2(v)$  in the catalyst bed occurs due to vibrational relaxation on the catalyst surface. A comparison between the measured rate of vibrational relaxation on the surface with upper bounds on proposed rates of  $NH_3$ -forming reactions from  $N_2(v)$  demonstrates that the abundantly produced, lower vibrational levels will quench on the surface faster than they can react to form  $NH_3$  (Figure 2) [1]. Relaxation of  $N_2(v)$  on the surface reduces the density of  $N_2(v)$  that can react to form  $NH_3$  by at least 100 $\times$ . As a result, surface reactions involving N radicals rather than  $N_2(v)$  are the source of the experimentally measured  $NH_3$  formation at the investigated operating conditions [2].

## References

- [1] Bayer et al. Plasma Sources Sci. Technol. In review  
[2] Bayer et al. ACS Catal. 13 (2023) 4, 2619-2630

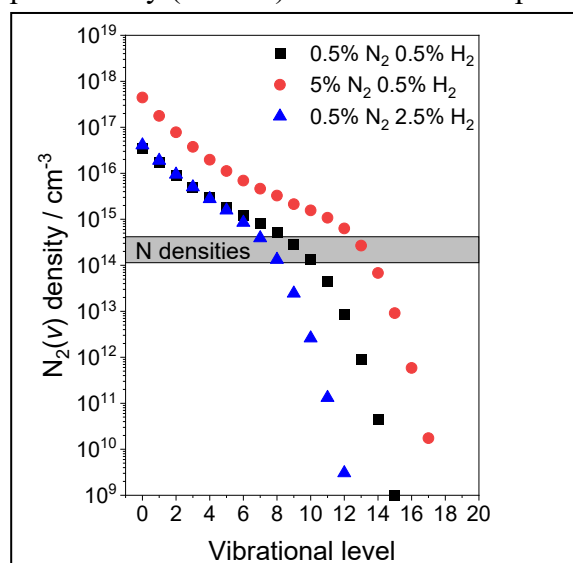


Figure 1 –  $N_2(v)$  and N densities at the inlet of the catalyst bed for different concentrations of  $N_2$  and  $H_2$  in the reactor.

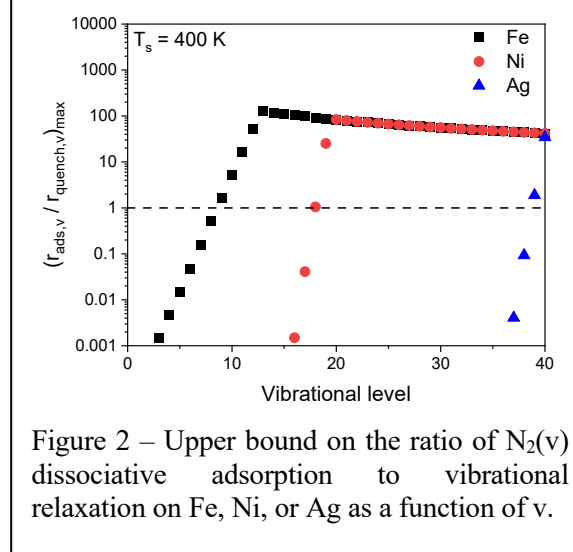


Figure 2 – Upper bound on the ratio of  $N_2(v)$  dissociative adsorption to vibrational relaxation on Fe, Ni, or Ag as a function of  $v$ .

# [PI-8] Computational Investigation of Mechanisms Leading to Reduction in Cell Viability by Changing Atmospheric Pressure Plasma Jet Configuration

Jordyn Polito<sup>a</sup> and Mark J. Kushner<sup>b</sup>

(a) Department of Chemical Engineering, University of Michigan, Ann Arbor, Michigan, USA  
(jopolito@umich.edu)

(b) Department of Elect. Engr. & Computer Sci., University of Michigan, Ann Arbor, Michigan, USA  
(mjkush@umich.edu)

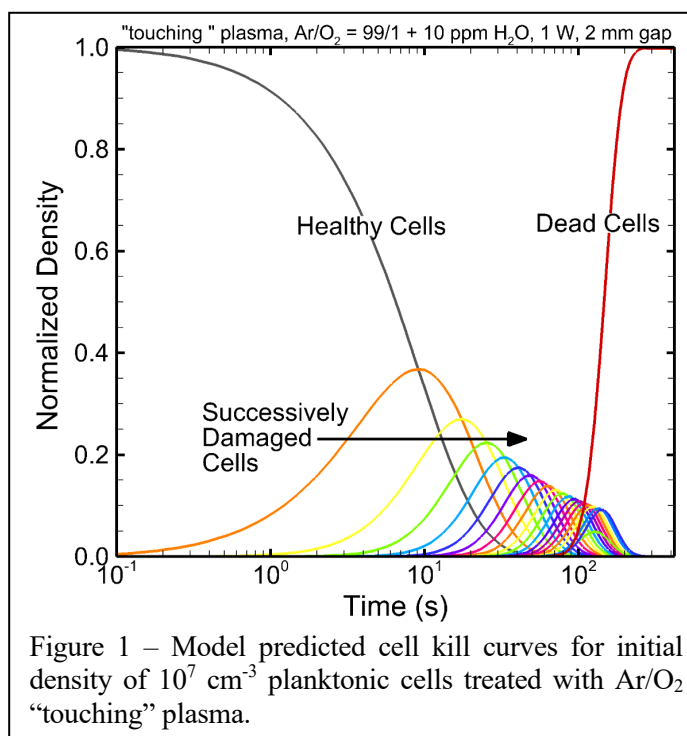
Cold atmospheric plasmas (CAPs) have been investigated as non-invasive sources of reactive oxygen and nitrogen species (RONS) for plasma medicine applications. Several plasma configurations, such as the kINPen and the COST-jet, have been studied for applications that reduce the viability of biological targets (i.e., disinfection and cancer treatment) [1]. When plasma-produced RONS are introduced to bacterial or cancer cell-containing medium, the mechanism by which reduction in viability occurs is thought to be as follows: RONS interactions at the cell membrane result in modifications of organic molecules located on the cell membrane, damaged molecules at the cell membrane interrupt cell signaling, causing uptake of RONS, and uptake of RONS induces oxidative stress, resulting in apoptosis [2]. Devices such as the kINPen (“touching”) produce a discharge that comes

into direct contact with the cell-containing medium whereas devices such as the COST-jet (“non-touching”) produce plasmas in which only the plasma effluent (not the discharge) comes into contact with the cell-containing medium. Studies have been performed to elucidate mechanisms leading to cell killing in different plasma configurations independently, however there are few direct comparisons between devices. Insight gained from direct comparison of mechanisms leading to reduction in cell viability between, for example, “touching” vs. “non-touching” plasma devices will lead to better understanding of these processes responsible for cell killing and will allow for design of plasma medical devices to be optimized based on the desired application.

In this work, we extend a reaction mechanism for the CAP treatment of small organic molecules in solution [3] to include RONS interactions with CFUs that result in cell damage. The 0D plasma chemistry model *GlobalKin* is used to provide predictions for cell killing as a result of using different plasma sources – “touching” vs. “non-touching” plasma jets. A comparison of the mechanisms for RONS production leading to cell death in both plasma configurations will be discussed. Ongoing efforts to validate the reaction mechanism and cell death model will also be discussed.

## References

- [1] J. W. Lackmann and J. E. Bandow, *Appl. Microbiol. and Biotechnol.*, **98**, (2014).
- [2] J. Van der Paal, et. al. *Chem. Sci.*, **7**, 489 (2016).
- [3] J. Polito, et. al. *J. Phys. D. Appl. Phys.*, **56**, 285202 (2023).



# [PI-9] Numerical Modeling of Plasma Assisted Deflagration to Detonation Transition in a Microscale Channel

Zhiyu Shi, Xingqian Mao and Yiguang Ju

Department of Mechanical and Aerospace Engineering, Princeton University, Princeton, NJ 08544, USA  
(zs3643@princeton.edu, xingqian@princeton.edu)

This work numerically studies the plasma assisted deflagration to detonation transition (DDT) of a  $H_2/O_2$  mixture in a microscale channel with detailed chemistry and transport. The effects of a repetitively-pulsed nanosecond discharge on fuel oxidation and DDT dynamics are investigated. The results show that the DDT onset time is non-monotonically dependent on the discharge pulse number.[1] With plasma discharge, the DDT is accelerated with a small plasma pulse number and the DDT onset time is reduced by  $52 \mu s$ . However, a large plasma pulse number delays the DDT and extends the DDT onset time by  $160 \mu s$ . The results show that without plasma a pronounced pressure gradient is generated due to the acoustic choking of the burned gas, which further triggers the DDT via auto-ignition in the induction zone at the flame front. For the DDT acceleration with small pulse numbers, the chemically active species generated by plasma such as H, O and  $O(^1D)$  introduce new reaction pathways and accelerate fuel oxidation at low temperatures. The relatively long lifetime species such as  $H_2(v)$ ,  $O_2(a^1\Delta_g)$ ,  $O_3$ , and  $HO_2$

amplify the heat release within the induction zone. This intensifies the reactivity gradient in the boundary layer and enhances the auto-ignition and shock-ignition coupling. The DDT occurs at the boundary layer in the induction zone. The results show that a direct auto-ignition initiating DDT occurs without the acoustic choking of the burned gas due to the elevated temperature when more plasma pulses are applied. The DDT onset is retarded due to a reduction in fuel quantity and therefore the decrease of heat release and flame acceleration. The results also show that the DDT is initiated when the ignition propagation velocity exceeds the local sonic speed both with and without plasma discharges, indicating the universality of the Zel'dovich gradient mechanism. This work advances the understanding of the non-monotonical dependence of the DDT onset time on plasma discharge. This provides guidance to control DDT in advanced detonation engines and fire safety of hydrogen fueled catalytic reactors in microchannels by non-equilibrium plasma discharge.

## References

[1] Z. Shi, X. Mao and Y. Ju, AIAA SCITECH 2023 Forum, 2023.

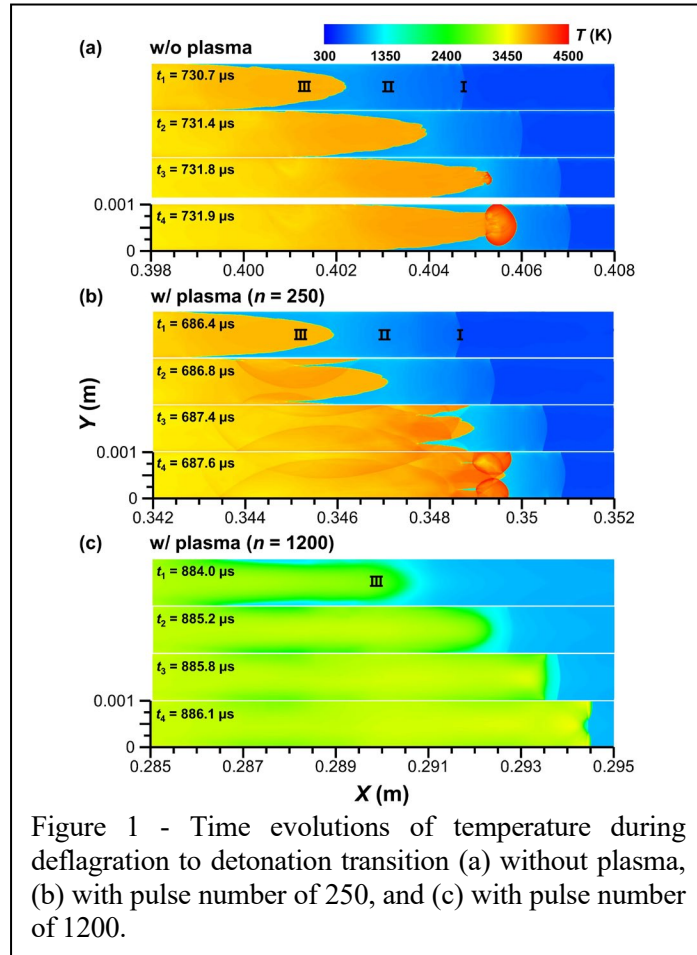


Figure 1 - Time evolutions of temperature during deflagration to detonation transition (a) without plasma, (b) with pulse number of 250, and (c) with pulse number of 1200.

# [PI-10] Synthesis of Dust Nanoparticles in RF Discharge Plasma

Y. Ussenov<sup>a</sup>, M. Shneider<sup>a</sup>, S. Yatom<sup>b</sup> and Y. Raitses<sup>b</sup>

(a) Department of Mechanical and Aerospace Engineering, Princeton University, Princeton,  
(yu3724@princeton.edu)

(b) Princeton Plasma Physics Laboratory, Princeton

Evaluating the charge of dust particles and gaining insights into the charging dynamics is essential, not just for enhancing the nanoparticle synthesis process but also for developing a comprehensive understanding of how particles interact with the surrounding plasma. Laser-stimulated electron photodetachment (LSPD) [1,2] stands out as a distinctive method for investigating these charging dynamics. It enables the immediate assessment of particle charge in saturated condition, given that the accurate measurement of electron density changes and information on particle properties such as size and density are available. Here we report on optimizing the nanoparticle growth process in capacitively coupled RF discharge dusty plasma with the aim to study LSPD from dust grains.

To optimize the nanoparticle growth process the argon/acetylene gas mixture ratios and gas pressure in a radio frequency (RF) capacitively coupled plasma have been varied. The growth of the dust particles is monitored by measuring a DC self-bias voltage of the RF discharge and analyzing the optical emission spectroscopy data. Dust particles have been grown at different ratios of Ar/C<sub>2</sub>H<sub>2</sub> mass flow rate and 300 – 600 mTorr range for constant 10 W RF power. The results were confirmed by the significant reduction in the discharge DC self-bias voltage (Figure 1), which is the consequence of the free electron absorption by the nanoparticles after the charging. The laser light scattered from 5 mW, He-Ne (633 nm) laser sheet was used to visually detect the nanoparticle cloud formation and its trapping. It also confirms the formation of the “void” in the central region of the dust cloud and the accumulation of the larger particles at the edge of the plasma boundary due to the ion drag force. Scanning electron microscopy of collected nanoparticles after several cycles of growth reveals the formation of amorphous carbon nanoparticles and agglomerates with sizes up to ~700-800 nm. The synthesized particles in the plasma environment will be used for the demonstration of LSPD-based real-time in-situ charge diagnostics in a dusty plasma.

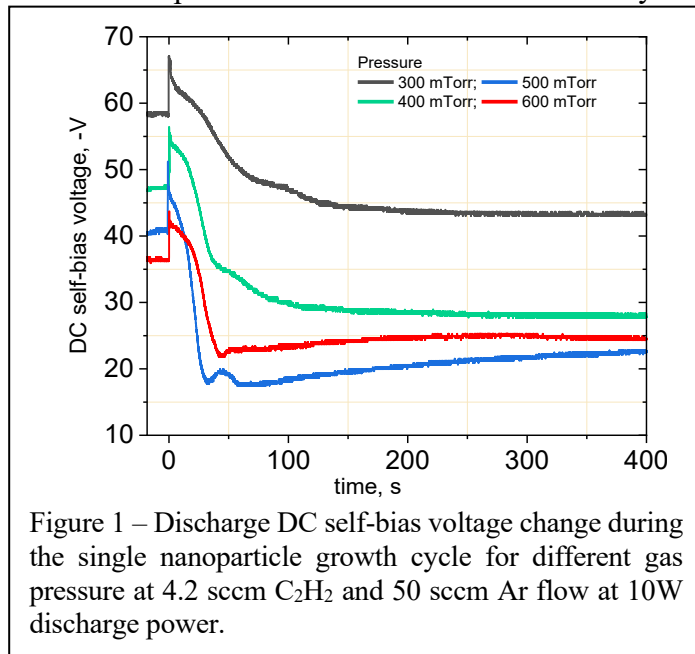


Figure 1 – Discharge DC self-bias voltage change during the single nanoparticle growth cycle for different gas pressure at 4.2 sccm C<sub>2</sub>H<sub>2</sub> and 50 sccm Ar flow at 10W discharge power.

This contribution is supported by the U.S. Department of Energy through contract DE-AC02-09CH11466.

## References

- [1] J.A. Staps, M.J.T. Donders, B. Platier, J. Beckers, J. Phys. D: Appl. Phys. 55 08LT01 (2022)
- [2] M. N Shneider, Y. Raitses, S. Yatom, J. Phys. D: Appl. Phys. 56 29LT01 (2023); J.Phys.D:Appl.Phys. 56 439501 (2023)

# [PI-11] Atmospheric Pressure Plasma Jet Treatment of Polypropylene Materials with Non-Smooth Interfaces

Kseniia Konina<sup>a</sup>, Joshua Morsell<sup>b</sup>, Jordyn Polyto<sup>a</sup>, Steven Shannon<sup>b</sup> and Mark Kushner<sup>a</sup>

(a) University of Michigan, Ann Arbor, MI 48109-2122 USA (kseniak@umich.edu)

(b) North Carolina State University, Raleigh, NC, 27607 USA

Atmospheric Pressure Plasmas (APPs) are widely used for polymer treatment [1], particularly in commercial packaging and biocompatible polymer manufacturing. The treatment helps tailor surface properties, for example, enhancing hydrophilicity. Plasma can also induce cross-linking, affecting resistance to temperature and photon fluxes. Plasma source, gas composition, and surface type can significantly influence treatment outcomes. Researching complex systems is required in order to control desired effects on surfaces. In this study, an atmospheric pressure plasma jet (APPJ) in contact with polypropylene surfaces with step barriers is investigated computationally and experimentally.

The computational platform *nonPDPSIM* was used in this study [2]. *nonPDPSIM* is a 2D model developed to solve plasma and hydrodynamics equations on unstructured meshes. The fundamental equations encompass Navier-Stokes, Poisson's, continuity, and Boltzmann's equations. Gas phase chemistry is addressed using a plasma-chemistry mechanism for rare gases flowing into humid air, while surface chemistry is addressed through a surface-kinetic model. Using a He APPJ to treat polypropylene generally limits the reactive oxygen and nitrogen species (RONS) fluxes to the treated surfaces. This results from the gas composition in typical APPJs that primarily operate with noble gases which provides a shield to the ambient. The primary influence on surface composition stems from photons and ion fluxes.

Consequently, functionalization is dominated by cross-linking, chain scission and radical formation with little oxygen attachment during treatment (Fig. 1). Upon exposure to ambient air after treatment, we expect radical sites will acquire oxygen functionalization.

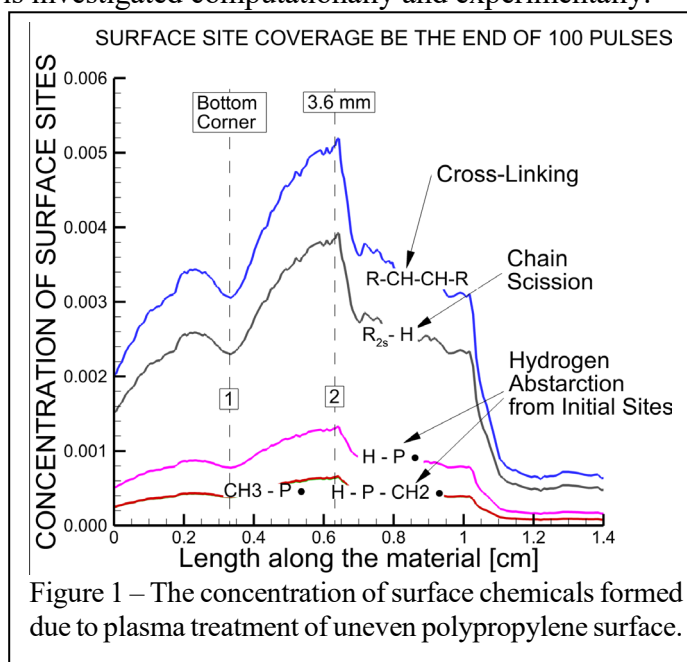


Figure 1 – The concentration of surface chemicals formed due to plasma treatment of uneven polypropylene surface.

## References

[1] J. P. Booth et al, *Plasma Sources Sci. Technol.* **31**, 103001 (2022).

[2] S. A. Norberg et al, *Plasma Sources Sci. Technol.* **24**, 035026 (2015).

# [PI-12] Ammonia Generation in a “Hybrid” High Repetition Rate Ns Pulse / RF Discharge Sustained over a Catalytic Surface

Matthew Berry and Igor V. Adamovich

Department of Mechanical and Aerospace Engineering, The Ohio State University, Columbus, OH 43210  
(berry.991@osu.edu, adamovich.1@osu.edu)

Ammonia generated during the plasma-chemical / plasma-catalytic synthesis in a “hybrid” ns pulse / RF discharge sustained at a high pulse repetition rate, 10 kHz, is measured by Fourier Transform Infrared Spectroscopy (FTIR). The plasma flow reactor is similar to the one used in our previous work [1]. The ns pulse discharge is operated in burst mode, with a pulse repetition rate of 10 kHz, burst repetition rate of 10 Hz, up to 200 pulses per burst. The pulse peak voltage is 15 kV, with pulse duration of approximately 100 ns. During each pulse burst, additional energy is coupled to the plasma by the sub-breakdown 13.56 MHz RF bursts 70  $\mu$ s long, generated between the ns pulses. The RF peak voltage is kept sufficiently low, 1 kV, to prevent additional ionization, dissociation, and electronic excitation of the N<sub>2</sub>-H<sub>2</sub> mixture in the reactor. This was verified by taking the ICCD plasma emission images during the RF bursts. The burst mode operation is used to increase the peak N<sub>2</sub> vibrational temperature, enhanced by the vibration-vibration (V-V) exchange, above what was done in our previous work [2]. The measurements are made in a 10% H<sub>2</sub>-N<sub>2</sub> mixture, at the pressure of P=190 Torr and temperature of T=573 K. The ammonia yield is measured *ex situ*, in the exhaust of the plasma flow reactor through an external absorption cell, 1.2 m long, using FTIR absorption spectroscopy. The measurements are made with and without a receptacle filled with Ni/ $\gamma$ -Al<sub>2</sub>O<sub>3</sub>, Co/ $\gamma$ -Al<sub>2</sub>O<sub>3</sub>, and Ru/ $\gamma$ -Al<sub>2</sub>O<sub>3</sub> catalyst pellets placed in the reactor. The ns pulse discharge is operated while monitored until the ammonia yield reaches steady state. After this, the sub-breakdown voltage RF waveform is turned on, the ammonia again monitored until steady state is reached, and then turned off. The results quantify the effect of N<sub>2</sub> vibrational excitation on the ammonia yield, compared to the mechanism driven by the reactions of the plasma-generated N and H atoms on the catalyst surface.

## References

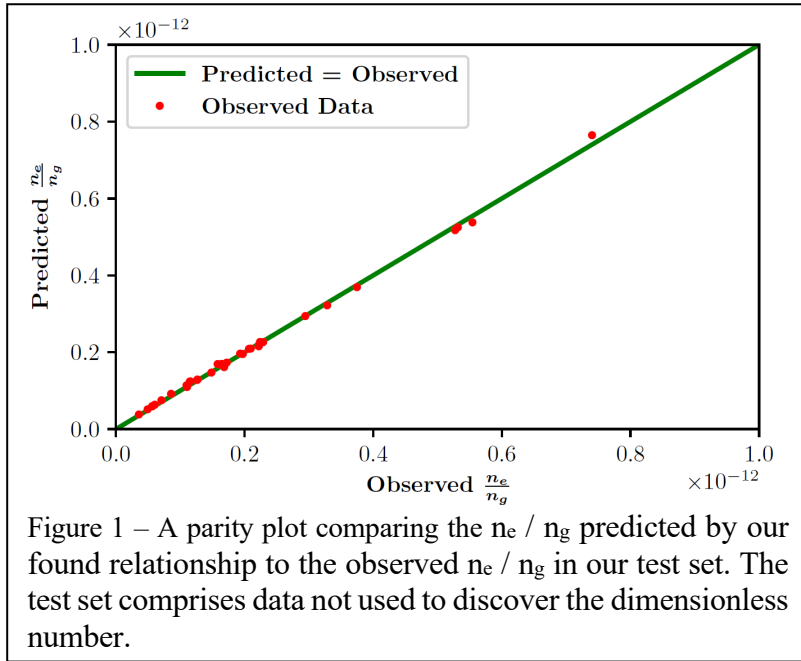
- [1] X. Yang et al, Plasma Sources Sci. Technol. **32**, 064003 (2023).
- [2] I. Gulko et al, Plasma Sources Sci. Technol. **29**, 104002 (2020).

# [PI-13] Data-Driven Dimensionless Number Discovery in a Nanosecond Pulsed Low Temperature Plasma

Victor Miller, Ketong Shao and Ali Mesbah

Department of Chemical and Biomolecular Engineering, University of California, Berkeley  
(vmiller1671@berkeley.edu, ketong\_shao@berkeley.edu, mesbah@berkeley.edu)

Emerging applications of low-temperature plasmas (LTPs), such as medicine or chemical synthesis, entail interactions with complex interfaces, which are generally not well-understood. Establishing scaling relations from plasma and surface diagnostics can aid in understanding of how various plasma and interface variables scale with each other and with manipulable process parameters, isolating underlying behavior and shedding light on fundamental mechanisms of plasma-interface interactions. Scaling relations can be established with dimensionless numbers [1]. In this work, we extend the dimensionless number discovery method of [2] to study the behavior of an atmosphere-pressure nanosecond pulsed He plasma.



Process inputs include voltage, flow rate, reactor volume, pulse time, off-pulse time, and packing bead diameter (zirconia). We measure the off-pulse electron temperature by optical emission spectroscopy (OES) and the current. A 0D model is used to infer the electron temperature and the electron density; it also serves to suggest what discharge parameters might be relevant. We predict how the ratio of electron density to gas density ( $n_e / n_g$ ) varies with process inputs and reactor geometry; we also predict how the ratio of electron temperature to gas temperature varies ( $T_e / T_g$ ).  $n_e / n_g$  is related to the degree of ionization;  $T_e / T_g$  is related to the energy that goes into the electrons versus the surrounding gas; both are important parameters for plasma behavior.

As a sample result, Figure 1 illustrates the capacity of the discovered dimensionless number to predict  $n_e / n_g$  for data points outside the training set is very strong. The key finding of this work is that a combination of physics and data can yield interpretable, flexible models. The next steps are (i) to improve the discovery method to yield more whole-number exponents, (ii) to extend this method to find dimensionless time-dependent equations, and (iii) to account for more complex discharges with many collisional processes, such as atmospheric air discharges.

## References

- [1] G. Barenblatt. Cambridge Texts in Applied Mathematics. *Scaling*, Cambridge University Press, 2003
- [2] X. Xie, A. Samaei, J. Guo, W. K. Liu, and Z. Gan; Nat Comms, **13**, 1, 7562, 2022



# [PI-14] Electron-Field Instability: Excitation of Electron Plasma Waves by an Electric Field

Lucas Beving<sup>a</sup>, Scott Baalrud<sup>b</sup>, and Matthew Hopkins<sup>a</sup>

(a) Sandia National Laboratories (lpbevin@sandia.gov)

(b) University of Michigan (baalrud@umich.edu)

Electric fields are common in plasmas, especially ambipolar fields in quasineutral regions, and affect transport by driving currents and, in some cases, instabilities. The condition for instability in collisionless plasmas is understood via the Penrose criterion [1], which quantifies the relative drift between different populations of particles that must be present for wave amplification via inverse Landau damping. For example, electric fields drive drifts between electrons and ions that can excite the ion-acoustic instability. Here, we use particle-in-cell (PIC) simulations and linear stability analysis to show that electric fields can drive a fundamentally different type of kinetic instability, named the electron-field instability.

This work builds on earlier theoretical work [2], where such an instability was predicted, but the authors were unsure of the validity of their linearizing assumptions. PIC simulations allow us to test their predictions in a fully nonlinear setting, precluding any linearizing assumptions.

One hallmark of a plasma instability is the exponential growth of fluctuations in the electric field. We observe such growth of the electric field in our simulations as shown in Fig. 1. The simulations represented in Fig. 1 utilized an applied field of -800 V/m, which leads to relatively fast growth of the instability and short simulation times. Alternatively, simulations with smaller applied fields, which are more representative of quasineutral plasma regions, also drive instability, but at a slower rate.

In general, this instability excites electron plasma waves with wavelengths  $> 30\lambda_{De}$ , has a growth rate that is proportional to the electric field strength, and does not depend on the relative drift between electrons and ions, which does not satisfy the Penrose criterion. Fluctuations formed by the instability oscillate near the electron plasma frequency, further distinguishing it from the ion-acoustic instability, which oscillates near the ion plasma frequency. The ubiquity of electric fields in plasmas suggests that this instability is possible in a host of systems, including low-temperature and space plasmas. In fact, damping from neutral collisions in such systems is often not enough to completely damp the instability, adding to the robustness of the instability across plasma conditions.

This work was supported by DOE grant No. DE-SC0022201. This work used the capabilities of the SNL Plasma Research Facility, supported by DOE SC FES. SNL is managed and operated by NTESS under DOE NNSA contract DE-NA0003525.

## References

- [1] O. Penrose, Phys. Fluids, **3** 258 (1960).
- [2] B. Fried, M. Gell-Mann, J. Jackson, and H. Wyld, J. Nucl. Energy. **1**, 190 (1960).

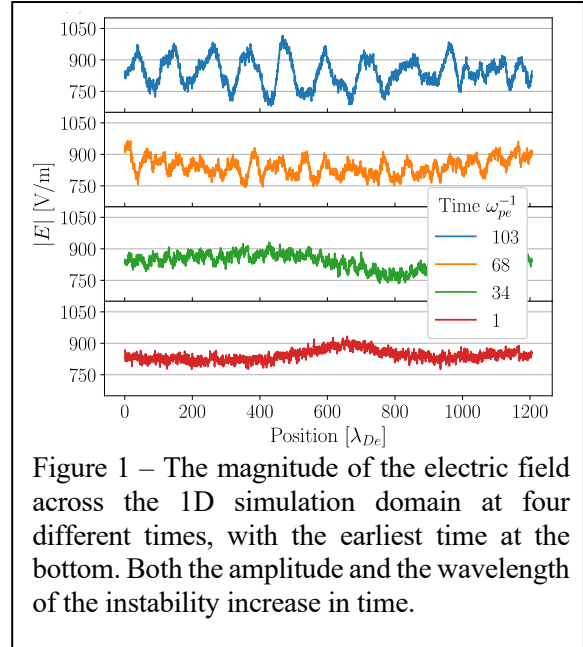


Figure 1 – The magnitude of the electric field across the 1D simulation domain at four different times, with the earliest time at the bottom. Both the amplitude and the wavelength of the instability increase in time.

# [PI-15] Interpretable Attention-Based Transfer Learning for Plasma Catalysis

Ketong Shao and Ali Mesbah

University of California, Berkeley (ketong\_shao@berkeley.edu, mesbah@berkeley.edu)

The integration of heterogeneous catalysis with low-temperature plasma (LTP) processes has been a topic of significant interest, with notable success observed in enhancing energy efficiency, exemplified by plasma-catalytic ammonia synthesis [1]. The pursuit of effective catalyst selection for LTP processes, as well as the elucidation of design principles for LTP-assisted chemical reactors, has become increasingly important. However, a significant challenge arises in obtaining experimental data that can identify surface species and measure binding energies relevant to LTP-catalytic behavior. Traditional diagnostics methods, which have proven effective in thermal heterogeneous catalysis, encounter difficulties when applied to LTP systems during experiments [2]. Herein, density functional theory (DFT) calculations have emerged as an indispensable tool for modeling plasma-surface interactions and have shown promise in unraveling the intricacies of LTP-catalytic processes [3]. However, DFT calculations for charged surfaces within LTP-catalytic processes are not only expensive, but also significantly more involved due to plasma-surface interactions.

To address these challenges, we are developing a machine learning architecture based on graph neural networks and natural language processing that harnesses the power of cross-domain transfer learning from thermal catalysis. This model architecture leverages two large pretrained neural networks from literature, which are trained using millions of thermal catalysis data points. As shown in Fig. 1, the left part is a graph neural network which is fixed to maintain the knowledge from thermal catalysis. An adaptor is added to account for system and simulation mismatches (i.e., catalytic system and software difference). The right part is a pretrained attention-based network [4], which is fine-tuned to capture charge-surface interactions. We will employ this architecture to study plasma-catalytic ammonia synthesis. The proposed model will enable rapidly screening out uninteresting catalyst candidates. This reduces the number of DFT calculations required for LTP-catalysis studies by narrowing down more expensive investigations to promising candidates. Furthermore, attention-based networks are physically interpretable, which will allow us to quantify the interactions between plasma and catalyst due to charge effects, as well as to identify the most important process parameters from scarce data.

This project is being carried out in collaboration with Prof. Yiguang Ju' group. We have obtained DFT-calculated structures for ammonia synthesis under the presence of charged particles using five different metal atoms and seven different molecules. Our current progress includes perturbing the optimized structures to expand our dataset and establishing a preliminary attention-based hybrid graph neural network.

## References

- [1] K. M. Bal et al. *PSST*. 27.2, 024001, (2018).
- [2] J. Hong et al. *ACS Sustain. Chem. Eng.* **6.1**, 15-31 (2018).
- [3] S. Zhang et al. *J. Phys. D: Appl. Phys.* **54.21**, 213001 (2021).
- [4] J. Zhang et al. *Joule*. **7.8**, 1832-1851 (2023)

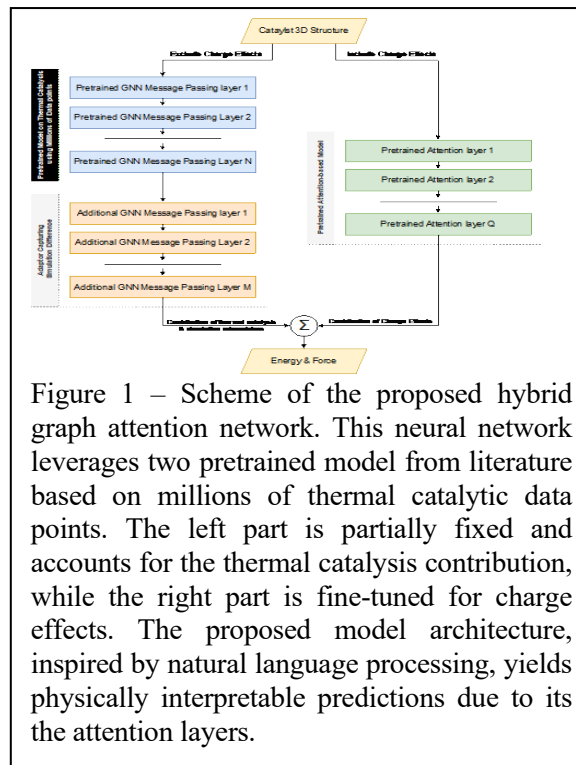


Figure 1 – Scheme of the proposed hybrid graph attention network. This neural network leverages two pretrained model from literature based on millions of thermal catalytic data points. The left part is partially fixed and accounts for the thermal catalysis contribution, while the right part is fine-tuned for charge effects. The proposed model architecture, inspired by natural language processing, yields physically interpretable predictions due to its the attention layers.

# [PI-16] Spatially- and Time-Resolved Measurements of HO<sub>2</sub> Radicals in a Ns Pulse Atmospheric Pressure Plasma Jet

Hamzeh Telfah, Sai Raskar, and Igor V. Adamovich

Nonequilibrium Thermodynamics Laboratory, Department of Mechanical and Aerospace Engineering, The Ohio State University, Columbus, OH 43210 (telfah.1@osu.edu, raskar.1@osu.edu, adamovich.1@osu.edu)

The absolute, spatially-resolved, and time-resolved number density of the hydroperoxyl radical is measured in a quasi-two-dimensional, atmospheric pressure “curtain” plasma jet powered by a train of ns discharge pulses. The plasma is sustained in an H<sub>2</sub>O vapor – O<sub>2</sub> – He flow with a co-flow of dry air, impinging on a copper foil target. The water vapor is added to the baseline O<sub>2</sub>-He flow in a bubbler filled with distilled, deionized water. The measurements are made using the previously developed pulsed Cavity Ring Down Spectroscopy (CRDS) diagnostic near 1.5 μm [1, 2]. The ring-down cavity is formed between two high-reflectivity mirrors placed at the ends of the stainless steel “arms” purged with dry air, with the plasma jet placed in the gap between the arms. Both the water vapor in the jet and HO<sub>2</sub> generated in the plasma have been measured. The results exhibit a rapid accumulation of HO<sub>2</sub> during the ns pulse discharge burst, which was in fair agreement with modeling prediction if power density is reduced, followed by the decay in the afterglow on a ms time scale, which in turn, was in large discrepancy with the kinetic modeling predictions, even with reduced power density. In the O<sub>2</sub>-He plasma jet (without the water vapor added) impinging on a liquid water surface, HO<sub>2</sub> has not been detected. The most likely reason is the rapid decay of the metastable He atoms and O atoms generated in the plasma in the evaporation/mixing layers, which precludes the efficient generation of H atoms, which are the dominant precursors for HO<sub>2</sub> generation. The present approach demonstrates the feasibility of time-resolved, *in situ* CRDS measurements of radicals and excited species in the ambient air plasma environments extended along the laser beam path.

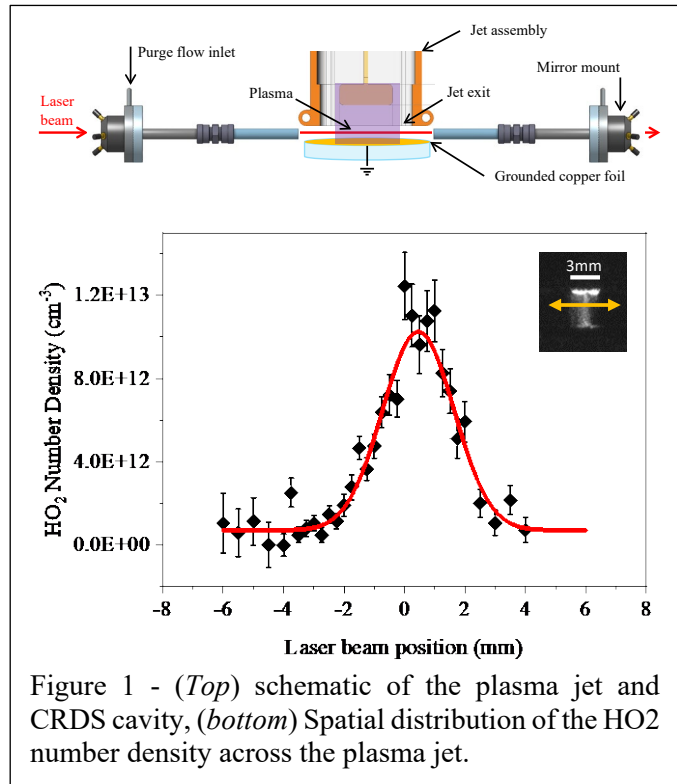


Figure 1 - (Top) schematic of the plasma jet and CRDS cavity, (bottom) Spatial distribution of the HO<sub>2</sub> number density across the plasma jet.

## References

- [1] E.R. Jans, X. Yang, I.W. Jones, T.A. Miller, J.F. Stanton, and I.V. Adamovich, *Combustion and Flame* **241** (2022) 112097.
- [2] H. Telfah, E. Jans, S. Raskar, and I.V. Adamovich, “Kinetics of HO<sub>2</sub> Radical Formation and Decay in Ns Pulse O<sub>2</sub>-He Plasmas over a Liquid Water Surface”, *Plasma Sources Science and Technology* **31** (2022) 115019.

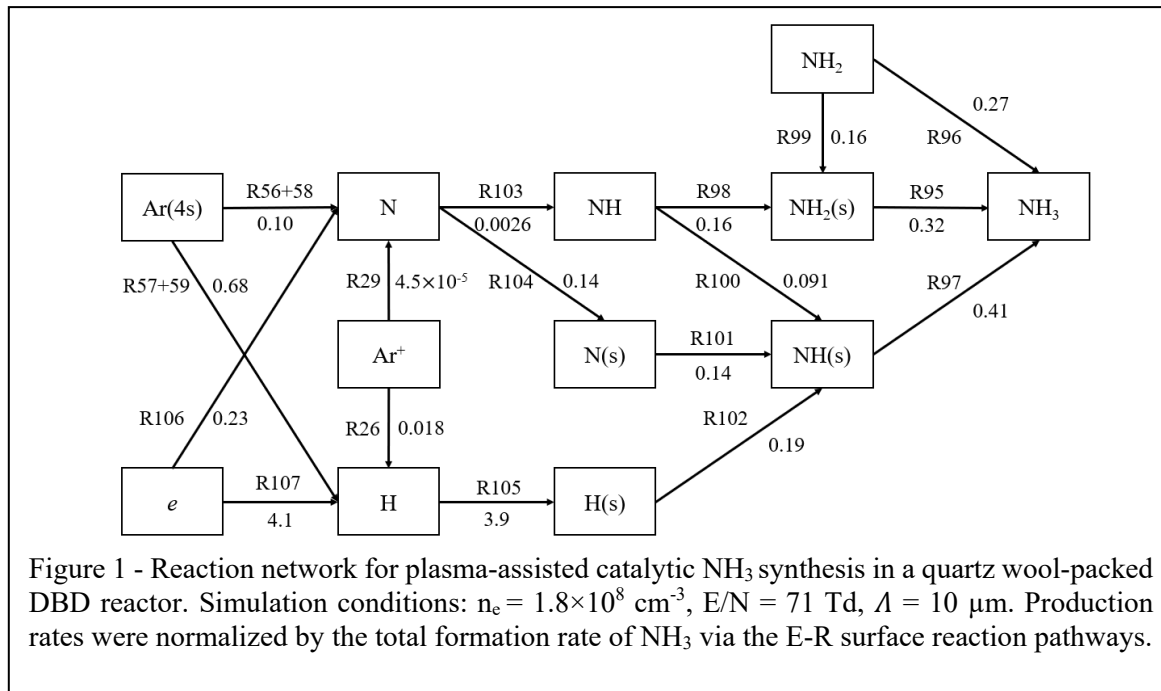
# [PII-1] Kinetic Modeling Analysis of Ar Addition to Atmospheric Pressure N<sub>2</sub>-H<sub>2</sub> Plasma for Plasma-Assisted Catalytic Synthesis of NH<sub>3</sub>

Zihan Lin <sup>a</sup>, Shota Abe <sup>b</sup>, Zhe Chen <sup>a</sup>, Surabhi Jaiswal <sup>a</sup> and Bruce E. Koel <sup>a</sup>

(a) Department of Chemical and Biological Engineering, Princeton University (zhl030613@gmail.com)

(b) Princeton Plasma Physics Laboratory (sabe@pppl.gov)

Zero-dimensional kinetic modeling of atmospheric pressure Ar-N<sub>2</sub>-H<sub>2</sub> nonthermal plasma was carried out to gain mechanistic insights into ammonia formation during plasma-assisted catalytic synthesis of ammonia. The kinetic model was developed for a coaxial dielectric barrier discharge (DBD) quartz wool-packed bed reactor operating at near room temperature using a kHz-frequency plasma source. With 30% Ar mixed in a 1:1 N<sub>2</sub>-H<sub>2</sub> plasma at 760 Torr, we find that NH<sub>3</sub> production is dominated by Eley-Rideal (E-R) surface reactions, which heavily involve surface NH<sub>x</sub> species derived from N and H radicals in the gas phase, while the influence of excited N<sub>2</sub> molecules is negligible. This is contrary to the commonly proposed mechanism that excited N<sub>2</sub> molecules created by Penning excitation of N<sub>2</sub> by Ar(4s) and Ar(4p) plays a significant role in assisting NH<sub>3</sub> formation. Our model shows that the enhanced NH<sub>3</sub> formation upon Ar dilution is unlikely due to the interactions between Ar and H species, as excited Ar atoms have a weak effect on H radical formation through H<sub>2</sub> dissociation compared to electrons. We find that excited Ar atoms contribute to 28% of the N radical production in the gas phase via N<sub>2</sub> dissociation, while the rest is dominated by electron-impact dissociation. Furthermore, Ar species play a negligible role in the product NH<sub>3</sub> dissociation. N<sub>2</sub> conversion sensitivity analyses were carried out for electron density ( $n_e$ ) and reduced electric field (E/N), and contributions from Ar to gas-phase N radical production were quantified. The model can provide guidance on potential reasons for observing enhanced NH<sub>3</sub> formation upon Ar dilution in N<sub>2</sub>-H<sub>2</sub> plasmas beyond changes to the discharge characteristics.



## Reference

[1]. Z. Lin, S. Abe, Z. Chen, S. Jaiswal, B.E. Koel, *J. Phys. Chem. A* (2023), under review. <https://arxiv.org/abs/2310.03307>.

## [PII-2] The Role of Dielectric Properties of Biological Targets in Non-thermal Plasma Treatment

Sophia Gershman<sup>a</sup>, Julia Sutter<sup>b</sup>, Jascha Brettschneider<sup>b</sup>, Sara Mamchur<sup>c</sup>, Fred Krebs<sup>b</sup>, Vandana Miller<sup>b</sup>

(a) US DOE Princeton Plasma Physics Laboratory, Princeton, NJ, USA (sgershma@pppl.gov)

(b) Department of Biological Sciences, Drexel University, Philadelphia, PA, USA

(c) Center for Molecular Virology and Gene Therapy, Institute for Molecular Medicine and Infectious Disease and Department of Microbiology and Immunology, Drexel University College of Medicine, PA

The current understanding of the effects of nonthermal plasma (NTP) on living cells extends beyond plasma induced chemistry to include physical effects such as electric and electromagnetic fields. In addition, there is a growing recognition of the feedback effects of the treated cell suspensions on the properties of the applied NTP. The concept of adaptive plasma that changes as it both alters the substrate and adjusts in response to the properties of the treated material has been suggested as a way to control plasma applications.[1] In this study we explore the changes in the properties of the applied NTP depending on the type and the viability of cells during an in vitro treatment of cell suspensions.[2] Cell suspensions are treated with NTP produced by a floating electrode dielectric barrier discharge and therefore become a part of the overall electrical circuit. Operando electrical measurements are used to determine the load impedance and changes thereof for various cell suspensions. We compare the changes in the impedance of cell media, live Viro cells, and cells of reduced viability, since these changes affect the properties of the power delivered during NTP treatment. We show that the effective capacitance of the circuit during discharge for heat inactivated and lysed cells compared to the live cells. A similar trend is observed for plasma inactivated cells. The measured increase in equivalent capacitance correlates with the trends in the dielectric permittivity of the cell suspensions. This study confirms that the control of the power input conditions and treatment time are insufficient for the control of NTP dose in biomedical applications.[2]

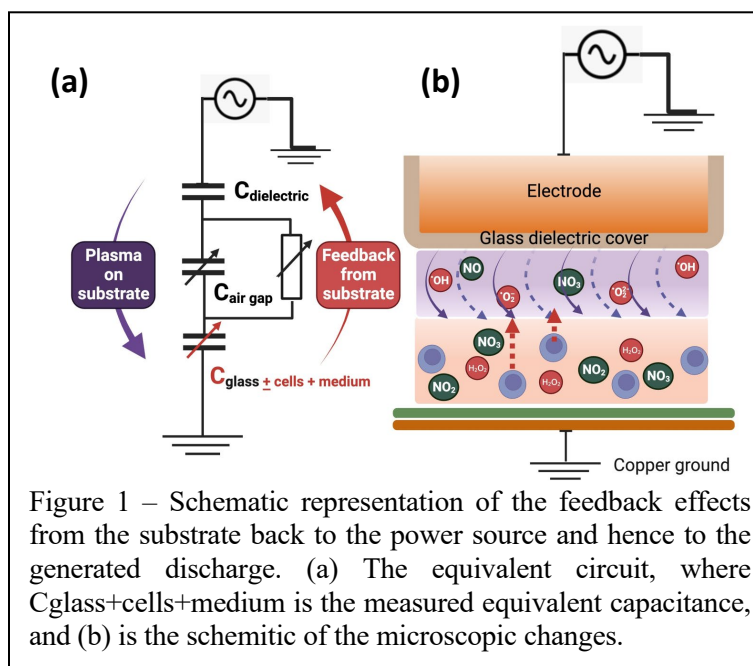


Figure 1 – Schematic representation of the feedback effects from the substrate back to the power source and hence to the generated discharge. (a) The equivalent circuit, where  $C_{\text{glass+cells+medium}}$  is the measured equivalent capacitance, and (b) is the schematic of the microscopic changes.

### References

- [1] M. Keidar, et al. Trends Biotechnol 36, 586-593 (2018).
- [2] J. Sutter, et al., Plasma 6(3), 577-591 (2023).

# [PII-3] Study of Surface Interactions During Plasma Catalytic Dry Reforming of Methane

Michael Hinshelwood and Gottlieb S. Oehrlein

Department of Materials Science and Engineering and the Institute for Research in Electronics and Applied Physics, University of Maryland, College Park, MD 20742, USA (oehrlein@umd.edu)

Dry reforming of methane (DRM) at atmospheric pressure is a potential process for converting methane and carbon dioxide into synthesis gas ( $H_2$  and  $CO$ ), which may be used for producing other valuable products such as methanol or ammonia [1]. Catalysts are prone to coking during the DRM process which degrades the reaction efficiency. Atmospheric-pressure non-equilibrium plasma may be a useful tool for enhancing the DRM reaction or preventing coke build up. The surface mechanisms resulting in these potential benefits are not understood. To study the interaction of plasma and catalyst we use a remote plasma-catalysis setup with a standard design plasma jet. The plasma plume is interacted with a  $Ni-SiO_2/Al_2O_3$  catalyst, a material common in DRM. Diffuse reflectance infrared Fourier transform spectroscopy (DRIFTS) is used to analyze adsorbed species on the catalyst surface and Fourier transform infrared spectroscopy (FTIR) is used to quantify products downstream of the plasma-catalyst coupling.

Ar gas is flown through the jet, while gas mixtures of Ar,  $CH_4$  and  $CO_2$  are introduced downstream of the plasma into the reaction chamber, producing a similar effect as a shielding gas. This prevents coke formation within the plasma jet and allows for reactive species produced from  $CH_4$  or  $CO_2$  entrainment in the plume to be formed closer to the catalyst surface.

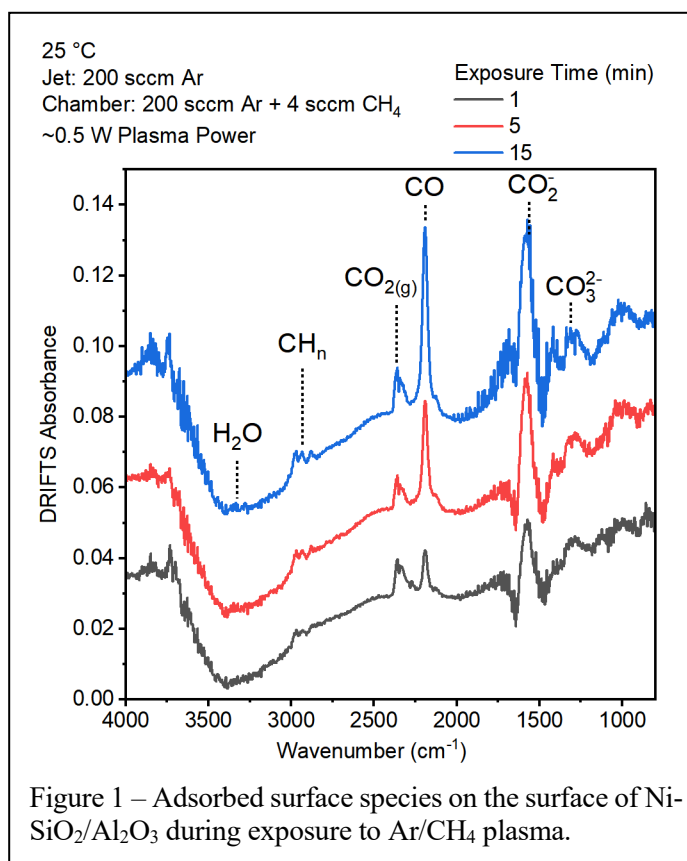
DRIFTS measurements reveal that exposure to Ar plasma with Ar/ $CH_4$  chamber gas results in the buildup of hydrogenated carbon, carbonate, and CO species on the catalyst surface. This is shown in figure 1.

Similar species may form during catalyst coking and deactivation [2]. Variation of such peaks with catalyst temperature and plasma composition can shed light on surface interactions important for plasma dry-reforming. Time-dependent correlations of surface species and downstream products will be discussed to inform development of future reaction systems.

This material is based upon work supported by the U.S. Department of Energy, Office of Science, Office of Fusion Energy Sciences under award number DE-SC0020232.

## References

- [1] Knoll, A. J., S. Zhang, M. Lai, P. Luan, and G. S. Oehrlein, *J. Phys. D: Appl. Phys.* **52**, 225201 (2019)
- [2] Zhang, S., Y. Li, A. Knoll, and G. S. Oehrlein, *J. Phys. D: Appl. Phys.* **53**, 215201 (2020)



## [PII-4] Particle-In-Cell Simulations of the Anode Sheath in DC Discharges

Grant M. Gorman<sup>a</sup>, Matthew M. Hopkins<sup>a</sup>, and Vladimir I. Kolobov<sup>b</sup>

(a) Sandia National Laboratories (gmgorma@sandia.gov)

(b) The University of Alabama in Huntsville (vladimir.kolobov@uah.edu)

The behavior of plasma in the anode region of a DC discharge is complex due to its dependence on the geometry of the anode, gas type and pressure, and discharge current. The anode plasma sheath displays interesting phenomena such as self-organization into complicated stationary or moving patterns and sign reversal of the potential drop in the anode sheath. Understanding this behavior is an ongoing effort due to its importance in developing a general theory for gas discharges and designing charged particle sources. A recently developed kinetic theory has identified four different regimes of differing behavior in the anode region that depend on relative values of characteristic length scales such as spatial discharge dimensions, electron mean free path, electron energy relaxation length, and the distance over which the electrons gain energy equivalent to the first atomic excitation potential,  $\lambda_e$ . [1]

This poster will overview the characterization and properties of these four regimes and describe our initial efforts to use Sandia's massively parallel PIC-DSMC plasma simulation code, Aleph, to model the electron-diffusion-dominated regime, where the electron mean free path is larger than the discharge tube radius and  $\lambda_e$ . In this regime, the length of the anode region is comparable to the electron mean free path, leading to a highly anisotropic electron energy distribution function and longitudinal electron transport that can occupy a mode of positive or negative anode potential drop. [2]

### References

[1] V. Kolobov and V. Nemchinsky, APS GEC Abstract: SR3.00004 (2020).

[2] V. Martens, Elsevier **218**, 112675 (2023).

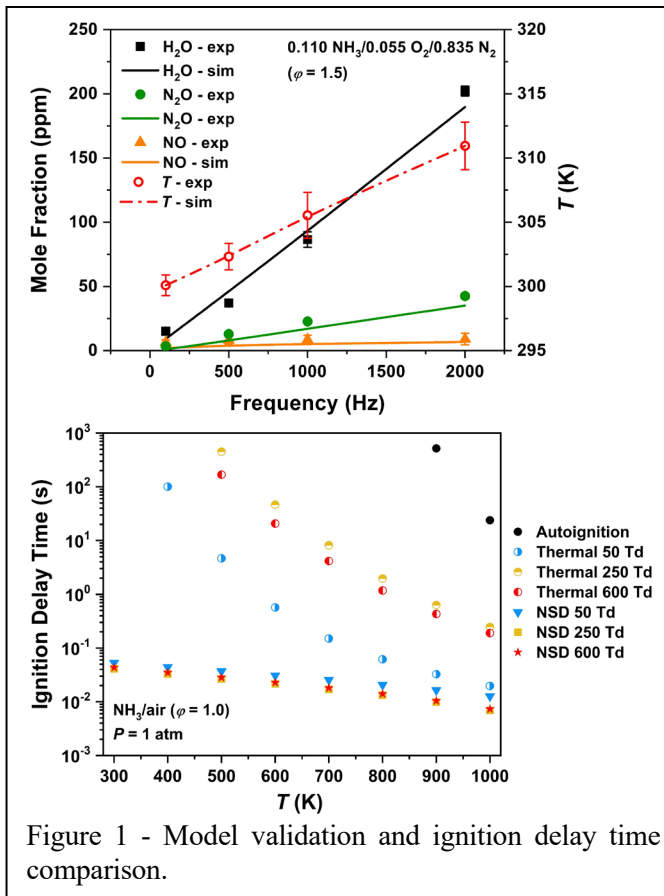
This work used the capabilities of the SNL Plasma Research Facility, supported by DOE SC FES. SNL is managed and operated by NTESS under DOE NNSA contract DE-NA0003525.

# [PII-5] Ignition Enhancement and NO<sub>x</sub> formation of NH<sub>3</sub>/air mixtures by Non-equilibrium Plasma Discharge

Xingqian Mao, Hongtao Zhong, Ning Liu, Ziyu Wang and Yiguang Ju

Department of Mechanical and Aerospace Engineering, Princeton University, Princeton, NJ 08544, USA  
(xingqian@princeton.edu)

This work computationally studies plasma assisted low temperature NH<sub>3</sub>/air ignition and NO<sub>x</sub> formation in a repetitively-pulsed nanosecond discharge at atmospheric pressure by using an experimentally-validated plasma-combustion kinetic model [1]. The results show that plasma discharge significantly enhances low temperature NH<sub>3</sub> ignition. Compared with thermal ignition, the ignition delay time is shortened by 2-5 orders of magnitude due to the kinetic enhancement of excited species and radicals. The radicals (NH<sub>2</sub>, NH, H and O) produced through electron impact dissociation and quenching of electronically excited N<sub>2</sub><sup>\*</sup>, O(<sup>1</sup>D) and N(<sup>2</sup>D) promote OH production and further accelerate NH<sub>3</sub> oxidation. The results show that there exists a non-monotonic dependence of ignition delay time on the reduced electric field strength. The optimum ignition enhancement is achieved at 250 Td at which the production of electronically excited species and radicals is most efficient. The vibrationally excited species produced at lower electric fields (<100 Td) are less effective in enhancing ignition



because they only induce gas heating through the fast vibrational-translational relaxation by NH<sub>3</sub> and H<sub>2</sub>O. At a higher electric field, although the efficient production of NH<sub>2</sub>, NH, H, O and OH by plasma creates new low temperature reaction pathways in enhancing low temperature NH<sub>3</sub> ignition, the ignition is inhibited through NH + NO = N<sub>2</sub>O + H and chain-termination reaction NH<sub>2</sub> + HO<sub>2</sub> = NH<sub>3</sub> + O<sub>2</sub>. The ignition delay times at different equivalence ratios show that the ignition enhancement by plasma is more effective at fuel-lean conditions due to the faster generation of N<sub>2</sub>(B), O(<sup>1</sup>D) and O from air, leading to accelerated NH<sub>3</sub> oxidation via O(<sup>1</sup>D) + NH<sub>3</sub> → NH<sub>2</sub> + OH, NH<sub>3</sub> + O = NH<sub>2</sub> + OH and NH<sub>2</sub> + O = NH + OH. The sensitivity analysis shows that the reactions involving O and O(<sup>1</sup>D) production are more effective on NH<sub>3</sub> ignition enhancement than the fuel dissociation by electrons. Moreover, the ignition is also enhanced by NO<sub>x</sub> formation in plasma via reactions NH<sub>2</sub> + NO = NNH + OH and NO + HO<sub>2</sub> = NO<sub>2</sub> + OH. This work advances the understanding of non-equilibrium excitation and NO<sub>x</sub> formation by plasma discharge on low temperature NH<sub>3</sub> ignition [2].

## References

- [1] H. Zhong, X. Mao, N. Liu, Z. Wang, T. Ombrello and Y. Ju, Combust. Flame **256**, 112948 (2023).
- [2] X. Mao, H. Zhong, N. Liu, Z. Wang and Y. Ju, Combust. Flame (In press).



# [PII-6] Molecular Dynamics Simulation of Vapor-Phase Nucleation of Metal Nanoparticles in a Reactive Plasma Atmosphere

Louis E. S. Hoffenberg<sup>a</sup>, Alexander Khrabry<sup>b</sup>, Yuri Barsukov<sup>b</sup>, Igor D. Kaganovich<sup>b</sup>, and David B. Graves<sup>a</sup>

(a) Princeton University Department of Chemical and Biological Engineering  
(lhoff@princeton.edu, dgraves@princeton.edu)

(b) Princeton Plasma Physics Laboratory  
(akhrabry@pppl.gov, yvbarsuk@pppl.gov, ikaganov@pppl.edu)

Metallic nanoparticles (NPs) offer a wide range of applications in electronics, energy, biology, catalysis, and the production of carbon nanomaterials like carbon nanotubes (CNTs). Synthesis of NPs from the vapor phase using plasma methods such as spark discharge generation is promising for industrial scalability. The behavior of nucleating systems in reactive environments, especially reactive *plasma* environments, is understudied. Moreover, charge-induced dipole interactions between ions and neutrals are thought to play a key role in the nucleation, coalescence, and aggregation of NPs in dusty plasmas [1]. Because the length scales and timescales associated with vapor-phase NP formation are too small to effectively probe experimentally, a promising alternative is molecular dynamics (MD) simulation. MD can give strong insight into the nanoparticle formation process with its atomic resolution. In this work, we use MD simulations with a reactive forcefield to study iron vapor nucleation in the presence of ions, radicals, and molecular species relevant to the production of CNTs (i.e., H, H<sub>2</sub>, C, CH, CH<sub>2</sub>, CH<sub>3</sub>, CH<sub>4</sub>, C<sub>2</sub>, C<sub>2</sub>H, C<sub>2</sub>H<sub>2</sub>, and ions). The effects of atomic-scale phenomena on metal vapor nucleation and nanoparticle behavior in a plasma environment will be discussed.

## References

[1] S. L. Girshick, *J. of Vac. Sci. Technol.* **38.1**, 011001 (2020).

## [PII-7] Improved Matching and Power Measurements in PICI Reference RF Jet

Mahreen Khan<sup>a</sup>, Josh Morsell<sup>b</sup>, Steven Shannon<sup>b</sup>, and Peter Bruggeman<sup>a</sup>

(a) Department of Mechanical Engineering, University of Minnesota  
(b) Department of Nuclear Engineering, North Carolina State University  
(fmahreen@umn.edu, pbruggem@umn.edu)

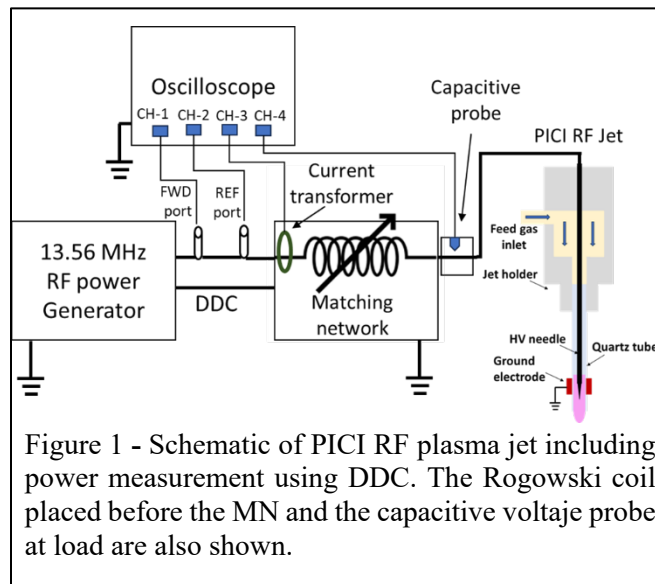
Two factors are imperative for ensuring the reliability of RF-based plasma applications: efficient energy deposition into the load and the accurate measurement of the deposited RF power in the plasma. Commercially available matching networks (MN) are not readily accessible for matching high capacitance miniaturized RF plasma jets thereby posing a significant challenge in achieving ideal tuning. Here, we propose the implementation of a MN featuring a variable inductor. This approach enhances the matching of the PICI RF plasma jet and leads to increased power deposition. The MN managed to operate the plasma jet with only 5 W supplied from RF generator.

Among the most employed tools for power measurement are voltage (V) and current (I) probes. The direct application of V-I probes at the plasma load is challenging in miniaturized RF plasma jets. Despite using meticulously calibrated probes at the plasma jet load, instances may occur when the measured phase shift between V and I will surpass  $90^\circ$  (yielding unrealistic power measurements) due to the inaccuracy in the phase shift measurement [1]. To avoid the load influence, a different approach to power measurement was used by placing V-I probes before the MN [2]. Nonetheless, this requires a subtractive power method to account for the power losses in the MN.

Given a need for the detailed calibration of V-I probes, we explored a more robust alternative—an electrical sampling method utilizing a Dual-Directional Coupler (DDC). The V-I probes have been effectively replaced by the DDC while using the subtractive power method. DDC-based power measurements were performed using two approaches for estimating the matcher losses: (i) ensuring the same current in plasma-on and plasma-off conditions (using a Rogowski coil), (ii) maintaining a maximum load voltage in plasma-on and plasma-off conditions (using a capacitive voltage probe). Both measurements are conducted simultaneously and *in situ* (Figure 1). A precise calibration of the DDC is carried out using [3], and the coupling factors are employed to estimate the discharge power in the PICI RF jet. Measurements based on both approaches and with V-I probe measurements are found to be in good agreement. The DDC-based power measurement is straightforward, reproducible, and a real-time monitor of power which helps in immediate adjustments during operation and accurately controls the plasma processes.

### References

- [1] Mahreen et al., Rev. Sci. Instrum. **93** 123514 (2022).
- [2] S Hofmann et al., Plasma Sources Sci. Technol. **20** 065010 (2011)
- [3] M Dünnebier et al., Plasma Sources Sci. Technol. **24** 065018 (2015)



## [PII-8] Understanding Ionic Interactions and Distributions at Plasma-Liquid Interfaces and Their Influence on Liquid Phase Chemistry

Foluke Jennifer Ganzallo and Selma Mededovic Thagard

Department of Chemical and Biomolecular Engineering, Clarkson University, 13699, New York, USA  
(ganzalfj@clarkson.edu)

The study of plasma-liquid interactions is a complex and diverse field of research, giving rise to various applications. Ions play a crucial role in interfacial aqueous chemistry, particularly their mobility and distribution within the interface and the subsurface, all of which are controlled by electrostatic forces and different modes of transport. Plasma sheaths and electrical double layers result from these ionic interactions, and they play a vital role in controlling rates of chemical reactions at the plasma-liquid interface.

In this study, the behavior of ions subjected to an electric field was investigated by examining transformation (oxidation) pathways of ionic salts in the bulk liquid. A point-plane pulsed DC reactor with a gas discharge contacting the surface of a liquid was employed to oxidize alkali metal halide and ammonium halide salts for both positive and negative polarity discharges (Figure 1). It was found that the production rates of anion oxidation products measured in the liquid were higher for the positive polarity discharge, while the opposite was true for the oxidation products of cations. This behavior was explained by the interfacial concentrations of these ions which are controlled by the extent of their polarizability. The response of anions to the electric field generated by the plasma was also found to be dependent on the polarizing power of the accompanying cation in the salt solution. The cationic response to the electric field, however, only depended on the cation's polarizing power.

Based on these findings, a physical description of the ionic behavior at the plasma-liquid interface was proposed.

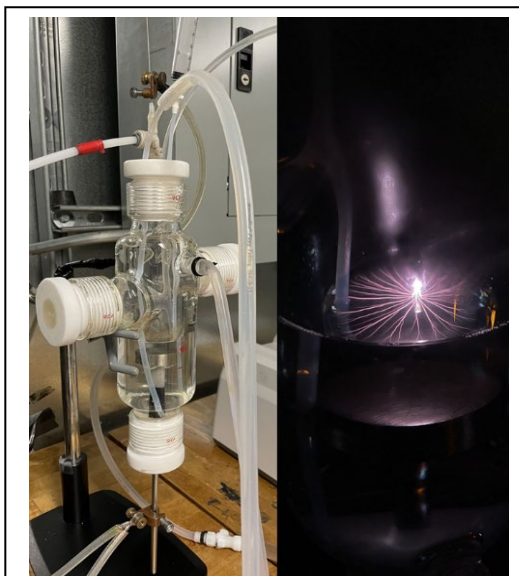


Figure 1 – Left: point-plane gas discharge reactor used in the experiments. Right: discharge in argon contacting the surface of a liquid.

## [PII-9] CH<sub>3</sub> Radical Generation in Microplasmas for Up-Conversion of Methane

Mackenzie Meyer<sup>a</sup>, Sanjana Kerketta<sup>a</sup>, Ryan Hartman<sup>b</sup> and Mark J. Kushner<sup>a</sup>

(a) University of Michigan (maemeyer@umich.edu, sanjana.kerketta@lamresearch.com, mjkush@umich.edu)

(b) New York University (ryan.hartman@nyu.edu)

Conversion of methane (CH<sub>4</sub>) into value-added compounds can be achieved through use of atmospheric pressure low-temperature plasmas generated in a dielectric barrier discharge (DBD). These plasmas can be formed in microchannels (< 0.1 mm square), commonly used in microfluidics due to controllable mass transfer between adjacent flows.

One novel approach to CH<sub>4</sub> up-conversion involves generating CH<sub>3</sub> radicals in the plasma, transporting the radicals to a liquid solvent in contact with the plasma, and capturing the CH<sub>3</sub> in the liquid through use of organic radical receptors or transition metal complexes. Once captured, the CH<sub>3</sub> radicals can be used to generate compounds of interest to the pharmaceutical industry.

The generation of CH<sub>3</sub> radicals in an Ar/CH<sub>4</sub>/H<sub>2</sub>O plasma generated in a microchannel is investigated using a 2D plasma hydrodynamics model (*nonPDPSIM*) and a 0D plasma chemistry model (*GlobalKin*). Results of *nonPDPSIM* examine the dynamics of the ionization wave (IW) and fluxes of CH<sub>3</sub> to the solvent surface over one pulse, while results of *GlobalKin* examine the chemistry over 20 pulses.

Many radicals and long-lived species are formed in the plasma, as shown in Figure 1 using *GlobalKin*. CH<sub>3</sub> is largely formed by electron-impact dissociation of CH<sub>4</sub> (43% of the CH<sub>3</sub> produced over the last pulse), CH<sub>2</sub> reacting with CH<sub>4</sub> (28%), and dissociative excitation transfer (DET) of CH<sub>4</sub> by Ar excited states (9%). CH<sub>3</sub> is consumed by formation of C<sub>2</sub>H<sub>6</sub> (88% of the CH<sub>3</sub> consumed over the last pulse), as well as formation of C<sub>3</sub>H<sub>8</sub> (10%) and CH<sub>3</sub>OH (0.5%).

The fluxes of CH<sub>3</sub> to the solvent layer are examined using *nonPDPSIM*. When the solvent is parallel to the IW propagation direction, the CH<sub>3</sub> flux is maximized at the top and bottom of the layer. However, when the solvent is placed perpendicular to the IW propagation, enhancement of the CH<sub>3</sub> flux occurs as the IW terminates on the solvent layer.

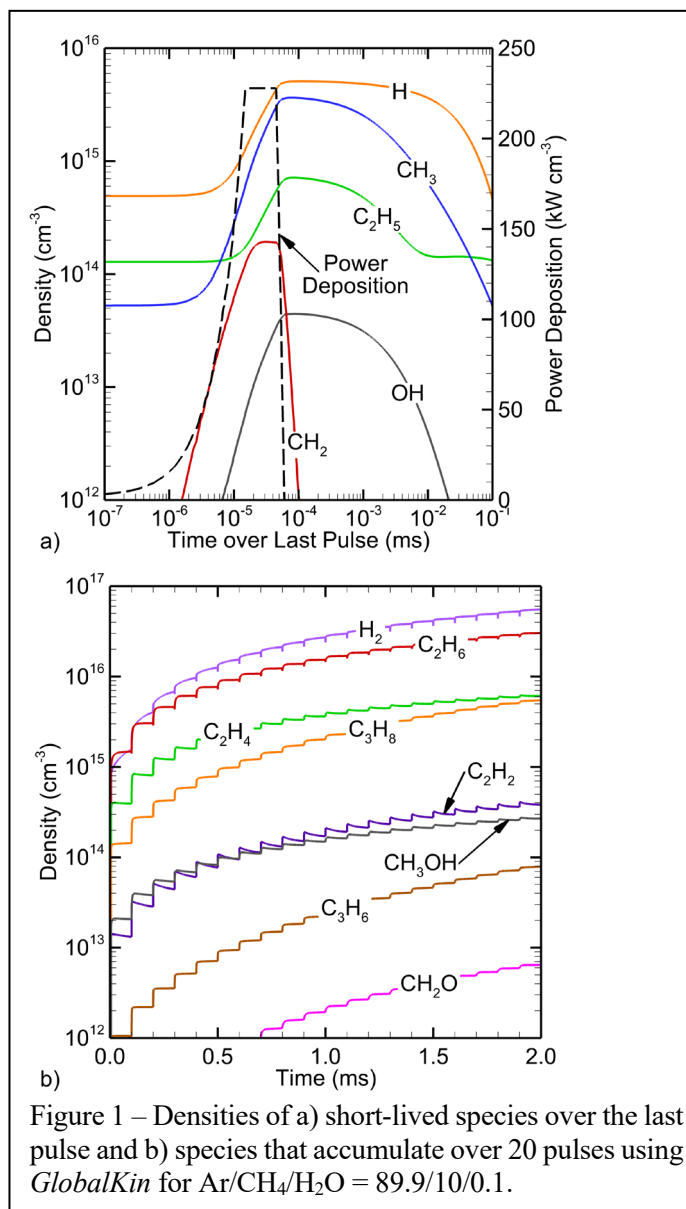


Figure 1 – Densities of a) short-lived species over the last pulse and b) species that accumulate over 20 pulses using *GlobalKin* for Ar/CH<sub>4</sub>/H<sub>2</sub>O = 89.9/10/0.1.

## [PII-10] Nickel Nitride on Plasma-Assisted Ammonia Synthesis over Nickel Catalysts

Yiteng Zheng<sup>a</sup>, Christopher Kondratowicz<sup>b</sup>, Zihan Lin<sup>a</sup>, Ari Gilman<sup>a</sup> and Bruce E. Koel<sup>a</sup>

(a) Department of Chemical and Biological Engineering, Princeton University, Princeton, New Jersey

(b) Department of Mechanical and Aerospace Engineering, Princeton University, Princeton, New Jersey  
(bkoel@princeton.edu)

The synergy between heterogeneous catalysts and excited gas-phase species generated by nonthermal plasma has been studied and has shown promising performance for multiple catalytic applications, such as ammonia synthesis, steam reforming of hydrocarbons, and dry reforming of methane. Among these reactions, plasma-assisted catalytic ammonia synthesis from  $N_2 + H_2$  is one of the most studied processes due to its simplicity and the high demand for ammonia as a feedstock for fertilizer production, and as a possible energy carrier. In order to optimize catalysts for plasma-assisted catalytic ammonia synthesis, a wide range of metals catalysts have been evaluated, and the reported activity trend in the presence of plasma was different from that of traditional thermal catalytic ammonia synthesis, and Ni and Co catalysts were reported to be more active than the benchmark Ru catalyst. Extensive experimental and computational efforts have been performed to understand the relationship between the plasma parameters and catalytic activity on Ni catalysts. Despite these efforts, fundamental structure-activity relationships for these catalysts are still missing. While Ni catalysts for plasma-assisted catalytic ammonia synthesis are always assumed to be in metallic form, Ni nitride was reported to be more active than metallic Ni catalysts for electrochemical ammonia synthesis. In traditional thermal catalytic ammonia synthesis, Ni nitride formation has usually been considered as negligible due to its poor thermal stability at the elevated temperatures. In plasma-assisted catalytic ammonia synthesis,  $NH_3$  can be produced at lower temperatures, and Ni nitride species could be formed and may be stable on catalyst surfaces. While there has been evidence obtained for Ni catalyst activation by surface accumulation of N-containing species, thus far there has been no in-depth catalytic study reported in the literature up to now on the formation and effects of Ni nitride in plasma-assisted ammonia synthesis. Herein, we report such results from a systematic catalytic study of the effect of Ni nitride on ammonia synthesis.

# [PII-11] Microkinetic Model for Low-Temperature Plasma Assisted Catalysis by Fe and Ni Catalysts for Ammonia Synthesis

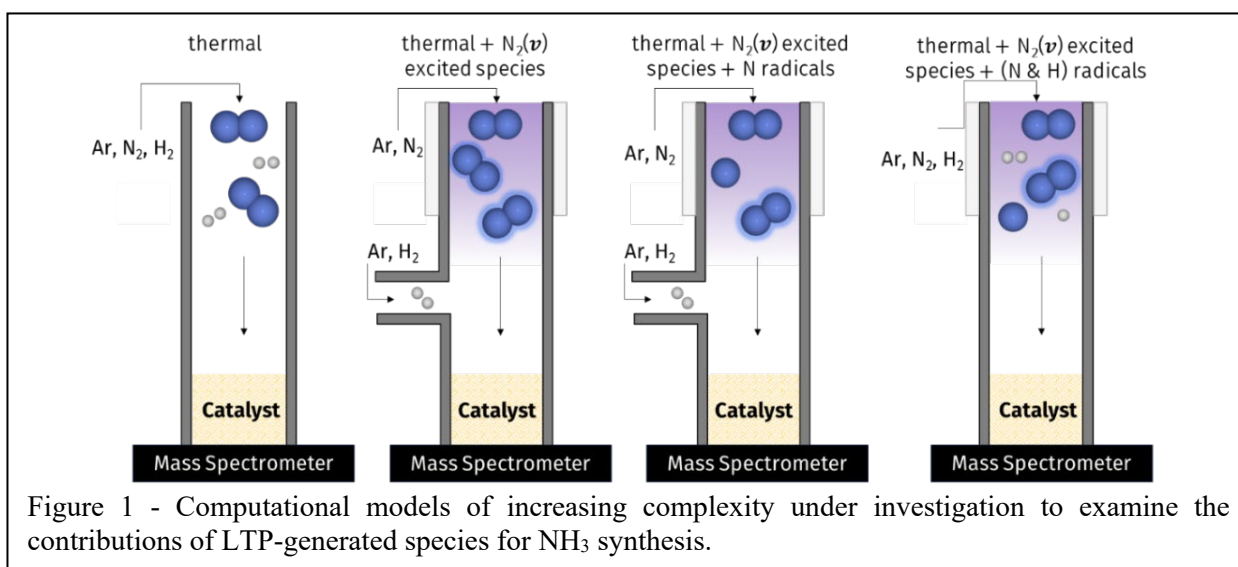
Oluwatosin Ohiro<sup>a</sup>, Brain Bayer<sup>b</sup>, Peter J. Bruggeman<sup>c</sup>, Aditya Bhan<sup>b</sup> and Bryan Goldsmith<sup>a</sup>

(a) Department of Chemical Engineering, University of Michigan. (bgoldsm@umich.edu)

(b) Department of Chemical Engineering, University of Minnesota. (abhan@umn.edu)

(c) Department of Mechanical Engineering, University of Minnesota. (pbruggem@umn.edu)

Combining heterogeneous catalysis with low temperature plasma (LTP) can produce ammonia ( $\text{NH}_3$ ) at near ambient temperatures and pressures by reacting plasma-derived species from  $\text{N}_2$  and  $\text{H}_2$ . However, LTP-assisted ammonia synthesis is a complex process consisting of many synergistic or competing effects that can give rise to the observed catalytic performance. One major challenge operating LTP reactions is determining the optimum level of ionization for molecular vibrational excitation and radical formation. In particular, there is uncertainty about which chemical species from a radiofrequency-driven atmospheric pressure jet predominantly contribute to the formation of  $\text{NH}_3$ . Multiple studies have attributed the increased  $\text{NH}_3$  formation rate due to vibrationally excited nitrogen chemical species ( $\text{N}_2(v)$ ) formed under LTP conditions. [1]  $\text{N}_2(v)$  species are postulated to reduce the activation barrier for  $\text{N}_2$  dissociation. A recent experimental study found a one-to-one consumption/production of N radicals and  $\text{NH}_3$  species on Fe, Ni and Ag catalysts, suggesting that N radical species facilitate the increased ammonia production rates, not  $\text{N}_2(v)$  species.[2] Herein, we construct various microkinetic models using density functional theory (DFT) based inputs to describe LTP-assisted ammonia synthesis (Figure 1) on Fe(110) and Ni(111) catalysts. Model inputs include equilibrium and rate constants for various gas phase and surface reactions, including  $\text{N}_2(v)$  and H radical concentrations measured from experiments. Our work seeks to elucidate the various contributions of LTP generated species (i.e.,  $\text{N}_2(v)$  and radical species) to the overall rate and determine which model best rationalizes our experimental measurements from a radiofrequency-driven atmospheric pressure jet-coupled catalytic reactor.



## References

[1] P. Mehta, P. Barboun, F. A. Herrera, J. Kim, P. Rumbach, D. B. Go, J. C. Hicks and W.F. Schneider. *Nat. Catal.* **1**:269–275 (2018).

[2] B. Bayer, P. J. Bruggeman and A. Bhan. *ACS Catal.* **13**(4):2619–30 (2023).

# [PII-12] Spatio-Temporal Electric Field Distributions in an Atmospheric Plasma Jet Impinging on a Microchannel Array Surface

Sai Raskar<sup>a</sup>, Kseniia Konina<sup>b</sup>, Igor V. Adamovich<sup>a</sup>, and Mark J. Kushner<sup>b</sup>

(a) Department of Mechanical and Aerospace Engineering, Ohio State University, Columbus, OH 43210  
(raskar.1@osu.edu, adamovich.1@osu.edu)

(b) Department of Electrical Engineering & Computer Science, University of Michigan, Ann Arbor, MI 48109 (kseniak@umich.edu, mjkush@umich.edu)

The electric field distribution in the ionization waves propagating over a microchannel array dielectric surface, with the channels either empty or filled with distilled water, is measured by ps Electric Field Induced Second Harmonic (EFISH) generation, developed in our previous work [1].

The surface ionization wave is initiated by the atmospheric pressure N<sub>2</sub>-Ar plasma jet impinging on the surface vertically and powered by ns pulse discharge bursts, shown in Fig. 1. The results show that the electric field inside the microchannels, specifically its horizontal component, is enhanced by up to a factor of 2. The field enhancement region is localized within the channels. The vertical electric field inside the channels lags in time compared to the field measured at the ridges, indicating the transient reversal of the ionization wave propagation direction across the channels (toward the jet). This is consistent with the phase-locked plasma emission images and confirmed by the kinetic modeling predictions, which show that the ionization wave “jumps” over the empty channels and propagates into the channels only after the jump between the adjacent ridges. When the channels are filled with water, the wave speed increases by up to 50%, due to the higher effective dielectric constant of the surface. No evidence of a significant electric field enhancement near the dielectric surface (ceramic or water) has been detected, within the spatial resolution of the present diagnostic, ~100 μm.

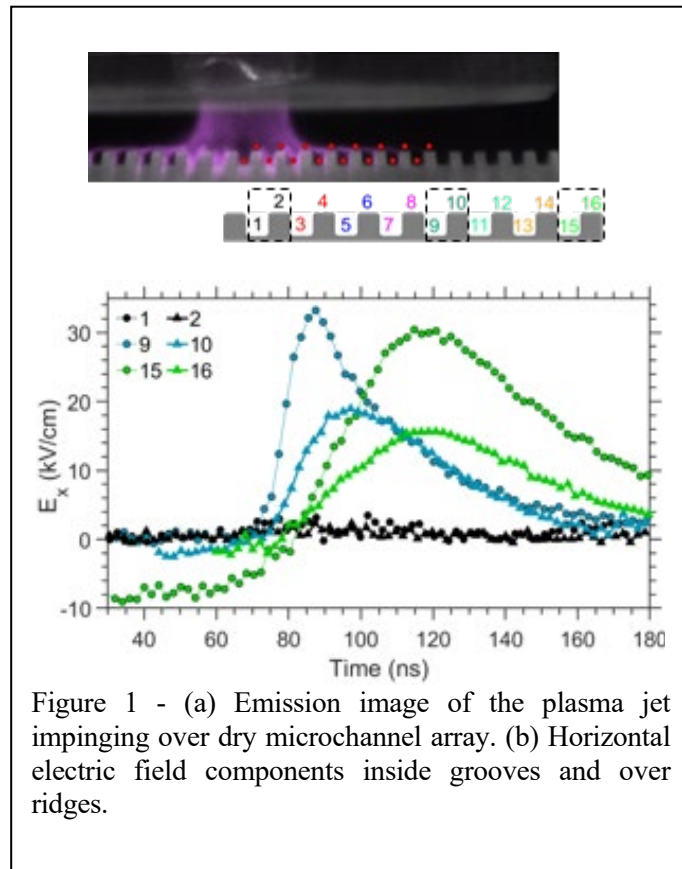


Figure 1 - (a) Emission image of the plasma jet impinging over dry microchannel array. (b) Horizontal electric field components inside grooves and over ridges.

Simulations of the SIW are performed using nonPDPSIM, a two-dimensional plasma hydrodynamics model [2]. The simulation includes the solution of Navier-Stokes equations for the neutral gas flow, coupled with the transport equations for charged particles and Poisson’s equation for the electric potential. Photoionization is represented using Green’s function approach.

## References

- [1] K. Orr, X. Yang, I. Gulko, and I.V. Adamovich, *Plasma Sources Sci. Technol.* 29 (2020) 125022.
- [2] S. A. Norberg, E. Johnsen, and M. J. Kushner, *Plasma Sources Sci. Technol.* 24 (2015) 035026.

## [PII-13] Measurements and Kinetic Modeling of O<sub>2</sub> Vibrational Kinetics in O<sub>2</sub>-Ar Mixtures Partially Dissociated by a Ns Pulse Discharge

Keegan Orr<sup>a</sup>, Fabrizio Esposito<sup>b</sup>, Iole Armenise<sup>b</sup>, and I.V. Adamovich<sup>a</sup>

(a) Ohio State University (orr.282@osu.edu, adamovich.1@osu.edu)

(b) Institute for the Plasma Science and Technology (fabrizio.esposito@cnr.it, iole.armenise@cnr.it)

Kinetics of O<sub>2</sub> vibrational excitation is studied during O atom recombination in an O<sub>2</sub>-Ar mixture partially dissociated by a burst of ns discharge pulses in a heated flow at T=400-800 K and P=200-600 Torr. The discharge generates a diffuse volumetric plasma, without well-pronounced filaments. The O atom number density is measured by ps Two-Photon absorption LIF (TALIF), calibrated in xenon. Time resolved vibrational level populations of molecular oxygen in the ground electronic state, O<sub>2</sub>(v=8-13,17-20), are measured by ps Laser Induced Fluorescence on the O<sub>2</sub> Schumann Runge bands, with absolute calibration by NO LIF in a NO-N<sub>2</sub> mixture with a known composition. The ozone number density is monitored by single pass absorption of radiation produced by a broadband deuterium lamp light source. The temperature of the gas is monitored by Rayleigh scattering thermometry. The results indicate a rapid initial decay of the O<sub>2</sub>(X,v=8-20) molecules generated by electron impact in the discharge, on ~20 μs time scale, due to the V-V exchange and V-T relaxation. This decay is followed by a much slower decay, on the time scale much longer compared to the characteristic time for V-V relaxation, ~1 ms. This indicates an additional process of O<sub>2</sub>(v) generation by chemical reactions initiated by the O atom recombination, and possibly ozone chemistry. Comparison of the experimental data with the master equation kinetic modeling predictions is used to infer the state-specific rates of chemical reactions generating vibrationally excited O<sub>2</sub>. The state-specific rates of O<sub>2</sub> vibrational energy transfer processes used in the kinetic model, specifically, the rates of vibration-translation (V-T) relaxation and dissociation in O<sub>2</sub>-O collisions, are predicted by the previously published Quasi Classical Trajectory (QCT) calculations.



# [PII-14] Studies of Catalyst Nanoparticles Synthesis Using Metal Arc Discharge: Experiment and Modeling

S. Musikhin, Y. Raitses and V. Nemchinsky

Princeton Plasma Physics Laboratory (smusikhin@pppl.gov)

The use of single-walled carbon nanotubes (SWCNTs) in structural materials promises significant enhancement in the construction's life span, mechanical, and even electrical characteristics, and thus—the reduction of CO<sub>2</sub> emissions. One of the scalable techniques of SWCNT production is the arc discharge method. Previous efforts mainly focused on the arc with two graphite electrodes, one of which contained catalyst powder [1]. A more scalable and sustainable method is the metal arc in a methane atmosphere in which the metal anode is continuously evaporated to produce catalyst nanoparticles, while methane is decomposed to generate carbon and H<sub>2</sub>, with no CO<sub>2</sub> formation.

SWCNT synthesis requires precise control over the catalyst particle size distribution [2]. Implementation of the control knobs typical to gas-phase synthesis, such as adjusting the flowrates or quenching the gas mixture, is limited because of the arc's dynamic instabilities [3] and strong gradients of atom density, temperature, pressure, and chemical composition [4]. Here, we evaluate an alternative approach: The size of metal particles can be limited by the formation of a non-reactive coating, such as a carbon shell. This study aimed to determine what defines the catalyst nanoparticle size in a chemically active environment and to develop a simple model able to predict the catalyst size and concentration for the given conditions.

We use a simple, yet accurate, monodisperse model [5] to monitor cluster formation at different stages in a chemically active gas mixture (Ar-CH<sub>4</sub>). The model includes iron cluster nucleation and growth, thermal processes, methane adsorption, and cluster coverage with carbon atoms. The modeling results are validated experimentally using a DC metal arc in the Ar-CH<sub>4</sub> atmosphere at sub-atmospheric pressure.

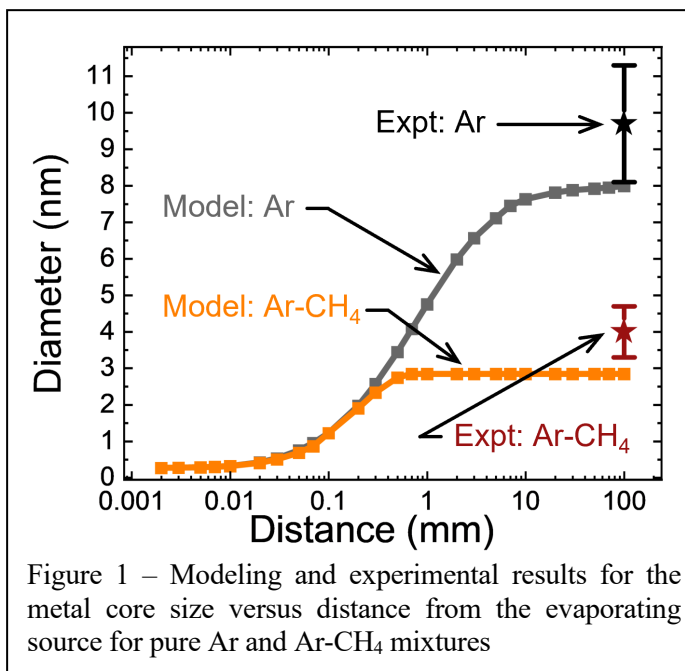


Figure 1 – Modeling and experimental results for the metal core size versus distance from the evaporating source for pure Ar and Ar-CH<sub>4</sub> mixtures

This work is supported by the U.S. Department of Energy through contract DE-AC02-09CH11466.

## References

- [1] S. Yatom et al., Carbon **125**, 336 (2017)
- [2] M.C. Diaz et al., J. Phys. Chem. C, **123** (2019)
- [3] S. Gershman et al., J. Phys. D: Appl. Phys. **49** (2016)
- [4] V. Vekselman et al., Plasma Sources Sci. Technol. **26** (2017)
- [5] V.A. Nemchinsky and M. Shigeta, Model. Simul. Mater. Sci. Eng **20** (2012)

# [PII-15] Femtosecond TALIF to Measure Atomic Sodium Densities in a Glow Discharge with NaCl Solution Electrode

Tanubhav Srivastava<sup>a</sup>, Arthur Dogariu<sup>b</sup>, Anatoli Morozov<sup>b</sup> and Peter Bruggeman<sup>a</sup>

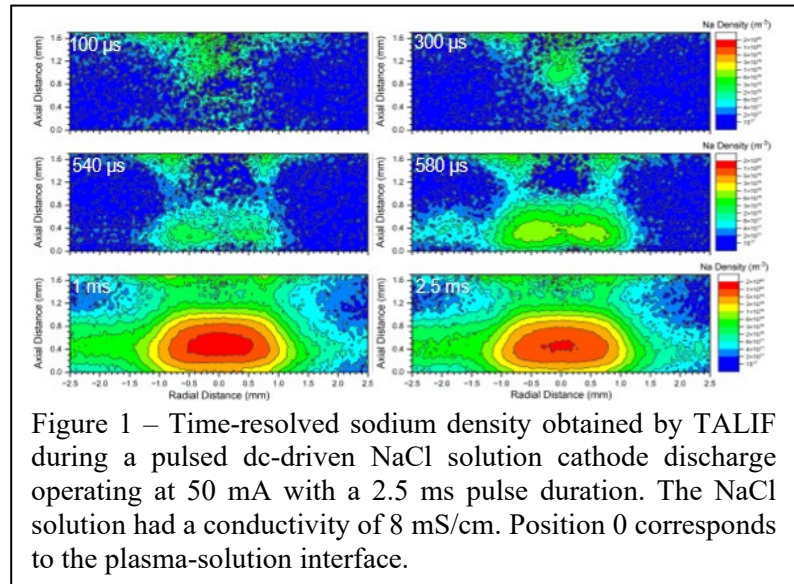
(a) Department of Mechanical Engineering, University of Minnesota (sriva203@umn.edu, pbruggem@umn.edu)

(b) Department of Mechanical and Aerospace Engineering, Princeton University (adogariu@princeton.edu)

(c) Department of Aerospace Engineering, Texas A&M University

Plasma-liquid interactions have been studied intensively during the last decade [1]. However, there remains a myriad of complex plasma-liquid interfacial phenomena which are yet to be investigated in detail. One such phenomenon is the transfer of solutes across the plasma-liquid interface enabled by the large energy flux supplied by plasmas to the liquid phase. A recent study has shown a correlation between self-organized patterns at the plasma-liquid interface for liquid anode discharges and solute transfer into the transfer [2]. Nonetheless, the mechanism of solute transfer in these discharges is not understood, with phenomenon such as electrospray [3] and chemical vapor generation (CVG) [4] suggested as possible mechanisms.

In this work, we report on Two-photon Absorption Laser Induced Fluorescence (TALIF) measurements of sodium densities using a broadband femtosecond-pulsed laser in a pulsed dc-driven NaCl solution cathode and anode discharges with as goal to investigate the mechanism of sodium transfer from the liquid to the plasma phase. For liquid cathode discharges, sodium densities near the plasma-liquid interface of the order of  $10^{20} \text{ m}^{-3}$  were observed, requiring a timescale on the order of 1 ms to achieve such densities as shown in Figure 1. The sodium density was found to be quadratically dependent on solution conductivity and correlates with the number of droplets injected into the plasma as detected by Mie scattering. For the liquid anode discharge, random flashes of sodium were observed resulting in average sodium densities at least on order of magnitude lower. The sodium density was also surprisingly located at a finite distance from the liquid surface. These findings are consistent with different mechanisms of sodium transfer from the liquid to the plasma phase for solution anode and cathode which will be discussed in detail.



This work was supported by the US Department of Energy, Office of Science, Office of Fusion Energy Sciences, General Plasma Physics Program under award DE-SC0024480 and DE-SC-0020232.

## References

- [1] P. J. Bruggeman et al., Plasma Sources Sci. Technol. **25**, 053002 (2016).
- [2] T. Srivastava et al., Plasma Sources Sci. Technol. **31**, 085010 (2022).
- [3] N. Shirai et al., Plasma Sources Sci. Technol. **29**, 025007 (2020).
- [4] J. Orejas et al., Spectrochemical Acta Part B: Atomic Spectroscopy. **209**, 106786 (2023).

# [PII-16] Mechanistic Insights into Plasma-Assisted Catalysis by *Operando* DRIFTS

James L. Trettin, Bruce E. Koel, and Michele L. Sarazen

Department of Chemical and Biological Engineering  
Princeton University, 50 Olden St, Princeton, NJ, 08540  
(jt2150@princeton.edu)

Given the critical need to limit our dependence on fossil fuels for energy and chemicals, it is vital to engineer chemical reactions that sustainably produce platform molecules using renewable electricity to limit greenhouse (GHG) emissions. One such reaction is the dry reforming of methane (DRM) that converts methane and carbon dioxide into syngas, which is a mixture of carbon monoxide and hydrogen that is valuable for upgrading to higher order hydrocarbons and liquid oxygenates via Fischer-Tropsch chemistry. [1]

While thermal DRM is limited by the activation of thermodynamically stable methane and by catalyst deactivation from adsorbed carbonaceous species, we propose a plasma-assisted catalytic approach. It is proposed that this direct electron process activates methane and carbon dioxide in a plasma discharge and reacts these species on a heterogeneous catalyst to tailor the selectivity to desired products. [2] This process benefits from its use renewable electricity and could possibly be used to directly synthesize important chemicals from methane and carbon dioxide. Furthermore, plasma-assisted catalysis has been shown to benefit from a synergistic effect due to the interactions of the plasma discharge on the catalyst surface and the effect of the catalyst material on the plasma discharge. [3] Thus, one primary challenge facing effective catalyst design for plasma-assisted catalysis is a lack of fundamental understanding of plasma/catalyst interactions during reaction.

In this work, we demonstrate the use of a dielectric barrier discharge (DBD) plasma jet interfaced with a diffuse reflectance (DR) reaction chamber for *operando* infrared Fourier transform spectroscopy (DRIFTS). We study the plasma-assisted oxidation of carbon monoxide on Pt/Al<sub>2</sub>O<sub>3</sub> as a suitable probe reaction for evaluating the strengths and limitations of the jet/cell configuration for mechanistic studies of plasma/catalyst interactions. Our work here has revealed the ability for certain plasma discharges to oxidize the active metal catalyst and to alter active metal nanoparticle restructuring mechanisms, which has significant impacts on reaction rates.

## References

- [1] Carapellucci, R.; Giordano, L. Steam, Dry and Autothermal Methane Reforming for Hydrogen Production: A Thermodynamic Equilibrium Analysis. *J Power Sources* **2020**, *469*, 228391.
- [2] Feng, J.; Sun, X.; Li, Z.; Hao, X.; Fan, M.; Ning, P.; Li, K. Plasma-Assisted Reforming of Methane. *Advanced Science* **2022**, 2203221.
- [3] Neyts, E. C.; Ostrikov, K. (Ken); Sunkara, M. K.; Bogaerts, A. Plasma Catalysis: Synergistic Effects at the Nanoscale. *Chem Rev* **2015**, *115* (24), 13408–13446.

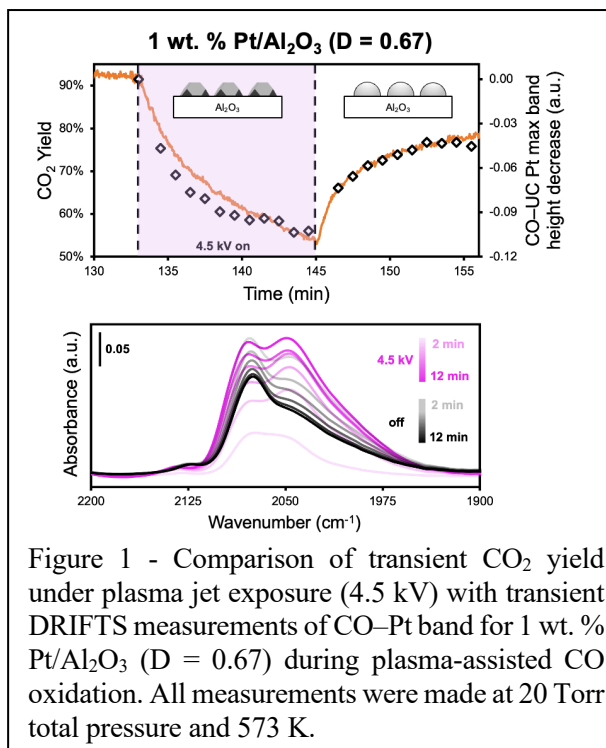


Figure 1 - Comparison of transient CO<sub>2</sub> yield under plasma jet exposure (4.5 kV) with transient DRIFTS measurements of CO–Pt band for 1 wt. % Pt/Al<sub>2</sub>O<sub>3</sub> (D = 0.67) during plasma-assisted CO oxidation. All measurements were made at 20 Torr total pressure and 573 K.

## List of Participants

Last Name	First Name	Email	Institution
Adamovich	Igor	adamovich.1@osu.edu	Ohio State University
Arumuganainar	Sonia	seka@princeton.edu	Princeton University
Bayer	Brian	bayer116@umn.edu	University of Minnesota
Bentz	Brian	bzbentz@sandia.gov	Sandia National Laboratories
Berry	Matthew	berry.991@osu.edu	Ohio State University
Beving	Lucas	lpbevin@sandia.gov	Sandia National Laboratories
Bhan	Aditya	abhan@umn.edu	University of Minnesota
Bruggeman	Peter	pbruggem@umn.edu	University of Minnesota
Frank	Jonathan	jhfrank@sandia.gov	Sandia National Laboratories
Ganzallo	Foluke (Jennifer)	ganzalfj@clarkson.edu	Clarkson University
Gershman	Sophia	sgershma@pppl.gov	PPPL
Goldsmith	Bryan	bgoldsm@umich.edu	University of Michigan
Gorman	Grant	gmgorma@sandia.gov	Sandia National Laboratories
Hansen	Nils	nhansen@sandia.gov	Sandia National Laboratories
Hinshelwood	Michael	mhinshel@umd.edu	University of Maryland
Hoffenberg	Louis	lh0534@princeton.edu	Princeton University
Hopkins	Matthew	mmhopki@sandia.gov	Sandia National Laboratories
Jeon	Jisu	jisujeon@umich.edu	University of Michigan
Ju	Yiguang	yju@princeton.edu	PPPL
Kaganovich	Igor	ikaganov@pppl.gov	PPPL
Khan	Mahreen	fmahreen@umn.edu	University of Minnesota
Kliwer	Christopher	cjkliew@sandia.gov	Sandia National Laboratories
Koel	Bruce	bkoel@princeton.edu	PPPL
Konina	Kseniia	kseniak@umich.edu	University of Michigan
Kushner	Mark J.	mjkush@umich.edu	University of Michigan
Lin	Zihan	zh1030613@gmail.com	Princeton University
Liu	Ning	nl7@princeton.edu	PPPL
Mao	Xingqian	xingqian@princeton.edu	Princeton University
Mededovic Thagard	Selma	smededov@clarkson.edu	Clarkson University
Meyer	Mackenzie	maemeyer@umich.edu	University of Michigan
Miller	Victor	vmiller1671@berkeley.edu	UC-Berkeley
Musikhin	Stanislav	smusikhin@pppl.gov	PPPL
Oehrlein	Gottlieb	oehrlein@umd.edu	University of Maryland
Ohiro	Oluwatosin	oohiro@umich.edu	University of Michigan
Orr	Keegan	orr.282@osu.edu	Ohio State University
Podder	Nirmol	Nirmol.Podder@science.doe.gov	DOE
Polito	Jordyn	jopolito@umich.edu	University of Michigan
Raitses	Yevgeny	yraitses@pppl.gov	PPPL
Raskar	Sai	raskar.1@osu.edu	Ohio State University

Last Name	First Name	Email	Institution
Shaddix	Chris	crshadd@sandia.gov	Sandia National Laboratories
Shannon	Steven	scshanno@ncsu.edu	North Carolina State University
Shao	Ketong	ketong_shao@berkeley.edu	UC-Berkeley
Shi	Zhiyu	zs3643@princeton.edu	Princeton University
Shneider	Mikhail	shneyder@princeton.edu	Princeton University
Sickafoose	Shane	smsicka@sandia.gov	Sandia National Laboratories
Srivastava	Tanubhav	sriva203@umn.edu	University of Minnesota
Steinkamp	Mike	mjstein@sandia.gov	Sandia National Laboratories
Telfah	Hamzeh	telfah.1@osu.edu	Ohio State University
Trettin	James	jt2150@princeton.edu	Princeton University
Ussenov	Yerbolat	yu3724@princeton.edu	Princeton University
Villafana	Willca	wvillafa@pppl.gov	PPPL
Yatom	Shurik	syatom@pppl.gov	PPPL
Zheng	Yiteng	yitengz@princeton.edu	Princeton University